Beyond Reflex: Nociception, Neural Circuits, and the Transformation of Threat into Memory in *Drosophila melanogaster*

Jessica Jones

A dissertation

submitted in partial fulfillment of the

requirements for the degree of

Doctor of Philosophy

University of Washington

2025

Reading Committee:

John C Tuthill, Chair

Sama Ahmed

Jay Z Parrish

Program Authorized to Offer Degree:

Neuroscience

University of Washington

Abstract

Beyond Reflex: Nociception, Neural Circuits, and the Transformation of Threat into Memory in *Drosophila melanogaster*

Jessica Jones

Chair of the Supervisory Committee:

John Tuthill

Department of Neurobiology and Biophysics

A fly flinches, jumps, runs—not randomly, but in a sequence carved by neurons that have been waiting for danger. For any animal, survival depends on knowing when the world has become dangerous—and reacting fast enough to avoid harm. This ability, called nociception, begins with specialized sensory neurons that detect mechanical, thermal, or chemical threats and ends with circuits that orchestrate escape and shape future behavior. In *Drosophila melanogaster*, nociception has been dissected in detail in larvae, but the adult system remains largely uncharted: how are its nociceptors wired, how do they drive different forms of escape, and how are their sensory properties tuned to the life of the adult fly? This thesis traces the anatomy and logic of escape in *Drosophila melanogaster*, revealing how a specific class of abdominal nociceptors initiates a spectrum of behaviors that begin with milliseconds of alarm and end with seconds of altered state.

In this thesis, I combine connectomics, optogenetics, calcium imaging, single-cell RNA sequencing, and computational modeling to build a multi-level understanding of adult nociceptor function. I begin with a behavioral screen for neurons capable of driving aversion, focusing on a genetically defined subset of abdominal class IV multidendritic neurons (md). Connectomic reconstruction shows that md neurons project to two distinct downstream pathways: circuits for rapid, reflexive escape behaviors (running, jumping) and ascending circuits for arousal and behavioral modulation. Within the ascending pathway, a pair of inhibitory/peptidergic neurons emerges as a candidate mechanism for regulating both the magnitude and persistence of nociceptive responses, balancing sensitivity with stability.

I next examine the molecular identity of md neurons. Single-cell RNA sequencing reveals a shift from the larval polymodal profile toward a mechanosensory-biased expression program, with strong enrichment of Piezo, ppk, and ppk26, and downregulation of thermosensory channels such as TrpA1 and Painless. Yet functional imaging reveals robust heat responses but no detectable mechanosensory activity, pointing to post-transcriptional regulation or context-dependent tuning.

Together, these findings define the first steps of a complete circuit map for adult *Drosophila* nociceptors and show how parallel pathways coordinate rapid escape with longer-term state modulation. They also reveal that molecular identity does not always predict sensory function—reminding us that in neural systems, what a cell expresses and what it does are related, but not the same. This work offers both a detailed model for nociceptive control in a compact brain and a broader framework for thinking about how evolution balances urgency, persistence, and sensitivity in the face of danger. We also begin to discuss the ethical implications this type of study might present to us.

TABLE OF CONTENTS

FIGURE TABLE OF CONTENTS

TABLES *WITH* CONTENT

Dedication

This thesis is dedicated to all my mothers.

Chapter 1: Main Introduction

Background

Nociception and Pain as a Biological Alarm System

Pain is a fundamental force, like hunger or gravity, that continuously influences our behavior. It plays a crucial role in self-preservation, education, and the resilience of our species. Beyond signaling immediate harm, pain also serves as a memory, a mechanism by which the nervous system guides future choices towards survival. This capacity to detect and respond to potentially harmful stimuli, known as **nociception**[1], is among the oldest and most essential biological functions. In mammals, pain is usually thought of as an emotional and sensory experience; in simpler animals, it's often dismissed as a reflex. But across the tree of life, from jellyfish to humans, nociception takes many forms, and its relationship to pain is more complicated—and more interesting—than any binary label can capture.

Primitive nervous systems, like those found in cnidarians, already show dedicated responses to noxious stimuli[2,3]. By the Cambrian explosion, the rise of bilaterian animals brought with it more specialized nociceptive circuits—ones capable of driving not just movement, but state changes[4]: arousal, vigilance, aversion, and perhaps even the scaffolding for what humans experience as pain. These circuits encode value, shape memory, and modulate motivation beyond purely reflexive responses.

Pain may not be universal, but its logic is. While many species depend on nociception to avoid harm, the sensitivity and behavioral consequences of that signal vary widely. Some animals—like the naked mole rat[5]—have lost specific pain modalities through evolutionary

tradeoffs, without losing the ability to learn, make decisions, or form social bonds. This divergence suggests that pain is not just a consequence of complexity, but a selective adaptation: a cognitive lens shaped by ecological need.

"Pain is the psychical adjunct of an imperative protective reflex."

–Sir Charles Sherrington

Pain does not require a neocortex, contrary to Sherrington's original assumption of pain *(see quote)*. What it likely does require is a way to detect damage, relay that signal to integrative centers, modulate the signal based on experience or internal state, and adapt future behavior. Recent efforts—like the "Gibbons Criteria[6]"—attempt to formalize this by outlining essential criteria needed to support something analogous to pain in nonhuman species: dedicated nociceptors[7], interneurons to integrate and transmit signals[8], neurochemical modulation[9,10], behavioral flexibility, and memory of noxious stimuli[11,12]. The more of these features an animal has, the stronger the case that it may experience a pain-like state.

The Case for Drosophila melanogaster

You may know the fruit fly as a nuisance circling a ripened banana. But in the wild, *Drosophila melanogaster* navigates an environment full of danger. It must assess whether to risk a landing on a hot surface, evade a parasitoid wasp[13,14], or tolerate pain for the sake of shelter. Each decision carries a cost. This raises the integral question of this thesis: *can an insect, like the*

fly, form an internal state based on threat? Can it feel something like pain? These questions beg binary answers—yes or no, present or absent. But the circuits that might support such states reveal something more nuanced: a nervous system that detects, integrates, remembers, and adapts to threat in ways that challenge simple categorization.

Drosophila is uniquely positioned to answer this question. Flies have genetically defined mechanosensory and nociceptive neurons distributed across their bodies, expressing conserved transduction molecules like TRPA1[15], *painless*[16], and Piezo[17]. When activated, these neurons drive stereotyped escape responses—rolling in larvae[8], running or jumping in adults—that mimic vertebrate responses to similar threats. The fly's genetic accessibility allows us to label, activate, silence, or reconstruct individual neurons with unprecedented precision.

More importantly, *Drosophila* is small enough to map in its entirety—down to the last synapse—but complex enough to exhibit choice, learning, and internal state shifts.

"To understand the functioning of a network, one must know its elements and their interconnections."

–Sporns et.al.[18]

The advent of **connectomics,** the study of the complete set of neural connections in a nervous system referred to as the **connectome,** has revealed the complete wiring diagram of the fly nervous system, providing an unprecedented opportunity to trace how nociceptive signals flow from

sensory detection through circuit integration to behavioral output. Recent work has shown that flies can modulate escape depending on context, learn to avoid harmful stimuli, and integrate competing drives[19,20]. The nervous system that enables these behaviors is compact, but sophisticated—and increasingly, it looks less reflexive and more cognitive than previously assumed.

In the context of this thesis, I focus on the adult fly abdomen. But adult flies start as larvae. As my thesis advisor would call it, larvae are essentially a "wet tubular bag"[21]. This "bag" though then dissolves into a soup in a chrysalis, then reforms as a flying machine, yet its bottom section remains largely intact. The *Drosophila* abdomen offers a uniquely advantageous model for studying nociception due to its remarkable developmental conservation[21–23]. Despite the dramatic metamorphosis of the head and thorax, the abdomen maintains significant architectural and cellular continuity with its larval form[24–27], including highly conserved nociceptors central to this research[28,29]. This preservation extends to their dendritic field organization, innervation patterns, and central connectivity[26], allowing researchers to trace form-function relationships across development. This blend of structural conservation[22] and functional innovation[30,31], combined with the ability to modify the interpretation of preserved sensory signals to support new behaviors, makes the *Drosophila* abdomen an ideal system to dissect the intricacies of nociceptive processing.

This is where *Drosophila* becomes more than a model system. It becomes a Rosetta Stone for understanding how our neural circuits have changed—within a lifetime and across many, many evolutionary lifetimes—to convert sensory threat into adaptive behavior.

Thesis Overview: From Genes to Circuits to Behavior

This thesis investigates the nociceptive circuits of *Drosophila melanogaster* using a multi-level approach that spans molecular identity, circuit architecture, and behavioral output. I focus on a particular class of abdominal sensory neurons—**the adult abdominal md nociceptors**—whose morphology resembles vertebrate free nerve endings[32]. These neurons are surprisingly one of the few cell-type preserved during metamorphosis[14,23,33,34]. These neurons have large, complex dendritic arbors that tile the dorsal and ventral abdomen and send axons into the ventral nerve cord, where they interface with a range of downstream targets.

Circuit Architecture and Connectomic Analysis

In Chapter 2, I begin with a systematic optogenetic screen of somatosensory neuron classes, which reveals that abdominal md neurons are uniquely capable of driving both rapid escape responses and sustained place avoidance—behavioral signatures consistent with affective processing. Most other somatosensory classes—proprioceptors, touch receptors, and other mechanosensory populations—elicit only transient effects such as grooming or pausing, without producing long-term spatial aversion.

Using spatially targeted optogenetic stimulation in tethered flies, I demonstrate that md neuron activation triggers stereotyped escape behaviors: rapid increases in forward velocity and jumping. Critically, these coordinated responses require intact connections between the ventral nerve cord and brain—decapitated flies exhibit only reflexive kicking and site-specific grooming, never coordinated escape. This establishes that nociceptor-mediated escape relies on ascending and descending integration with central brain circuits, not just local spinal-like reflexes.

Connectomic reconstruction reveals the anatomical basis for this integration: md axons form spatially organized, somatotopic terminal arbors in the abdominal ganglion and dedicate nearly half of their synaptic output to ascending interneurons that project to the brain. This contrasts sharply with other somatosensory classes (tactile bristles, proprioceptors), which predominantly connect to local motor circuits. Within the ascending pathways, I identify distinct neural populations that mediate different behavioral components: some drive rapid jumping via the giant fiber system, others modulate walking velocity through premotor circuits, and still others support sustained place avoidance through connections to learning and memory centers.

In Chapter 3, connectome-based modeling predicts that without some of these modulatory ascending pathways, notably a pair of GABAergic and serotonergic ascending neurons, the nociceptive network becomes hyperexcitable, suggesting these circuits are essential not just for escape, but for calibrating behavioral state—a core feature of pain processing in vertebrates. The circuit architecture supports behavioral complexity that extends far beyond simple reflexes: optogenetic activation produces immediate running and jumping, but also longer-term reductions in exploration and persistent changes in spatial preference that scale with repetition, transitioning from reflex to learned behavior.

Sensory Tuning and Transcriptomic Identity

In Chapter 3, I first examine the sensory properties and molecular identity of md neurons found in Chapter 2: Calcium imaging from md axons in the abdominal ganglion reveals robust responses to noxious heat (40°C) but minimal responses to isolated mechanical stimulation—a surprising finding given the neurons' extensive peripheral innervation and morphological similarity to mechanosensory free nerve endings.

Single-cell transcriptomic analysis from the Fly Cell Atlas provides a potential explanation for this paradox. Adult md neurons show developmental transcriptomic remodeling compared to their larval precursors: upregulation of mechanosensitive channels (*ppk*, *Piezo*, *Balboa*, *Cirl*) paired with downregulation of thermosensitive and polymodal receptors (*TrpA1*, *painless*, *Gr28b*, *pyrexia*). This molecular signature would predict mechanosensory specialization, yet the physiological data tell a different story.

Rather than viewing this as a contradiction, these findings may reflect evolution of sophisticated multimodal integration. Unlike their larval predecessors, which function as broadly tuned danger detectors responding to any sufficiently intense stimulus, adult md neurons may require combinatorial stimuli—integrating thermal and mechanical information—to discriminate between benign environmental contacts and genuine threats. This represents an elegant evolutionary solution that leverages existing neural architecture while refining sensory specificity to meet the demands of three-dimensional flight environments where false alarms carry high energetic costs.

The developmental shift from larval polymodal responsiveness to adult multimodal integration may reflect adaptation to changing ecological demands. Ground-dwelling larvae face relatively simple threat categories where any intense stimulus warrants escape rolling. Flying adults must support more nuanced behavioral decisions in complex environments where escape can involve jumping, flight initiation, or directional running. The transcriptomic changes suggest functional refinement rather than simple modality switching—a "software update" that preserves the nociceptive "hardware" while tuning its activation requirements.

Toward a Circuit-Level Understanding of Pain

Taken together, these findings support the idea that *Drosophila melanogaster* meets several key criteria for pain-like processing: dedicated nociceptors, sophisticated circuit integration, state-dependent modulation, memory formation, and adaptive decision-making. The anatomy is there. The behavior is there. The molecular machinery is there. But perhaps most importantly, the circuits reveal a logic that transcends simple reflexes—a system capable of transforming sensory threat into adaptive behavioral states.

This thesis posits that pain-like processing arises from the universal challenge for mobile organisms to transform harmful sensory data into adaptive behaviors. By studying the compact neural circuits of flies, the research reveals sophisticated solutions to this ancient problem, where these circuits not only detect and react to threats but also learn, remember, and apply that memory to future actions. Through modern connectomics, transcriptomics, and behavioral analysis, this work aims to uncover the fundamental origins of pain, offering insights into fly biology and a foundational understanding of how nervous systems across the animal kingdom convert sensory experience into adaptive behavior.

References.

1. Julius, D. & Basbaum, A. I. Molecular mechanisms of nociception. *Nature* **413**, 203–210 (2001).

2. Mechanical stimulation in the sea-anemone *Calliactis parasitica*. *Proc. R. Soc. Lond. Ser. B - Biol. Sci.* **143**, 226–238 (1955).

3. Grimmelikhuijzen, C. J. P. & Westfall, J. A. The nervous systems of Cnidarians. in *The Nervous Systems of Invertebrates: An Evolutionary and Comparative Approach* (eds Breidbach, O. & Kutsch, W.) vol. 72 7–24 (Birkhäuser Basel, Basel, 1995).

4. Chen, C.-L. *et al.* Ascending neurons convey behavioral state to integrative sensory and action selection brain regions. *Nat. Neurosci.* **26**, 682–695 (2023).

5. Smith, E. St. J., Park, T. J. & Lewin, G. R. Independent evolution of pain insensitivity in African mole-rats: origins and mechanisms. *J. Comp. Physiol. A* **206**, 313–325 (2020).

6. Gibbons, M. *et al.* Can insects feel pain? A review of the neural and behavioural evidence. in *Advances in Insect Physiology* vol. 63 155–229 (Elsevier, 2022).

7. Dubin, A. E. & Patapoutian, A. Nociceptors: the sensors of the pain pathway. *J. Clin. Invest.* **120**, 3760–3772 (2010).

8. Burgos, A. *et al.* Nociceptive interneurons control modular motor pathways to promote escape behavior in Drosophila. *eLife* **7**, e26016 (2018).

9. Adel, M. & Griffith, L. C. The Role of Dopamine in Associative Learning in Drosophila: An Updated Unified Model. *Neurosci. Bull.* **37**, 831–852 (2021).

10. Jovanoski, K. D. *et al.* Dopaminergic systems create reward seeking despite adverse consequences. *Nature* (2023) doi:10.1038/s41586-023-06671-8.

11. Aso, Y. *et al.* Specific Dopaminergic Neurons for the Formation of Labile Aversive Memory. **20**, 1445–1451 (2010).

12. Yu, D., Akalal, D.-B. G. & Davis, R. L. *Drosophila α/β Mushroom Body Neurons Form a Branch-Specific, Long-Term Cellular Memory Trace After Spaced Olfactory Conditioning*. (2006).

13. Moore, L. D., Chris Amuwa, T., Shaw, S. R. & Ballinger, M. J. Drosophila are hosts to the first described parasitoid wasp of adult flies. *Nature* **633**, 840–847 (2024).

14. Hwang, R. Y. *et al.* Nociceptive Neurons Protect Drosophila Larvae from Parasitoid Wasps. *Curr. Biol.* **17**, 2105–2116 (2007).

15. Neely, G. G. *et al.* TrpA1 Regulates Thermal Nociception in Drosophila. *PLOS ONE* **6**, e24343 (2011).

16. Tracey, W. D., Wilson, R., Laurent, G. & Benzer, S. painless, a Drosophila Gene Essential for Nociception. **113**, 261–273 (2003).

17. Kim, S. E., Coste, B., Chadha, A., Cook, B. & Patapoutian, A. The role of Drosophila Piezo in mechanical nociception. *Nature* **483**, 209–212 (2012).

18. Sporns, O., Tononi, G. & Kötter, R. The human connectome: A structural description of the human brain. *PLoS Comput. Biol.* **1**, e42 (2005).

19. Anderson, D. E. & Adolphs, R. A Framework for Studying Emotions across Species. **157**, 187–200 (2014).

20. Tyng, C. M., Amin, H. U., Saad, M. N. M. & Malik, A. S. The Influences of Emotion on Learning and Memory. *Front. Psychol.* **8**, 1454 (2017).

21. Dutta, D. *et al.* Regional Cell-Specific Transcriptome Mapping Reveals Regulatory Complexity in the Adult Drosophila Midgut. *Cell Rep.* **12**, 346–358 (2015).

22. Schönbauer, C. *et al.* Spalt mediates an evolutionarily conserved switch to fibrillar muscle fate in insects. *Nature* **479**, 406–409 (2011).

23. Kimura, K. & Truman, J. Postmetamorphic cell death in the nervous and muscular systems of Drosophila melanogaster. *J. Neurosci.* **10**, 403–411 (1990).

24. Currie, D. A. & Bate, M. The development of adult abdominal muscles in *Drosophila:* myoblasts express *twist* and are associated with nerves. *Development* **113**, 91–102 (1991).

25. Roy, S., Shashidhara, L. S. & VijayRaghavan, K. Muscles in the Drosophila second thoracic segment are patterned independently of autonomous homeotic gene function. *Curr. Biol.* **7**, 222–227 (1997).

26. Fernandes, J. J. & Keshishian, H. Patterning the dorsal longitudinal flight muscles (DLM) of *Drosophila* : insights from the ablation of larval scaffolds. *Development* **122**, 3755–3763 (1996).

27. Bate, M., Landgraf, M. & Gomezbate, M. Development of Larval Body Wall Muscles. *Int. Rev. Neurobiol.* **43**, 25–44 (1999).

28. Grueber, W. B., Jan, L. Y. & Jan, L. Y. Tiling of the Drosophila epidermis by multidendritic sensory neurons. **129**, 2867–2878 (2002).

29. Shimono, K. *et al.* Multidendritic sensory neurons in the adult Drosophila abdomen: origins, dendritic morphology, and segment- and age-dependent programmed cell death. **4**, (2009).

30. Syed, M. H., Mark, B. & Doe, C. Q. Steroid hormone induction of temporal gene expression in Drosophila brain neuroblasts generates neuronal and glial diversity. *eLife* **6**, e26287 (2017).

31. Truman, J. W. Steroid Receptors and Nervous System Metamorphosis in Insects. *Dev. Neurosci.* **18**, 87–101 (1996).

32. Messlinger, K. Chapter 17. Functional morphology of nociceptive and other fine sensory endings (free nerve endings) in different tissues. in *Progress in Brain Research* vol. 113 273–298 (Elsevier, 1996).

33. Williams, D. W. & Truman, J. W. Cellular mechanisms of dendrite pruning in *Drosophila* : insights from in vivo time-lapse of remodeling dendritic arborizing sensory neurons. *Development* **132**, 3631–3642 (2005).

34. Zhong, L., Hwang, R. Y. & Tracey, W. D. Pickpocket Is a DEG/ENaC Protein Required for Mechanical Nociception in Drosophila Larvae. *Curr. Biol.* **20**, 429–434 (2010).

Glossary of Key Terms

The following terms are used throughout this thesis and represent core concepts in nociception research and circuit neuroscience.

Term	Definition
Nociception	The detection and neural processing of potentially harmful stimuli by specialized sensory neurons; among the oldest and most essential biological functions, serving as a mechanism by which the nervous system guides future choices toward survival.
Pain	A fundamental force that continuously influences behavior; in mammals, an emotional and sensory experience. The relationship between circuit complexity and pain varies across the tree of life and is more complicated than any binary label can capture.
Nociceptor	A specialized sensory neuron that detects mechanical, thermal, or chemical threats and initiates protective responses; the primary cellular substrate of nociception.
Connectome	The complete set of neural connections in a nervous system; provides an unprecedented opportunity to trace how nociceptive signals flow from sensory detection through circuit integration to behavioral output.
Connectomics	The study of the complete set of neural connections in a nervous system; requires knowing both the elements and their interconnections to understand network functioning.
Multidendritic (md) neurons	Adult abdominal nociceptors in *Drosophila* whose morphology resembles vertebrate free nerve endings; one of the few cell types preserved during metamorphosis with large, complex dendritic arbors that tile the dorsal and ventral abdomen.
Ascending neurons	Interneurons that transmit sensory information from the ventral nerve cord to the brain; md neurons form their strongest synaptic connections with ascending interneurons, enabling nociceptive signals to reach integrative brain centers.
Metamorphosis	The dramatic transformation from larva to adult; despite radical changes to head and thorax, the abdomen maintains significant architectural and

Term	Definition
	cellular continuity, making it ideal for studying developmental conservation of nociceptive circuits.
State changes	Long-lasting alterations in arousal, vigilance, aversion, and behavioral priorities beyond purely reflexive responses; encode value, shape memory, and modulate motivation, representing the scaffolding for what humans experience as pain.
Polymodal	Responsive to multiple types of stimuli (thermal, mechanical, chemical); characteristic of larval class IV da neurons that function as broadly tuned danger detectors responding to any sufficiently intense harmful stimulus.
Multimodal integration	The requirement for combinatorial stimuli (e.g., both thermal and mechanical) for robust activation; may represent an evolutionary solution enabling adult md neurons to discriminate between benign environmental contacts and genuine threats.
Place avoidance	Sustained spatial aversion to locations previously associated with noxious stimuli; a behavioral assay demonstrating that nociceptor activation produces genuine state changes rather than simple stimulus-response arcs.
Somatotopy	The ordered mapping of body surface onto neural tissue; md neurons exhibit anterior-posterior and dorsal-ventral organization in the abdominal ganglion that reflects their peripheral location on the abdomen.
Optogenetics	The use of light-activated ion channels (e.g., Chrimson) to control neural activity with temporal and spatial precision; enables systematic identification of neurons sufficient to drive specific behaviors.
Gibbons Criteria	A framework outlining essential features needed to support pain-like states in nonhuman species: dedicated nociceptors, interneurons to integrate signals, neurochemical modulation, behavioral flexibility, and memory of noxious stimuli. The more of these features an animal has, the stronger the case for pain-like experience.

Chapter 2

Ascending nociceptive pathways drive rapid escape and sustained avoidance in adult *Drosophila*

Jessica M. Jones[1], Anne Sustar[1], Akira Mamiya[1], Sarah Walling-Bell[1], Grant M. Chou[1], Andrew P. Cook[1], John C. Tuthill[1*]

[1] Department of Neurobiology and Biophysics, University of Washington, Seattle, Washington

* Correspondence: tuthill@uw.edu

(note: a version of this manuscript is in review. ***preprint****)*

Abstract

Nociception — the detection of harmful stimuli by the nervous system — contributes to both rapid escape and long-term avoidance behaviors. *Drosophila* larvae detect damaging heat, mechanical, and chemical stimuli with specialized multidendritic (md) neurons, and these cells are among the only sensory neurons that survive metamorphosis. However, it remains unknown which somatosensory neurons contribute to nociception in adult flies. In an optogenetic screen, we found that abdominal md neurons were the only somatosensory class to induce rapid escape and sustained place avoidance. Calcium imaging from abdominal md axons revealed that they are activated by thermal nociceptive stimuli (>40°C). Connectomic reconstruction showed that md axons form their strongest synaptic connections with ascending interneurons that project to the brain. Among these, we identified two classes of ascending neurons that mediate rapid escape responses and a third that supports sustained avoidance. Our findings reveal that adult *Drosophila* meet several core criteria commonly used to define pain: dedicated nociceptors, ascending pathways connecting peripheral sensors to integrative brain centers, and a capacity for sustained avoidance of noxious stimuli.

Introduction

The ability to detect and respond to harmful stimuli is a core survival function shared across the animal kingdom. This capacity, known as nociception, relies on specialized sensory neurons called nociceptors, which detect mechanical, thermal, or chemical stimuli with the potential to damage the body[1]. Nociceptor activation triggers fast, reflexive motor programs that help animals avoid injury. In some animals, such as humans, nociceptive responses also contribute to the perception of affective pain, the internal emotional experience that arises from noxious stimuli. Affective pain can motivate long-term behavioral changes, such as learning to avoid particular situations or stimuli[2].

Whether insects and other invertebrates experience pain has been debated for centuries[3]. Traditionally, insect behaviors were viewed as purely reflexive and lacking an affective component[4]. However, mounting evidence has demonstrated that insects exhibit hallmarks of affective pain, such as learned avoidance[5,6], behavioral prioritization following noxious stimuli[7], affective cognition[8], and sensory generalization across threat modalities[9]. These studies have shown that insects are capable of adapting their behavior to avoid nociceptive stimuli[10], one of the criteria for affective pain in vertebrate animal models[11–14]. Understanding the neural bases of reflexive and affective responses to nociceptive stimuli in insects could provide fundamental insights into the mechanisms and evolution of pain.

The fruit fly, Drosophila melanogaster, offers unique advantages for investigating these questions, including a compact, well-mapped nervous system[15–20] and powerful genetic tools to enable precise manipulation of specific cell-types. Nociception in *Drosophila* larvae is mediated by class IV dendritic arborization (da) neurons that tile the body wall and trigger escape responses to

damaging mechanical, thermal, and ultraviolet stimuli[21]. Class IV da neurons are multidendritic, polymodal nociceptors that express conserved transduction channels including *TrpA1*[22,23], *painless*[24], *ppk*[25], and *Piezo*[26]. Analyses of downstream neural circuits in the fly larva have identified ascending[27,28] and descending[29] pathways that relay information from class IV da neurons to higher brain centers and motor neurons, respectively, to coordinate escape behavior[30,31].

The transformation from larval to adult fly presents new challenges for the somatosensory system[32]. Adult flies possess a different body plan, and their increased mobility exposes them to different threats than ground-dwelling larvae. They also exhibit an expanded behavioral repertoire, including walking, jumping, grooming, courtship, mating, and flight. The somatosensory system of the adult fly is comprised of multiple classes of sensory neurons, including multidendritic neurons, bristles, chordotonal neurons, and campaniform sensilla (**Figure 2.1A)**, which serve a range of proprioceptive and exteroceptive functions[33]. Multidendritic neurons—class I (proprioceptors in the larva[34]) and class IV da neurons—are among the few sensory neurons that survive metamorphosis from the larval to adult stage, though they undergo extensive remodeling[35–38]. Class I neurons undergo programmed cell death within a week after eclosion, whereas class IV da neurons persist throughout adulthood[39,40]. During metamorphosis, the class IV da neurons are pruned and regenerated into lattice-like dendritic fields[39,40] that are distributed across the surface of the adult fly's abdomen, where they are positioned to detect external threats to the abdominal cuticle[41], similar to free-nerve endings in mammalian skin[42]. (Because the class I–IV nomenclature is not used in the adult fly, we refer to the surviving class IV da neurons as abdominal multidendritic (md) neurons). However, compared to other classes of somatosensory neurons, little is known about the sensory properties of abdominal md neurons, their downstream connectivity, and the behaviors they control.

Here, we investigate the cells and circuits that mediate nociception in adult *Drosophila*. We begin with an optogenetic screen of somatosensory neuron classes, which reveals that abdominal md neurons are the only class that triggers both rapid escape and sustained avoidance. Using *in vivo* calcium imaging, we find that md neurons detect nociceptive thermal stimuli. By combining optogenetics, behavioral analysis, and connectomic reconstruction, we map the central pathways downstream of md axons and identify ascending interneurons that contribute to escape and sustained avoidance. Overall, our results suggest that md neurons in the adult fly abdomen detect nociceptive stimuli and trigger behaviors that are consistent with the experience of pain.

Results

A screen for somatosensory neurons that produce avoidance behavior.

In some animals, nociceptive stimuli produce both rapid, reflexive escape responses and long-term avoidance. To systematically identify which somatosensory neuron classes produce these behaviors in adult flies, we conducted an optogenetic screen targeting genetically defined populations of somatosensory neurons in adult *Drosophila*[33]. We expressed the red-light activated channelrhodopsin Chrimson in distinct populations of somatosensory neurons and used a four-quadrant assay to quantify behavioral preference over time **(Figure 2.1A–B).** The fly's preference or aversion for stimulated regions of the arena served as a readout of stimulus valence, an approach analogous to affective pain assays in mammals[12].

Most classes of somatosensory neurons, including proprioceptors and touch receptors, elicited only transient behavioral effects, such as grooming or pausing, without producing sustained place avoidance **(Figure 2.1C)**. However, activation of abdominal md neurons labeled by *ppk*-GAL4 (the md(C) driver line) induced significant and sustained place avoidance **(Figure 2.1D).** Flies continued to avoid the stimulated region for at least 30 seconds after stimulus offset **(Figure 2.1D)**, with only a slight decrease in walking velocity (**Figure 2.1E)**. We confirmed these results in three driver lines that label abdominal md neurons, which produced similar avoidance responses. The magnitude of avoidance increased across consecutive trials of md neuron stimulation (**Figure 2.1D**). As a positive control, we activated thermosensory hot cells in the antenna, which have been previously shown to produce robust place avoidance in a similar experimental assay[9,43]. Activation of hot cells produced significantly greater place avoidance than md neurons in our experimental setup (**Figure 2.1C**).

We further classified the behavior of flies in the arena and observed that activating md neurons led to increases in jumping and walking velocity **(Figure 2.1E–F)**, escape behaviors that also occur in response to other aversive stimuli[44,45]. We noticed that walking velocity peaked then decayed rapidly after stimulus onset, so we further quantified these kinetics using repeated optogenetic stimulation of md neurons in a uniformly illuminated arena **(Figure S2.1A)**. We found that flies exhibited phase-locked increases in walking velocity even at higher stimulation frequencies (e.g., 2 Hz). Fast walking in response to optogenetic stimulation of md neurons was significantly straighter than normal walking **(Figure S2.1C–E)**. Overall, our results show that optogenetic activation of md neurons drives both reflexive escape behaviors (jumping and running) and sustained place avoidance.

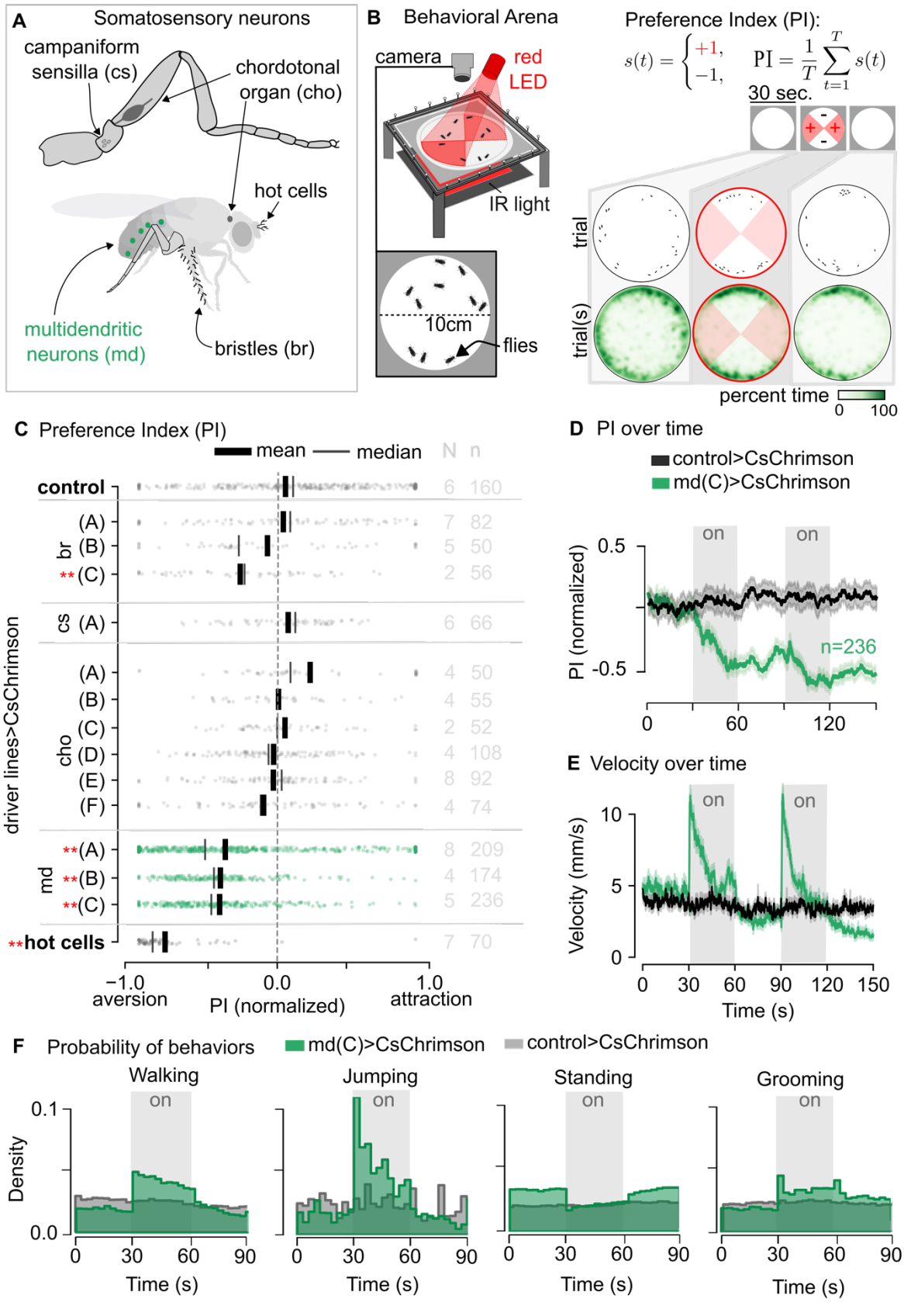
A
Somatosensory neurons
campaniform sensilla (cs)
chordotonal organ (cho)
hot cells
multidendritic neurons (md)
bristles (br)
B
Behavioral Arena
camera
red LED
IR light
10cm
flies
Preference Index (PI):
$s(t) = \begin{cases} +1, \\ -1, \end{cases}$
$\mathrm{PI} = \frac{1}{T}\sum_{t=1}^{T} s(t)$
30 sec.
trial
trial(s)
percent time
0
100
C
Preference Index (PI)
mean
median
N
n
control
(A)
br (B)
**(C)
cs (A)
(A)
(B)
cho (C)
(D)
(E)
(F)
**(A)
md **(B)
**(C)
**hot cells
driver lines>CsChrimson
−1.0
aversion
0.0
PI (normalized)
1.0
attraction
D
PI over time
control>CsChrimson
md(C)>CsChrimson
PI (normalized)
0.5
-0.5
on
n=236
0
60
120
E
Velocity over time
Velocity (mm/s)
10
5
0
0
30
60
90
120
150
Time (s)
F
Probability of behaviors
md(C)>CsChrimson
control>CsChrimson
Walking
Jumping
Standing
Grooming
Density
0.1
0.0
Time (s)

Figure 2.1. Activation of multidendritic (md) sensory neurons drives place aversion and changes in locomotion. (A) We tested classes of somatosensory neurons in an optogenetic screen. (B) Flies were placed in a 10 cm diameter bowl and their behavior was recorded under infrared light. A red LED delivered optogenetic stimulation during ON trials, and a preference index (PI) was calculated for each fly. Spatial density of flies by number across trials is plotted in green as the percent of time occupying a given region of the arena. (C) Preference indices are shown for different somatosensory neuron classes. The number of trials (N) and flies (n) are indicated for each class. The color scale represents the normalized attraction–aversion index, ranging from –1.0 to +1.0. Letters denote distinct lines labeling subsets of sensory neurons (see Methods for genotypes; md driver line expression is shown in Figure S1). Control flies were of a similar genetic background but lacked Chrimson expression (40B01-GAL4AD >CsChrimson). Red stars mark significant differences relative to controls. Box plots display median, mean, and individual data points. (D–E) Mean preference and velocity traces during 30-second optogenetic stimulation periods illustrate distinct responses between control and md(C)>CsChrimson flies. Gray bars indicate LED ON periods. PI measurements are shown for control flies (n=160) and md(C)>CsChrimson flies (n=236) across multiple trials. PI values were normalized from +1 (attraction) to -1 (aversion). (F) Behavioral probability distributions are plotted over time during 90-second recording periods. Bar heights were normalized within each group to sum to 1.

Spatially targeted activation of abdominal md neurons triggers stereotyped escape

To resolve the motor responses evoked by md neuron activation with higher temporal and spatial precision, we used optogenetic stimulation of md neurons in tethered flies walking on a spherical treadmill while we tracked the legs and abdomen in 3D **(Figure 2.2A, Figure S2.2A–B)**. In addition to enabling high fidelity 3D pose estimation, the tethered preparation allowed us to spatially target md neurons on the abdomen with a laser, thus excluding contributions from other cells labeled by the md GAL4 lines (**Figure S2.1**).

Transient (1 sec), spatially targeted (~350 μm) optogenetic stimulation of md neurons on the left side of the abdomen produced a rapid and robust increase in forward, but not rotational, velocity. Forward velocity increased to twice the baseline level within 500 ms of stimulus onset **(Figure 2.2B),** though the flies' heading angle did not significantly change **(Figure 2.2C).** This velocity increase was frequently accompanied by jumping behavior, during which the fly released the ball and retracted its leg **(Figure 2.2D–E).** Increases in walking speed occurred at a shorter latency (mean=100 ms) than jumping (mean=480 ms; **Figure 2.2E).**

Previous work has shown that flies and other insects exhibit some sensorimotor reflexes in the absence of descending input from the brain (i.e., in decapitated flies[46]). Decapitated flies may also jump[47] and attempt coordinated walking[48] during thermo- or optogenetic stimulation of specific neurons. To determine whether md neuron-mediated escape responses require the brain, we repeated our experiments in decapitated flies. While intact flies exhibited coordinated escape behaviors, such as increased forward locomotion and jumping, we found that decapitated flies performed leg kicking and site-specific grooming directed at the abdomen. Kicking and grooming were variable but occurred at a significantly higher percentage over the entire stimulus period than controls **(Figure 2.2F–G)**. Decapitated flies never displayed coordinated walking on the treadmill **(Figure 2.2F)**, indicating that ascending or descending projections to/from the brain are essential for escape initiation following md neuron activation. Interestingly, a study in mice also found that brain circuits are required to coordinate escape behavior[49].

Our findings collectively indicate that activation of abdominal md neurons in adult *Drosophila* drives escape responses: jumping and forward locomotion. The same stimuli in headless flies produced distinct motor reflexes: kicking and abdominal grooming. This suggests that nociceptor-mediated escape behaviors rely on ascending and descending signals to and from the central brain.

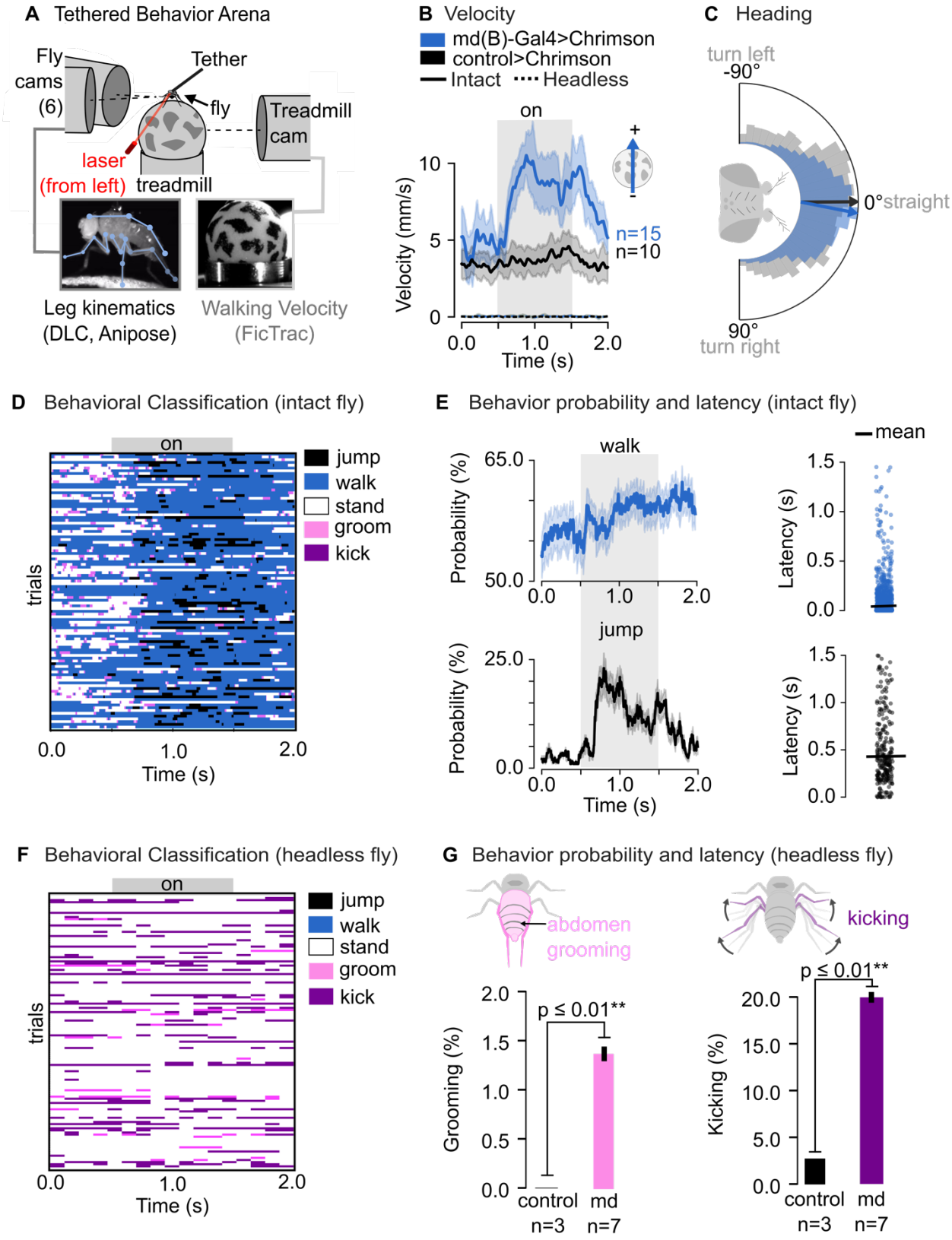
A Tethered Behavior Arena
Fly cams (6)
Tether
fly
Treadmill cam
laser (from left)
treadmill
Leg kinematics (DLC, Anipose)
Walking Velocity (FicTrac)
B Velocity
md(B)-Gal4>Chrimson
control>Chrimson
Intact
Headless
on
Velocity (mm/s)
n=15
n=10
Time (s)
C Heading
turn left
-90°
0°straight
90°
turn right
D Behavioral Classification (intact fly)
on
trials
jump
walk
stand
groom
kick
Time (s)
E Behavior probability and latency (intact fly)
walk
jump
Probability (%)
mean
Latency (s)
Time (s)
F Behavioral Classification (headless fly)
on
trials
jump
walk
stand
groom
kick
Time (s)
G Behavior probability and latency (headless fly)
abdomen grooming
kicking
Grooming (%)
Kicking (%)
p ≤ 0.01**
control n=3
md n=7

Figure 2.2. Md neuron activation drives escape behaviors that are absent in headless flies. (A) Flies were mounted on an air-supported spherical treadmill while seven cameras recorded fly behavior and treadmill movement. (B) Average velocity traces (±SEM) are shown for intact flies expressing CsChrimson in md(B) neurons (md(B)>CsChrimson) compared with controls (52A01-GAL4DBD>CsChrimson). Optogenetic activation increased walking velocity. (C) Heading distributions are plotted for control flies (gray) and md neuron–activated flies (blue) during stimulation. (D–E) Behavioral classifications of intact flies revealed transient increases in walking and jumping following stimulation. Panel D shows trial-wise classifications across flies, while panel E plots the mean probability of each behavior over time across flies. (F–G) Behavioral analysis was also performed in headless flies. Ethograms from individual flies across multiple trials (F) illustrate behaviors including walking, jumping, standing, grooming, and kicking. Quantitative probability analyses (G) Trial-wise classifications and mean behavior probabilities between groups compare controls (black) with kicking (purple) and abdomen grooming (pink). Statistical comparisons were made using independent t-tests. All behavioral classifications were derived from automated tracking algorithms. Detailed experimental procedures are provided in the Methods.

Abdominal md neurons are sensitive to noxious heat

Knowing that optogenetic activation of md neurons produces escape and sustained avoidance, we sought to understand the stimuli that they sense. The axons of md neurons project into the

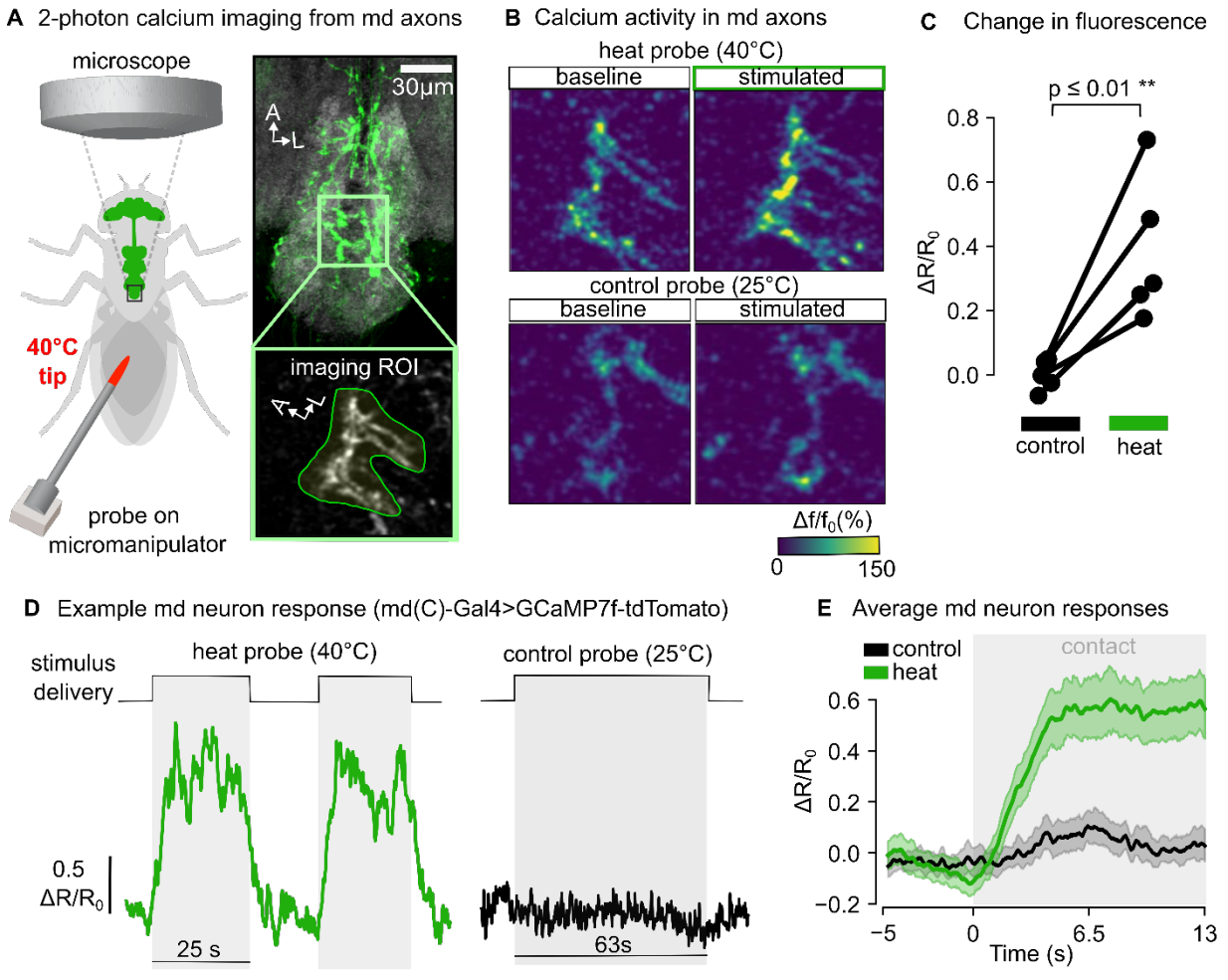

Figure 2.3. Calcium imaging from md axons reveals sensitivity to high temperature. (A) Two-photon calcium imaging from md axons in the abdominal ganglion. The schematic illustrates the imaging configuration with a temperature probe for thermal stimulation (left). A confocal image displays md neurons expressing GFP (green; md(C)-GAL4>UAS-GFP) within the ventral nerve cord, with the region of interest (ROI) outlined (scale bar = 30 μm). The ROI image shows GCaMP7f expression at md axon terminals (md(C)-GAL4>UAS-GCaMP7f-tdTomato). (B) Calcium responses of md neurons are compared under different temperature conditions: a 25°C probe (room temperature control) and a 40°C probe (heat stimulation). (C) Response magnitudes are quantified across flies, with ratio values plotted for each fly (n=5). All flies exhibited substantial increases in calcium responses during heat stimulation, with values ranging from ~0.2 to 0.8. (D) Representative GCaMP7f traces from md axons in a single fly are shown. The left trace captures calcium transients during 40°C probe stimulation over a 25-second recording period, while the right trace shows minimal activity ($\Delta R/R_0$ = 0.5 scale) during room-temperature probe application over 63 seconds. Stimulus timing is indicated by gray bars above each trace. (E) Average calcium responses over time are plotted, with the green trace representing mean ± SEM responses to the 40°C probe and black to the 25°C probe. Calcium levels remained elevated (~0.6 $\Delta R/R_0$) throughout the stimulation period (gray shading).

abdominal ganglion, the most posterior compartment of the fly ventral nerve cord (VNC). To characterize the sensory response properties of md neurons, we recorded their axonal calcium activity in the abdominal ganglion with *in vivo* two-photon imaging **(Figure 2.3A).** We expressed GCaMP7f and tdTomato in md neurons and quantified their activity as the ratio of green to red fluorescence while applying thermal and mechanical stimuli that had previously been shown to evoke class IV da neuron activity in larval *Drosophila*[50–53]. Gentle deflection of the abdomen with a 40°C metal probe elicited robust calcium responses in md axons (**Figure 2.3B)**. Elevated calcium levels were sustained throughout the duration of the stimulus **(Figure 2.3B–D).** We also observed increased calcium activity when we topically administered AITC, an agonist of Trp channels including *TrpA1*[54], to the abdominal surface **(Figure S2.3)**. This result suggests that *TrpA1* contributes to the detection of noxious thermal stimuli, as has been shown in *Drosophila* larvae[55]. Notably, we did not observe consistent mechanosensory responses when a room temperature (25°C) probe touched the abdomen (**Figure 2.3B)**. Overall, our results show that abdominal md neurons in adult *Drosophila* detect noxious heat **(Figure 2.3B–D)**, responding at the same high temperature (40°C) previously used in fly larvae[22,56].

The axons of nociceptive md neurons form a somatotopic map in the abdominal ganglion.

We next analyzed the spatial organization of md neuron axons in the abdominal ganglion using genetic labeling, light microscopy, and connectomics **(Figure 2.4A)**. Light microscopy images of GAL4 lines labeling md axons revealed 30 md neurons with extensive dendritic arbors distributed across the fly abdomen (**Figure S2.4**). We counted 16 ventral and 14 dorsal md neurons per fly, each spanning one tergite or sternite on either side. Md axons enter the abdominal ganglion via four different nerves and then project ventrally within the neuropil. For example, nerve 2 carries four axons (two per side) from segment 1, nerve 3 carries four axons, and the nerve trunk carries six from segments 6/7, with nerve 4 carrying the remaining 15.

We used morphological criteria to identify md axons in existing electron microscopy volumes of the female (FANC)[15,18] and male (MANC)[19] adult nerve cords (**Figure 2.4B**). In FANC, we manually proofread each md axon. The axons in MANC were already proofread after automated segmentation. These connectome reconstructions revealed that individual md axons arborize in multiple segments of the abdominal ganglion, with unique projections into each segment. Md axon projections are spatially segregated from abdominal mechanosensory bristle and gustatory axons, as previously described[57] **(Figure S2.4A–F).** Md axons in FANC and MANC have qualitatively similar terminal structure, synapse distribution, branching architecture, and input-output connectivity, suggesting that md neurons are similar in male and female flies, despite known sexual dimorphisms in other aspects of fly behavior and neural circuit organization[58].

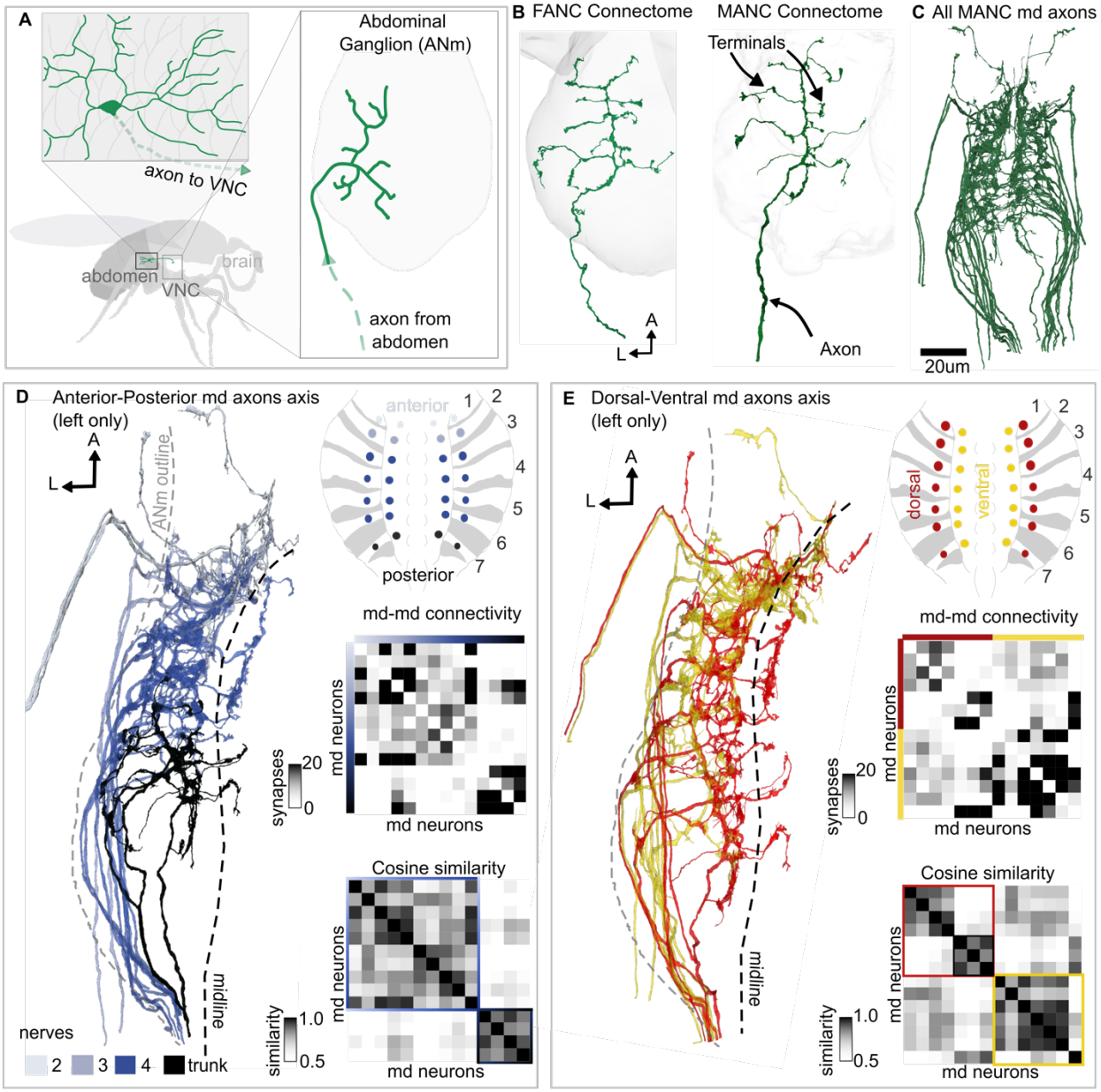

Figure 2.4. Axons of abdominal md neurons form somatotopically organized and stereotyped terminal arbors in the abdominal ganglion. (A) A schematic of the abdominal ganglion shows axonal projections from peripheral md neurons. Individual axons (green) arborize in stereotyped patterns within the neuropil (grey outline). (B) An anatomical overview depicts md neuron organization within the Female Adult Nerve Cord (FANC) and Male Adult Nerve Cord (MANC) connectomes, revealing consistent innervation patterns across datasets. (C) All md neurons reconstructed in MANC are shown (n=30). (D–E) Three-dimensional reconstructions of axon terminals demonstrate spatial organization along the dorsal–ventral and anterior–posterior axes. Axons display biased output distributions depending on peripheral soma position and exhibit like-to-like connectivity patterns when terminals are in close proximity. Pairwise cosine similarity analyses compare axonal arbor morphology (left) and synaptic connectivity (right) for md neurons grouped by dorsal (n=8) versus ventral (n=7) soma location in panel E, and by anterior–posterior position in panel D. Schematics illustrate the spatial organization of md neurons within abdominal segments 1–7. Color coding indicates cell body origins and nerve pathways, with trunk nerves 3 and 4 highlighted. Neurons with similar spatial locations on the abdomen exhibit more similar connectivity patterns.

To determine the relationship between each md neuron's peripheral location on the abdomen and their central projection into the abdominal ganglion, we used sparse genetic labeling with SPARC (Sparse Predictive Activity through Recombinase Competition)[59]. Labeling single neurons revealed a somatotopic organization of md axons within the abdominal ganglion (**Figure S2.4G–M**), which we then used to infer the peripheral origin of each md axon in the connectomes (**Figure 2.4D–E**). We found that md neurons from anterior abdominal segments terminate in the most anterior region of the abdominal ganglion, while md neurons on the posterior abdomen arborize posteriorly (**Figure 2.4D**). We also observed somatotopy along the dorsal-ventral axis. The axons of md neurons from the dorsal abdomen cross the midline of the abdominal ganglion before terminating, while ventrally originating neurons remain ipsilateral to the midline **(Figure 2.4E).** This crossing pattern is similar to the pattern of somatotopy described in the larval nervous system[60].

We also observed somatotopic structure in the downstream synaptic connectivity of md neurons. Dorsal md neurons are more likely to synapse on the axons of other dorsal neurons, and vice versa for ventral neurons. Dorsal md neurons exhibit more similar postsynaptic connectivity to other dorsal or ventral neurons, as measured by their cosine similarity **(Figure 2.4E, inset)**. We also observed clusters of downstream connectivity among anterior and posterior axons **(Figure 2.4D, inset)**. These results reveal that md axons are organized somatotopically in the fly abdominal ganglion, which may facilitate integration of correlated sensory signals by downstream circuits.

Nociceptive abdominal md axons are most strongly connected to ascending neurons

We next used the connectome to analyze the synaptic inputs and outputs of md neurons. We first analyzed presynaptic input to md axons, i.e., feedback from VNC neurons. All neurons in the

MANC connectome have a predicted neurotransmitter, based on a validated machine learning classifier[61]. Unlike other classes of sensory neurons that receive presynaptic inhibition (e.g., leg proprioceptors[62]), we found that md neurons primarily receive cholinergic input, which is typically excitatory in the fly CNS **(Figure S2.5A–E).** Excitatory feedback to md axons could contribute to sensitization, a hallmark of nociceptors in vertebrates[63,64] and larval *Drosophila*[65,66].

We next analyzed the postsynaptic VNC targets of all 30 md axons, focusing on neurons receiving ≥4 synapses from abdominal md neurons, a threshold previously used to filter for functionally relevant connections in MANC[67–69]. We identified 374 distinct postsynaptic neurons that we categorized into six morphological classes: ascending neurons, descending neurons, local interneurons, motor/efferent neurons, and other sensory neurons **(Figure 2.5A).** We found that md neurons form particularly strong connections onto ascending neurons **(Figure 2.5B–D).** Nearly half (49%) of md axon synapses are onto ascending neurons, whereas other somatosensory classes, tactile bristles and leg proprioceptors, have less than 30% of their synapses onto ascending neurons, with the majority onto local neurons **(Figure 2.5C).** Approximately 73% of the ascending neurons postsynaptic to md axons are cholinergic **(Figure 2.5E**), compared to 76% for bristles and 54% for proprioceptors. Overall, this connectivity suggests that sensory information from md axons is rapidly routed to the brain, compared to the tactile and proprioceptive systems, which predominantly feed into local VNC circuits.

A small number of ascending interneurons (~20) receive a disproportionately high number of synapses from md axons. These ascending neurons also receive most of their sensory input from md neurons vs. other sensory neuron classes **(Figure 2.5F)**, suggesting that these ascending neurons may be specialized for conveying nociceptive signals from abdominal md neurons to the brain.

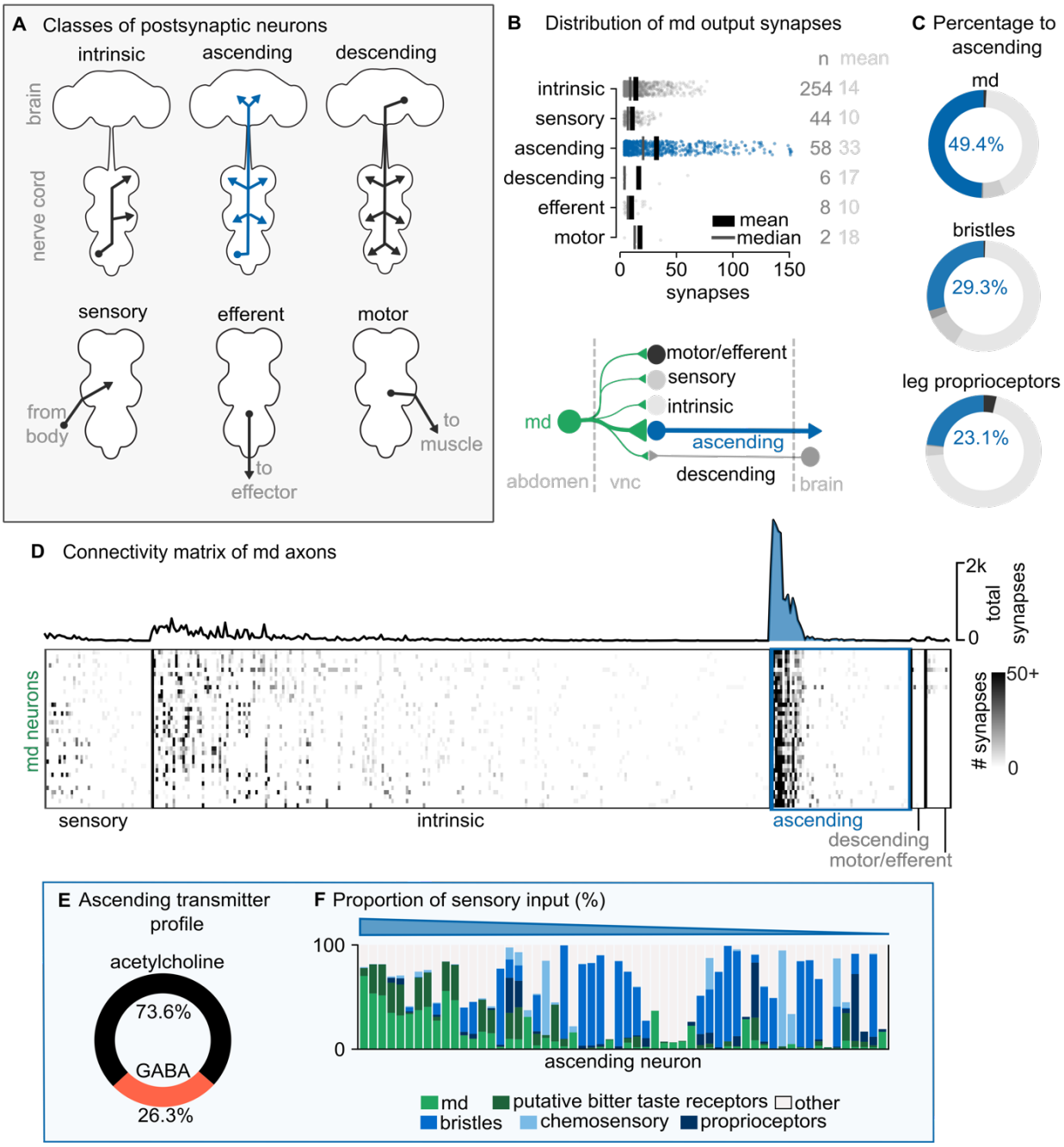

Figure 2.5. Ascending neurons are the main postsynaptic target of abdominal md sensory axons. (A) Classes of VNC neurons receiving input from md axons. (B) Md connectivity patterns are illustrated at the bottom, highlighting synaptic relationships with intrinsic, sensory, efferent, motor, descending, and ascending neuron types. The top panel quantifies synaptic connectivity by target class, with a strip plot displaying mean synapse counts and individual data points onto postsynaptic VNC neurons. (C) The percentage of synapses to ascending neurons is summarized in a pie chart, with comparisons to mechanosensory bristles and leg proprioceptors. (D) A connectivity matrix reveals strong connections to a small number of ascending neurons. Synapse counts between md neurons and their targets are represented as a heat map, with color intensity corresponding to connection strength (0 to >150 synapses). (E) The predicted neurotransmitter identities of ascending neurons are shown as a pie chart, grouped by transmitter percentage. (F) Sensory input proportions for each postsynaptic ascending neuron.

Different components of escape and sustained avoidance are mediated by distinct ascending pathways

We sought to identify genetic driver lines that label the primary ascending neurons downstream of md axons. We first searched in the MANC connectome for ascending neurons that received >20% of their input from md neurons. This resulted in 22 individual ascending neurons. We used NeuronBridge[70] to identify three split-GAL4 driver lines that labeled different anatomical subtypes of ascending neurons that fulfilled these criteria **(Figure 2.6A).** The ascending neurons labeled by these driver lines all arborize throughout the abdominal, hindleg, and wing neuropils. Within the brain, all the ascending axons arborize within the gnathal ganglion (GNG), a premotor center. However, individual ascending neurons within each driver line project to distinct brain areas, suggesting distinct functions.

We used optogenetic activation of each split-GAL4 line to test whether they recapitulate the behaviors we observed when activating the md sensory neurons in freely walking flies. Activating all three driver lines produced increases in walking velocity **(Figure 2.6C).** The line with neurons projecting to the anterior ventrolateral protocerebrum (AVLP; SS51024) was the only one among the three that displayed elevated jumping behavior **(Figure 2.6D–E).** We also noticed that this line increased jumping outside of the optogenetic stimulus period. The third driver line (SS01159) contained ascending axons that project to the AVLP, saddle (SAD), and lateral horn (LH), a higher-order olfactory region **(Figure 2.6A).** This driver line labeled a broader set of neurons than the other two but was the only one among the three that produced sustained place avoidance **(Figure 2.6B, F).** These results are consistent with a recent study showing that activation of this same driver line produced aversive learning in a similar spatial avoidance paradigm[45]. Overall, our

results suggest that ascending pathways downstream of md axons drive distinct, though partially overlapping, aspects of rapid escape and sustained avoidance behavior.

Finally, we analyzed the downstream connectivity of the different classes of ascending neurons using existing brain and nerve cord connectomes (MANC[19], FAFB[67,68], and BANC[16]). Matching cells labeled by each driver line to ascending neurons in the connectome revealed that they connect to distinct downstream circuits **(Figure S2.6).** SS51024 neurons are strongly connected to the giant

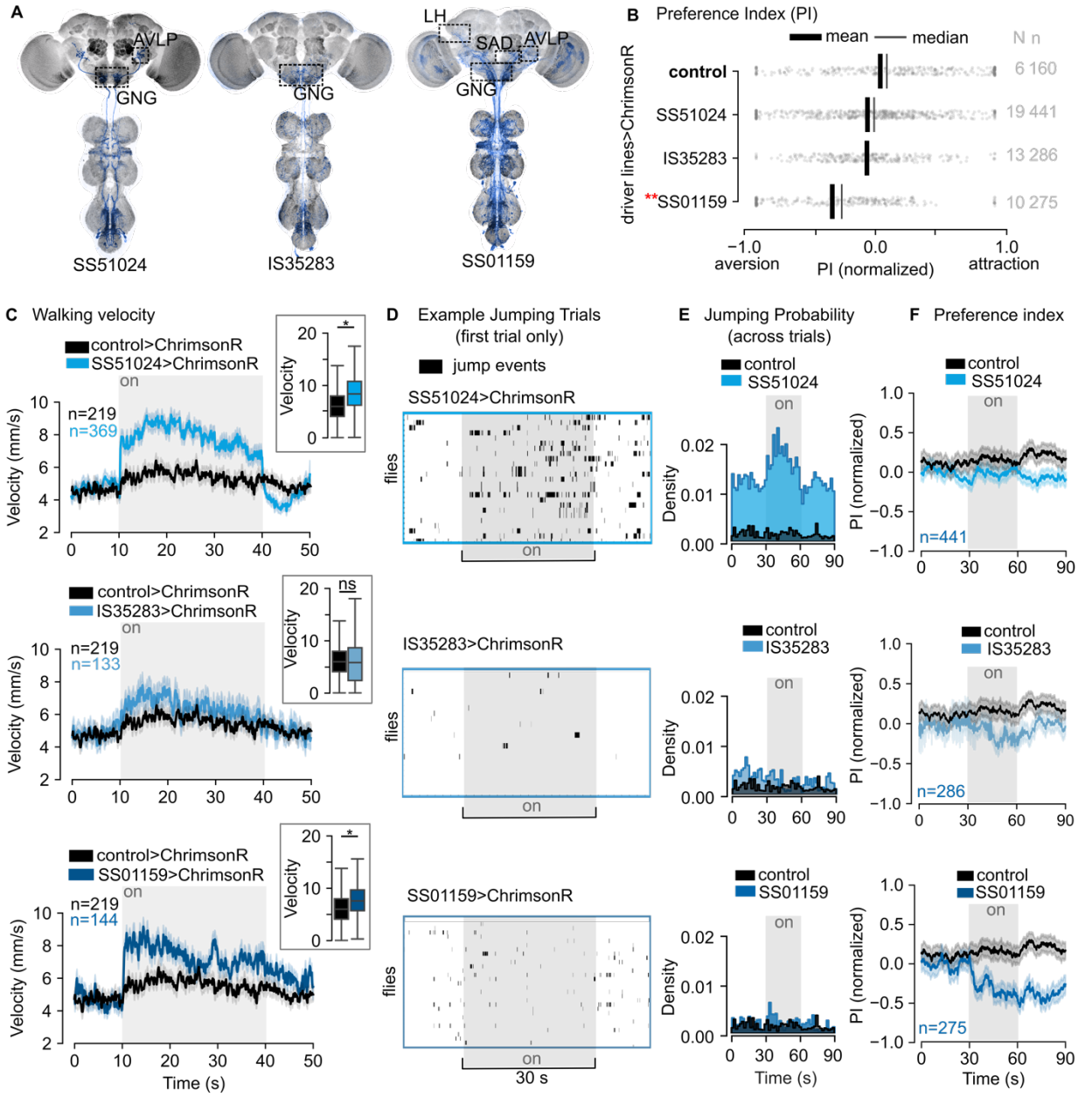

Figure 2.6. Optogenetic activation of ascending neurons produces escape and sustained avoidance. (A) Schematic shows the brain regions targeted by three genetic lines: SS51024, which projects to the AVLP and GNG regions; IS35283, which projects to the GNG; and SS01159, which projects to the LH, SAD, AVLP, and GNG regions. GFP expression is pseudocolored in blue. (B) The preference index is shown for all second-order driver lines, with a red star denoting statistical significance. Control flies carried the genotype 40B01-GAL4AD>CsChrimson. (C) Mean walking velocity traces are shown over time for control flies (black) and optogenetically stimulated flies (blue) over 50-seconds. The light stimulation period is indicated by grey bars. Sample sizes of flies were SS51024: n=369, IS35283: n=133, and SS01159: n=144 flies. Shaded areas represent the standard error of the mean. Insets show the change in velocity for the first 10 seconds during optogenetic activation between controls in black, and experimental genetic lines in blues. (D) Representative raster plots show jumping events (black bars) during the first trial for individual flies across the stimulation period. Each row represents one fly, with jumping events plotted against time. The light stimulation period (30 seconds) is indicated by grey shading. (E) Population-level histograms show jumping probabilities comparing control (black) and stimulated (blue) conditions across 90-second trial periods. Light stimulation occurred during the middle 30 seconds, indicated by grey shading. (F) Preference indices quantify behavioral responses over time, calculated as the difference between stimulated and control conditions. Statistical comparison to controls during stimulation period quantified in B. Sample sizes were SS51024: n=441 flies, IS35283: n=286, and SS01159: n=275. Values above zero indicate increased preference relative to controls, while values below zero indicate decreased preference. All traces show mean ± SEM. AVLP, anterior ventrolateral protocerebrum; GNG, gnathal ganglion; LH, lateral horn; SAD, saddle

fibers and other premotor networks that produce rapid takeoff responses[71,72]. IS35283 neurons primarily target walking control circuits, including connections to descending neurons that modulate locomotion speed and direction[48,73–75]. SS01159 neurons connect to brain regions associated with learned avoidance, including pathways to dopaminergic clusters that mediate aversive memory formation[76,77]. These anatomical analyses suggest potential circuits through which ascending neurons could transform nociceptive signals from abdominal md neurons into distinct escape and avoidance behaviors.

Discussion

Comparison of nociception to other somatosensory modalities

Several features distinguish md neurons from other somatosensory neurons in the adult fly. First, unlike proprioceptors and touch receptors, we found that md neurons drove both rapid escape and sustained place avoidance when optogenetically stimulated **(Figures 2.1, 2.2)**. Activating other somatosensory neurons in our optogenetic screen produced only transient effects, such as grooming or pausing, without sustained place avoidance. An exception was the bristle driver line b(C), which produced a significantly negative preference index, though not as low as any of the md driver lines. The b(C) line labels mechanosensory bristles on the eye, and closer inspection of the video revealed that optogenetic stimulation of this line produced sustained head grooming, similar to behavior seen in a previous study using this driver line[78].

Second, abdominal md neurons exhibit distinct connectivity patterns compared to other somatosensory neurons. While mechanosensory bristles and proprioceptors primarily connect to local motor circuits in the VNC, we found that md neurons dedicate a large fraction of their synaptic output to ascending neurons that project to the brain **(Figure 2.5)**. This connectivity pattern suggests that nociceptive information requires integration with higher-order circuits for threat assessment and long-term behavioral modification.

We also found that abdominal md neurons have distinct properties from other thermosensory neurons in adult *Drosophila.* Antennal "hot cells" detect warm ambient temperatures (30–35ºC) and drive thermotaxis behaviors, such as navigation toward the fly's preferred temperature[9,22]. In contrast, our results suggest that abdominal md neurons function as nociceptors that detect noxious heat (>35°C) **(Figure 2.3).** Hot cells detect heat using the gustatory receptor GR28B(D)[79], while

past work in the larva suggests that class IV da neurons rely on TRPA1[23]. The difference in temperature sensitivity between md neurons and hot cells is also reflected in their circuit organization: the ascending neurons downstream of md axons do not converge with lateral horn circuits downstream of antennal hot cells[80,81]. Additionally, hot cells guide turning behaviors that enable flies to navigate thermal gradients[9,22], whereas we did not find directional turning in response to unilateral md neuron activation. These differences suggest that the fly nervous system uses distinct thermosensory neurons and downstream circuits to detect and respond to innocuous and noxious temperatures.

The somatotopic organization we observed in abdominal md axon terminals **(Figure 2.4D–E)**—both anterior-posterior and dorsal-ventral organization—is similar to that described in the 3rd instar fly larvae[60]**.** Our cosine similarity analysis revealed that md neurons from similar abdominal regions share similar downstream connectivity, which could support spatially coordinated responses, though we did not observe directionality in escape responses following unilateral optogenetic stimulation. Analysis of postsynaptic connectivity revealed organizational principles beyond simple somatotopy (**Figure S2.5F**). Most postsynaptic partners receive input from all md neurons along the anterior-posterior axis, with few neurons receiving selective input from md neurons within the same nerve. However, dorsal and ventral-originating md neurons connect to different postsynaptic cells, with target neurons distributed along the dorsal-ventral axis. Neurons postsynaptic to dorsal md neurons arborize more medially in the VNC than those receiving ventral md input. This asymmetric organization suggests that VNC circuits may preferentially integrate threat information along the body's anterior-posterior axis while maintaining separate processing channels for dorsal vs. ventral stimuli. This organization could reflect distinct escape strategies in response to nociceptive stimuli from above versus below the fly.

Comparison of nociceptors across metamorphosis

Insects that undergo complete metamorphosis develop two distinct body forms during their lifetime: a larva specialized for feeding and growth, and an adult built for reproduction and dispersal. This transformation involves dramatic changes to the nervous system, which is extensively reorganized through the differentiation of adult-specific neurons, the programmed death of certain larval neurons, and the structural remodeling of others[82,83]. Multidendritic sensory neurons, including the abdominal md neurons, are among a small minority of identified neurons that are known to survive through metamorphosis. Other da neuron types also survive metamorphosis but are not labeled by the *ppk*-GAL4 lines we used in this study[37]. Multidendritic neurons have been extensively studied in the larvae of *Drosophila*[84] and the moth, *Manduca sexta* [85,86], but their physiology, downstream connectivity, and behavioral function had not been previously explored in adult flies.

We found that abdominal md neurons in the adult fly respond robustly to noxious heat (40°C) and a *TrpA1* agonist, as has been previously observed for the same cells in the larva. Our data suggest that detection of thermal nociceptive stimuli is conserved in these cells across metamorphosis **(Figure 2.3, Figure S2.3).** However, unlike in the larva[26,52,87], we did not observe md neuron calcium signals in response to mechanical deflection of the abdomen. We also did not observe consistent changes in md axon activity when we stretched, squashed, or punctured the abdomen with a glass pipette (*data not shown*)—stimuli that have been shown to evoke calcium activity in larval class IV da neurons. Larval class IV da neurons are sensitive to shear forces[88] and other mechanical stimuli that deform the larval body wall. Recent work has demonstrated that larval class IV da neurons can be activated by diffusible signals released from damaged tissue[89], which may produce responses on longer timescales than we tested in our calcium imaging experiments.

While we cannot rule out sensitivity to other mechanical stimuli, we did not observe responses to indentation or puncture of the abdomen in the adult fly. Their sensitivity to AITC suggests that adult md neurons retain *TrpA1* expression, and while *TrpA1* has been implicated in mechanosensation in other *Drosophila* sensory neurons[23], our results suggest that md neurons in the adult fly primarily function as thermal nociceptors. More work is needed to understand the natural contexts within which abdominal md neurons are active and how they contribute to escape and sustained avoidance.

Shifts in sensory tuning from larva to adult may reflect adaptation to different ecological challenges. Adult flies do not burrow into the substrate and are capable of rapidly escaping into the air to evade predators. Ground-dwelling larvae, on the other hand, encounter distinct threats during burrowing and feeding, including parasitism[90,91]. The behavioral responses we observed in adult flies—jumping, running, and place avoidance—are more elaborate than the stereotyped rolling responses characteristic of larvae. This expanded repertoire may reflect the adult fly's integration of nociceptive input with descending motor programs. We found that headless flies exhibited reflexive scratching and kicking, behaviors that may be suppressed by descending signals that drive escape.

In larvae, class IV da neurons connect to second-order interneurons that coordinate nociceptive responses. The most extensively studied are the Basin neurons, ascending interneurons that receive direct synaptic input from multiple md neuron types across body segments. Basin neurons are both necessary and sufficient for larval rolling escape responses[92–94]. Other pathways downstream of larval class IV da neurons include local circuits that coordinate segmental motor responses and descending neurons that modulate the magnitude of escape behaviors[30,95–97]. Unlike the organization we found in the adult **(Figure 2.5)**, larval class IV da neurons show less connectivity

bias toward ascending pathways, with substantial connectivity to local motor circuits that drive the stereotyped rolling response. It is not clear whether Basin neurons and other second-order nociceptive interneurons survive metamorphosis[32,98]. Reorganization of second-order pathways may contribute to the expanded behavioral repertoire we observed in adults, as the larval circuits were optimized for the rolling escape response rather than the jumping, running, and avoidance behaviors seen in adult flies.

Ascending Nociceptive Pathways

We found multiple ascending pathways positioned to transmit abdominal nociceptive signals to the brain **(Figure 2.6A–F).** Optogenetic activation of neurons labeled by SS51024, which connect to the giant fiber and other escape circuits, produced immediate reflexive escape without producing place avoidance (**Figure S2.6A,G**). In contrast, SS01159 neurons drove locomotion and sustained place avoidance; ascending cells within this line connect to the lateral horn[99–101], dopaminergic PAM neurons, and MBONs, supporting their role in forming associative memories of dangerous locations (**Figure S2.6C,S6I**). IS35283 neurons produced an intermediate phenotype: smooth locomotor changes without strong jumping or avoidance (**Figure S2.6B,S2.6H**). While these ascending neuron classes recapitulate key features of md neuron activation, we note that our experiments relied solely on optogenetic activation. Future work could use optogenetic silencing to test the necessity of these pathways for nociceptive behaviors, or recordings of ascending neuron activity during natural stimulation.

The sustained behavioral effects we observed following md neuron activation, including place avoidance lasting at least 30 seconds, suggest that nociceptor activation may trigger longer-lasting changes in internal state beyond immediate motor responses. These state changes could involve

neuromodulatory[102–105] systems that alter the fly's behavioral priorities, shifting from exploration to heightened vigilance. While our analyses focused on ascending excitatory pathways, the VNC circuits also contain inhibitory and neuromodulatory neurons that could contribute to long-lasting changes in internal state. The md sensory neurons may also release neuromodulators, as we observed high densities of dense-core vesicles in their synaptic terminals (**Figure S2.6E**). Neurotransmitter prediction algorithms also suggest that some of the ascending neurons labeled by IS35283 co-release serotonin along with acetylcholine[96,106]. These observations suggest that nociceptors and downstream neurons rely on neuromodulation to sustain altered behavioral states beyond the duration of the initial sensory stimulus.

Our connectomic analyses revealed that md neurons predominantly receive excitatory cholinergic input from other sensory neurons **(Figure S2.5A–C)**, including input from other sensory neurons (leg and abdominal bristles that sense innocuous touch, taste bristles, and other unknown sensory types**; Figure S2.5E)**. This lateral excitatory connectivity within the nociceptive system may amplify sensitivity[107–109] when noxious stimuli activate multiple classes of exteroceptive somatosensory neurons. Direct input from tactile bristle neurons to md neurons suggests that touch could enhance nociceptive responses under certain conditions, as occurs during tactile allodynia in vertebrates (**Figure S2.5E**). Further work is needed to test the role of tactile input and excitatory feedback to md neurons in the adult fly, particularly in response to combined thermal and tactile stimuli or following tissue injury.

Summary

Our findings reveal that adult *Drosophila* satisfy several of the criteria[10,110] commonly used to define the experience of pain: dedicated nociceptors, ascending pathways connecting peripheral sensors to integrative brain centers, and a behavioral capacity for long-term avoidance of nociceptive stimuli. The ability to trace genetically-defined neural circuits at synaptic resolution makes the fly a powerful system for dissecting the neural circuits and computations that underlie nociceptive behaviors. The identification of ascending nociceptive pathways opens the door to understanding how these signals are used by brain circuits to guide navigation, learning, and action selection. Understanding how evolution has sculpted diverse nervous systems to balance protecting the body and behavioral flexibility may inform approaches to understanding and treating pain-related disorders.

Acknowledgements and Support

We thank members of the Tuthill Lab for technical assistance and feedback on the manuscript. We thank the following people for providing feedback on the manuscript, reagents, equipment, and scientific guidance: Jay Parrish, Sama Ahmed, Wes Grueber, Ishmail Abdus-Saboor, Ellen Lesser, Gabrielle Sterne, Stefanie Hampel, Andrew Seeds, Kazuo Emoto, William Joiner, David Shepherd, and James Truman.

J.M.J. was supported by an HHMI Gilliam Fellowship and NIH T32 Predoctoral Training Program in the Neurosciences. Other support was provided by National Institutes of Health grants R01NS102333, R01NS128785, and U19NS104655, a Searle Scholar Award, a Klingenstein-Simons Fellowship, a Pew Biomedical Scholar Award, a McKnight Scholar Award, a Sloan Research Fellowship, the New York Stem Cell Foundation, and a UW Innovation Award to J.C.T., J.C.T is a New York Stem Cell Foundation – Robertson Investigator.

Author Contributions

J.M.J. and J.C.T. conceived the study and wrote the manuscript. J.M.J. analyzed the connectivity, calcium imaging, and optogenetic datasets. A.S. conducted SPARC experiments and created the gorgeous confocal images of the fly abdomen and VNCs. A.M. collected and processed calcium imaging data from md axons. G.M.C. and S.W.B. collected optogenetic activation data in tethered flies. A.P.C. proofread the md axons and connected neurons in FANC and helped annotate neurons in the BANC.

Lead contact

Further information and requests for resources and reagents should be directed to and will be fulfilled by the lead contact, John C. Tuthill (tuthill@uw.edu).

Data and Code Availability

Data is available on Dryad (10.5061/dryad.fbg79cp8k). Code for analyzing and visualizing md neuron connectivity in the EM dataset, calcium activity of md neurons, preference and velocity behavior during optogenetic experiments, and walking kinematics is located on GitHub (https://github.com/jesmjones/nociceptive_pathways_paper).

Methods

Key Resources Table

REAGENT or RESOURCE	SOURCE	IDENTIFIER
***Drosophila* Parental Stocks**		
w[1118]; P{y[+t7.7] w[+mC]=R40B01-p65.AD}JK22C	Bloomington	RRID:BDSC_89613
w[1118]; P{y[+t7.7] w[+mC]=R52A01-GAL4.DBD}attP2	Bloomington	RRID:BDSC_69141
w[*];Gr28b.d-GAL4	Gallio Lab (Northwestern University)	N/A
w[1118];+;P{y[+t7.7] w[+mC]=GMR52A06-GAL4}attP2	Bloomington	RRID:BDSC_38810
w[1118]; +;P{y[+t7.7] w[+mC]=GMR38B08-GAL4}attP2	Bloomington	RRID:BDSC_49541
W; VT17251-LexA (3012796);+	Hampel et. al[78]	N/A
w[1118];38g07AD / CyO;43c10DBD / TM6B	Phelps, Hildebrand, Graham, et al.[18]	N/A
w[1118]; P{y[+t7.7] w[+mC]= VT038873-p65ADZ}attP40 / +; P{y[+t7.7] w[+mC]=R32H08-GAL4.DBD}attP2 / +	Mamiya et al[111]	N/A
w[1118];P{y[+t7.7] w[+mC]= VT018774-p65ADZ}attP40 / +; P{y[+t7.7] w[+mC]=VT040547-GAL4.DBD}attP2 / +	Mamiya et al[111]	N/A
w[1118];P{y[+t7.7] w[+mC]=R55C05-p65.AD}attP40 / +; P{y[+t7.7] w[+mC]=VT017745-GAL4.DBD}attP2	Mamiya et al[111]	N/A
w[1118]; P{y[+t7.7] w[+mC]= 50C12-p65ADZp}JK22C / +; P{y[+t7.7] w[+mC]=R84H05-GAL4.DBD}attP2	Mamiya et al[111]	N/A
w[1118]; P{y[+t7.7] w[+mC]=R92D04-p65.AD}attP40 / +; P{y[+t7.7] w[+mC]=VT043140-GAL4.DBD}attP2 / +	Mamiya et al[111]	N/A
22E04-AD;10H03-DBD	Gorko et al[112]	N/A
w[1118];P{y[+t7.7] w[+mC]=GMR27H06-LexA}JK22C	Bloomington	RRID:BDSC_94664

w[*];P{ppk-GAL4.G}2;+	Gift from William Joiner, UCSD (via Jan lab, Wes Grueber)	N/A
w[*];+;{24c10-AD}attP2, {ppk-DBD}VK00027 /TM3 Sb	Seidner et. al.[113]	N/A
w[*];VT020126-p65ADZp; VT000357-ZpG.DBD / TM6B Tb	Sterne et al[114]	N/A
w[*];VT004985-p65ADZp in attP40; VT034810-ZpGDBD in attP2	Janelia Research Campus	N/A
w; R41C05-p65ADZp in attP40; VT026019-ZpGdbd in attP2	Shuai et al[45]	N/A
w[1118];+; P{y[+t7.7] w[+mC]=13XLexAop2-IVS-CsChrimson.mVenus}attP2	Bloomington	RRID:BDSC_55139
+ DL;+ DL; 10X UAS ChrimsonR mCherry (attp2)/TM3 Sb	UAS-ChrimsonR was gifted from Janelia (outcrossing was done by Anne Sustar, University of Washington to Dickinson Lab stock W-03)	N/A
w[1118];+; P{y[+t7.7] w[+mC]=20XUAS-IVS-CsChrimson.mVenus}attP2	Bloomington	RRID:BDSC_55136
y[1] w[*] P{y[+t7.7] w[+mC]=13XLexAop2-mCD8::GFP}su(Hw)attP8	Bloomington	RRID:BDSC_32204
w[*]; P{pJFRC7-020XUAS-IVS-mCD8::GFP}attP2	Gift from Gerry Rubin	N/A
P{UAS-phiC31}attP18; Star/CyO; Pri/TM6B	Gift from Rachel Wilson	N/A
TI{20XUAS-SPARC2-S-mCD8::GFP}CR-P40	Bloomington	RRID:BDSC_84148
Chemicals, peptides, and recombinant proteins		
All-trans-retinal	Santa Cruz Biotechnology	Cat#SC-221196
AITC (allyl isothiocyanate)	Sigma-Aldrich	Cat#377120; CAS: 57-06-7
Paraformaldehyde	Fisher Scientific	Cat#15710-S; CAS: 30525-89-4
Normal goat serum	Fischer Scientific	Cat#50197Z
Triton X-100	FISHER SCIENTIFIC	Cat# AAA16046AE
Vectashield	Vector Laboratories	Cat#H-1000
DMSO	Fischer Scientific	Cat#BP231-100
Antibodies		
Chicken anti-GFP	Invitrogen	Cat# PA5-143569
Mouse anti-brp (nc82)	Developmental Studies Hybridoma Bank	RRID: AB_2314866

Goat anti-chicken Alexa 488	Invitrogen	Cat # A-11039
Goat anti-mouse Alexa 633	Invitrogen	Cat # A-11001
Software and algorithms		
FlyTracker	Eyjólfsson et al[115]	https://github.com/kristinbranson/FlyTracker
ImageJ	Schneider et al	https://imagej.nih.gov/ij/
DeepLabCut	Mathis et al[116]	https://github.com/DeepLabCut/DeepLabCut
Anipose	Karashchuk et al[117]	https://github.com/lambdaloop/anipose
FicTrac	Moore et al[118]	https://github.com/rjdmoore/fictrac
Neuroglancer	Maitin-Shepard et al[119]	https://github.com/google/neuroglancer
CAVEclient	Dorkenwald et al[120]	https://github.com/seung-lab/CAVEclient
NetworkX	SciPy	https://networkx.org/
scikit-learn	Pedregosa et al[121]	https://www.jmlr.org/papers/v12/pedregosa11a.html
ScanImage 5.2	Vidrio Technologies	https://www.vidrio-technologies.com/scanimag-5/
MATLAB	MathWorks	https://www.mathworks.com/products/matlab.html
Python	Python Software Foundation	https://www.python.org/
SciPy		https://scipy.org/
CMTK (Computational Morphometry Toolkit)	Rohlfing & Maurer	http://nitrc.org/projects/cmtk
Deposited data		
Connectome data (FANC)	FlyEM - Janelia Research Campus	https://flyem.janelia.org/FANC
Connectome data (MANC)	FlyEM - Janelia Research Campus	https://flyem.janelia.org/MANC
Connectome data (BANC)	FlyEM - Janelia Research Campus	https://flyem.janelia.org/BANC
Connectome data (FAFB)	FlyEM - Janelia Research Campus	https://flyem.janelia.org/
Other		
FlyBowl apparatus	This paper; Simons and Dickinson[122]	N/A

Spherical foam ball	This paper	Diameter: 9.08 mm; weight: 0.13 g

Experimental Animals

All *Drosophila melanogaster* used in this study were raised on standard cornmeal molasses food and housed in an incubator kept at 25°C on a 14:10 light dark cycle.

***Drosophila* Genotypes Figure Table:**

Figure Identifier	Full Genotype	Figure(s)
40B01-AD (control)	w[1118]; P{y[+t7.7] w[+mC]=R40B01-p65.AD}JK22C > w[1118];+; P{y[+t7.7] w[+mC]=20XUAS-IV S-CsChrimson.mVenus}attP2	1C–E, 6A–C,E–F
52A01-DBD (control)	w[1118]; P{y[+t7.7] w[+mC]=R52A01-GAL4.DBD}attP2 > + DL;+ DL; 10X UAS ChrimsonR mCherry (attp2)/TM3 Sb	2B–C
hot cell	w[*];HC-GAL4;10X-UAS-ChrimsonR-mCherry (attp2)	1C
b(A)	w[1118];+; P{y[+t7.7] w[+mC]=GMR52A06-GAL4}attP2/10X UAS ChrimsonR mCherry (attp2)	1C
b(B)	w[1118]; +; P{y[+t7.7] w[+mC]=GMR38B08-GAL4}attP2/10X UAS ChrimsonR mCherry (attp2)	1C
b(C)	W; VT017251-LexA (3012796) ; P{y[+t7.7] w[+mC]=13XLexAop2-IVS-CsChrimson.mVenus}attP2	1C
cs(A)	w[1118];38g07AD;43c10DBD/10X UAS ChrimsonR mCherry (attp2)	1C
cho(B) (hook flexion)	W;VT038873-p65ADZ in attP40;32H08-DBD/10X UAS ChrimsonR mCherry (attp2)	1C
cho(F) (hook extension)	W;VT018774-p65ADZ in attP40; VT040547-DBD/10X UAS ChrimsonR mCherry (attp2)	1C
cho(A) (claw extension)	W;55C05 AD;VT017745 DBD/10X UAS ChrimsonR mCherry (attp2)	1C
cho(D) (club)	w[1118]; P{y[+t7.7] w[+mC]= 50C12-p65ADZp}JK22C / +; P{y[+t7.7] w[+mC]=R84H05-GAL4.DBD}attP2/10X UAS ChrimsonR mCherry (attp2)	1C
cho(C) (claw flexion)	W;92D04 AD;VT006391 DBD/10X UAS ChrimsonR mCherry (attp2)	1C
cho(E) (neck chordotonal)	W ;22E04-AD;10H03-DBD/10X UAS ChrimsonR mCherry (attp2)	1C

md(A)	w[1118];P{y[+t7.7] w[+mC]=GMR27H06-LexA}JK22C/P{y[+t7.7] w[+mC]=13XLexAop2-IVS-CsChrimson.mVenus}attP2	1C
md(C)	w[*];P{ppk-GAL4.G}2; P{y[+t7.7] w[+mC]=20XUAS-IV S-CsChrimson.mVenus}attP2	1C–E
md(B)	w[*];+;{24c10-AD}attP2; {ppk-DBD}VK00027/ P{y[+t7.7] w[+mC]=13XLexAop2-IV S-CsChrimson.mVenus}attP2	1C
md(B)>Chrimson	w[*];+;{24c10-AD}attP2; {ppk-DBD}VK00027 ;10X UAS ChrimsonR mCherry (attp2)	2B–G
md(B)>GFP	w[*];+;{24c10-AD}attP2/ P{pJFRC7-02 20XUAS-IVS-mCD8::GFP}attP2; {ppk-DBD}VK00027	S1H
md(C)>GFP	w[*];P{ppk-GAL4.G}2/P{pJFRC7-02 20XUAS-IVS-mCD8::GFP}attP2	3A, S1I
md(C)+ (control)	w[*];P{ppk-GAL4.G}2	S1A–B
md(C)> CsChrimson	w[*];P{ppk-GAL4.G}2; P{y[+t7.7] w[+mC]=20XUAS-IV S-CsChrimson.mVenus}attP2	S1A–E
md(A)>GFP	y[1] w[*] P{y[+t7.7] w[+mC]=13XLexAop2-mCD8::GFP}su(Hw)attP8;P{y[+t7.7] w[+mC]=GMR27H06-LexA}JK22C	S1F
IS35283>Chrimson	w[*];VT020126-p65ADZp; VT000357-ZpG.DBD / 10X UAS ChrimsonR mCherry (attp2)	6A–F
SS51024>Chrimson	w[*];VT004985-p65ADZp in attP40; VT034810-ZpGDBD in attP2 / 10X UAS ChrimsonR mCherry (attp2)	6A–F
SS01159>Chrimson	w; R41C05-p65ADZp in attP40; VT026019-ZpGdbd in attP2 / 10X UAS ChrimsonR mCherry (attp2)	6A–F
SPARC	w[*];+;{24c10-AD}attP2/P{pJFRC7-02 20XUAS-IVS-mCD8::GFP}attP2 ;{ppk-DBD}VK00027	S4C,E
SPARC	P{UAS-phiC31}attP18; Star/{24c10-AD}attP2; Pri/{ppk-DBD}VK00027	S4A–B, S4D–G
SPARC	TI{20XUAS-SPARC2-S-mCD8::GFP}CR-P40; 24c10-AD}attP2; {ppk-DBD}VK00027	S4A–B, S4D–G
md(C)-GAL4>UAS-GCaMP7f-tdTomato	w[*];P{ppk-GAL4.G}2/P{w[+mC] = UAS-tdTom.S}2;PBac{y[+t7.7] w[+mC]=20XUAS-IVS-jGCaMP7f}VK00005	3B–E
md(C)-GAL4>UAS-GCaMP7f-tdTomato	w[*];P{ppk-GAL4.G}2/P{w[+mC] = UAS-tdTom.S}2; PBac{y[+t7.7] w[+mC]=20XUAS-IVS-jGCaMP7f}VK00005	S3

As in past studies[45,123,124], we used individual AD or DBD split-GAL4 lines crossed to various UAS constructs as genetic controls. These split-half lines have the same insertion sites and genetic background as the full split-GAL4 driver lines but do not produce a functional GAL4 or effector

expression without the complementary split-half. We prefer this approach, and have used it extensively in past work, because other commonly used "empty-GAL4" lines exhibit off-target expression in the VNC[125]. We also note that different Chrimson variants (ChrimsonR vs. CsChrimson) were used for different experiments due to genetic constraints (i.e., availability of LexA/GAL4 constructs, chromosomes, insertion sites, etc.). We did not observe any differences in behavior produced by different Chrimson variants.

Statistical Analysis

We performed statistical comparisons between two groups using paired or unpaired two-tailed Student's *t*-tests. We assumed data were normally distributed with similar variances across groups. We defined statistical significance as $p \leq 0.01$, and denoted it by stars in the relevant figure panels. We conducted statistical analyses with Python (SciPy).

Immunohistochemistry and Imaging of VNCs and abdomens

For confocal imaging of mcd8::GFP-labeled neurons in the VNCs, we dissected the VNC from 2-day old female adults in PBS. We fixed the VNC in a 4% paraformaldehyde PBS solution for 20 min and then rinsed the VNC in PBS three times. We put the VNC in blocking solution (5% normal goat serum in PBST) for 20 min, then incubated it with a solution of primary antibodies (chicken anti-GFP antibody, 1:50; anti-Brp mouse for neuropil staining, 1:50) in blocking solution for 24 hours at room temperature. At the end of the first incubation, we washed the VNC with PBS with 0.2% Triton-X (PBST) three times over two hours, then incubated the VNC in a solution of secondary antibody (anti-chicken-Alexa 488, 1:250; anti-mouse-Alexa 633, 1:250) dissolved in blocking solution for 24 hours at room temperature. Finally, we washed the VNC in PBST three times, once in PBS, and then mounted it on a slide with Vectashield (Vector Laboratories). We

acquired z-stacks of each VNC on a confocal microscope (Olympus FV1000). We aligned the morphology of the VNC to a female VNC template in ImageJ with the Computational Morphometry Toolkit plugin (CMTK32;http://nitrc.org/projects/cmtk).

SPARC labeling

To obtain the data in Figure S4, we combined a split-GAL4 driver (24c10-AD; ppk-DBD) with a PhiC31-based SPARC[59] cassette (UAS-SPARC-STOP-GFP) and a PhiC31 recombinase source (UAS-PhiC31) for sparse labeling of neurons. PhiC31 recombination irreversibly removes/inverts the STOP cassette in a stochastic subset of GAL4+ cells, which permits UAS-driven GFP expression only in recombined cells. For each experimental fly, we waited 3-7 days after eclosion, dissected the abdomen and VNC, and kept them as pairs. We fixed and stained the VNCs as described above. Abdomens were fixed and stained and mounted the same way, but before staining, we cut the abdomens along the dorsal midline with dissecting scissors to open the abdomen into a single sheet, removing gut and ovaries, and being careful not to disturb the epithelial area. We acquired z-stacks of abdomens on a Leica DMI6000 widefield microscope (low magnification) and Olympus FV1000 (high magnification).

We scored each fly for (i) GFP expression in *ppk*+ neuron soma and dendritic morphology on the abdomen, and (ii) labeling density per hemisegment. For single-neuron analyses, we included animals with ≤2 GFP+ *ppk* neurons per hemisegment (preferably single-neuron). We excluded animals with dense labeling (>3 cells/hemisegment) from single-cell morphological and functional datasets.

Optogenetics experiments in freely walking flies

For optogenetics experiments in freely walking flies (Figure 1), we housed adult flies on cornmeal-molasses food with dissolved all-trans-retinal (35 mM in 95% EtOH, Santa Cruz Biotechnology) and in the dark for at least 24 hr before experiments. We tested groups of 2-5 day old flies, separated by sex, in a 10 cm circular arena fitted with a glass top[122]. The arena was illuminated by infrared LEDs. For optogenetic activation, a red LED (625 nm-peak wavelength; ThorLabs) illuminated the arena from the top. Whole arena illumination experiments **(Figure 2.6C–E, Figure S2.1A–B)** had an LED intensity of 16.9 mW/mm^2 in the center of the arena. Due to the placement of the LED, the quadrant arena experiments **(Figure 2.1**, **Figure 2.6B, 2.6F)** had a left LED intensity of 6.5-6.7mW/mm^2, and a right LED intensity of 7.4-9.3mW/mm^2. Boundary points, or edges of quadrants, had illuminations of 1.0mW/mm^2 (left LED zone) and 1.4mW/mm^2 (right LED zone). Off arena zones with no LED had an illumination of <0.1mW/mm^2 during optogenetic activation. Fly behavior was recorded with a top-down view camera at 33 Hz (Basler acA1300-200 um; Basler AG) mounted with a lens (Computar). Videos were tracked using FlyTracker[115], an automated system for tracking group walking trajectories and custom python script for analysis.

To quantify spatial aversion **(Figure 2.1**, **Figure 2.6B, 2.6F)**, we tracked flies in a circular arena divided into four equal quadrants. We designated two opposing quadrants as the stimulus zones, illuminating them with a red LED, while the remaining two quadrants served as control zones, with the LED off. At each time point, we classified the fly's location as either within a stimulus (LED-on) zone or a control (LED-off) zone. We applied a binary scoring system: flies in the stimulus zones received a score of +1, and flies in the control zones received a score of –1. We then calculated a Preference Index (PI) for each fly. The resulting Preference Index ranges from –1 (complete avoidance of the LED zones) to +1 (complete preference for the LED zones), with 0

indicating no preference. We computed place preference statistics on a per-fly basis, across multiple trials.

In Figure 2.1B, to visualize spatial occupancy, we binned fly positions into a 2D histogram (3000 bins) for the time periods denoted by the trial (30 second bins), smoothed them with a Gaussian filter (sigma=50 pixels), and displayed them as a density heatmap where color intensity represents the frequency of occupancy at each location.

In **Figure S2.1,** we used a vector-based approach to analyze position data and quantify the directional consistency of fly trajectories during optogenetic stimulation trials. We grouped fly trajectory data by individual flies within each experimental trial. For each fly, we analyzed two predefined spatial regions of the arena: the *center* (the center 6cm of arena before the beveled edges) and the *surround* (the 2cm of border around the center that is beveled). We included only trials in which optogenetic stimulation was applied (opto condition of either 'left' or 'right') in the analysis. For each trial and arena region, we examined fly movement in two temporal windows: a **pre-stimulation** period (28–30 seconds) and a **post-stimulation** period (30–32 seconds). Within each period, we further analyzed time-series data to compute both instantaneous movement vectors and an overall **consistency** score. To compute movement vectors, we applied a sliding window across the trajectory data to extract incremental directional vectors between successive time points. We recorded each vector's angle and magnitude to characterize local movement behavior. To quantify **directional consistency**, we used a custom function. This metric captures the degree to which the fly moved in a consistent direction over the two-second window. High consistency values (close to 1.0) reflect straight walking, whereas lower values (typically < 0.5) indicate more variable or turning behavior.

Optogenetics experiments in tethered flies

We housed adult flies for optogenetics experiments in tethered flies on cornmeal-molasses food with dissolved all-trans-retinal (35 mM in 95% EtOH, Santa Cruz Biotechnology) and in the dark for at least 24 hr before experiments. We de-winged 2-5 day old flies and fixed them to a rigid tether (0.1 mm thin tungsten rod) with UV glue (KOA 300). We placed these flies onto a spherical foam ball (weight: 0.13 g; diameter: 9.08mm). We focused a red laser (638 nm; 1.2 kHz pulse rate; 30% duty cycle, Laserland) on the third segment of the abdomen (diameter of ~350 μm). We conducted optogenetic activation experiments on flies in which md(B) flies (24c10AD; ppkDBD split GAL4) expressed ChrimsonR, as well as control flies. Trials were 2 seconds in duration and consisted of 500 milliseconds prestimulus, 1 second with the laser on, and 500 milliseconds post stimulus. During each trial, each fly was recorded with 6 high-speed cameras (300 fps; Basler acA800-510 um; Basler AG) and the movement of the ball was recorded at 30 fps with a separate camera (FMVU-03MTM-CS) and processed using FicTrac[118]. The 3D positions of each leg joint were determined using DeepLabCut[116] and Anipose[117]. Kinematic analyses were performed with custom Python scripts.

Analysis of behavioral data

In Figure 2.2 and Figure S2.2, to classify discrete motor behaviors in tethered flies, we analyzed femur-tibia joint angles recorded from the fly's six legs over time. We used a threshold-based peak detection algorithm to identify significant movements within each joint's trajectory. Specifically, we define peaks as local maxima in the joint angle time series that exceed a minimum height of 50 degrees and do not surpass 190 degrees. We chose these thresholds empirically to capture robust

leg extensions while excluding small fluctuations or hyperextensions. We detected peaks separately for each leg and within each behavioral window.

We divided the behavioral data into consecutive, non-overlapping time windows of 35 frames. We chose this time window empirically to capture only one peak at a time. Within each window, we quantified which legs exhibit peak movement during the entire two-second trial (including the one-second stimulus period). We used this to classify the fly's behavior during that window.

We classified behavioral states according to the specific pattern of detected peaks across legs:

- **Grooming** when only the hind legs (either left and right L3/R3 or L2/R2 midlegs) show rhythmic movement, while the other legs remain still. This pattern is consistent with grooming behaviors directed toward the head or body.
- **Kicking** when only a single leg shows movement during the window, typically indicative of isolated defensive or reflexive motions.
- **Standing** when no leg shows peak movement during each sliding time window.
- If none of the above conditions are met, we labeled the behavior as ambiguous or unclassified.

We applied behavior classification separately to each trial within the dataset. For each trial, we processed time windows sequentially, and we assigned classified behaviors to each frame in the original dataset.

To classify behaviors in the free-walking arena (**Figure 2.1D–E, Figure 2.6C**), we binned fly velocity (100 milliseconds). We classified flies with walking velocities less than 1mm/s as standing. We classified walking velocities between 1 and 30mm/s, which is the average top speed

of flies walking in our arena, as walking. We classified flies that had large changes in x-y position as jumping. We applied these velocity bins to tethered flies to classify jumping and walking (**Figure 2.2D–E).**

We calculated the latency to jump following stimulus onset **(Figure 2.2E)** from annotated behavioral data for all trials. We filtered the data to include only frames occurring at or after the stimulus onset. We then grouped the dataset by trial and individual fly, and for each group, we identified the first occurrence of the "jumping" or "walking" behavior after stimulus onset. We calculated the latency to behavior as the difference between the frame number of the first behavioral event and the stimulus onset time. We assigned no latency value to trials in which no behavior occurred after stimulus onset.

To quantify the probability of behaviors over time (**Figure 2.2D–E),** we analyzed annotated behavioral data across individual flies. For each fly, we computed the number of frames labeled as a behavior and divided it by the total number of observed frames for that fly and time point. First, we counted all frames annotated as a given behavior for each fly and frame number. We then calculated total frame counts, regardless of behavior, for the same identifiers. We merged these counts by fly and frame number, and we computed the probability of the given behavior as the ratio of the number of frames for a given behavior to total time. We assigned a probability of zero for that time point to flies with no behavior annotations at a given frame.

In **Figure 2.2C**, we visualized heading angles of tethered walking flies using polar histograms to assess the distribution of movement orientations. We expressed behavioral trajectory data in degrees, normalized them to the range 0–360°, and converted them to radians for polar plotting. We binned angle values into 36 equal-width sectors (10° each) spanning 0 to 2π radians. We

computed the frequency of headings within each bin and normalized them to represent proportions rather than raw counts. We generated all plots using Matplotlib in polar projection mode.

Md and Postsynaptic Neuron Reconstruction in the connectome datasets

For the analyses in Figure 4, we first reconstructed md neurons and postsynaptic neurons in the female adult nerve cord (FANC[15]). We then matched sensory and postsynaptic partners in the male adult nerve cord (MANC[19]). We proofread automatically segmented neurons using Neuroglancer[119], an interactive software for visualizing, editing, and annotating 3D volumetric data. Proofreading entailed two types of edits: we split off neurites that did not belong to the cell of interest, and we merged segments of the neuron that the automated segmentation falsely missed. Light-level images of md genetic driver lines guided our identification. We reconstructed md axons from abdominal nerves 2, 3, 4, and the fused posterior trunk. In FANC, the dorsal side of the abdominal ganglion was cut during dissection, which prevented us from following axons completely out of the nerve cord.

We used the reconstructed FANC neurons as a reference to identify homologous neurons in the MANC dataset. MANC neurons matched to FANC neurons shared the same postsynaptic connectivity. We based nerve assignment on both single axon labeling of peripheral neurons and reconstructed md neurons matched in FANC. Janelia proofreaders reconstructed axons in MANC, and further proofreading was not possible. For both FANC and MANC, we excluded the most posterior *ppk*+ neurons associated with the genitals (4–6 neurons) for all analyses.

Past work found that applying a 3-4 synapse threshold mitigates the inclusion of false positive connections[62,67,69]. For the analyses in Figure 5, we similarly analyzed postsynaptic neurons based on a synapse threshold of ≥4 synapses. In FANC, we reconstructed the top 100 neurons, sorted by

the highest connectivity. We identified all objects in the automated segmentation that received ≥4 synapses from an md neuron. Synapses were detected automatically as described by Azevedo et al., 2024[15]. We then proofread those objects until they were associated with either a cell body or an identified descending or sensory process. We categorized a small number of objects as fragment segments, and we could not connect them to a cell body or an identified descending or sensory process. We deemed a neuron "proofread" once its cell body was attached, we reconstructed its full backbone, and we confidently attached as many branches as possible. Neuron annotations were managed by CAVE, the Connectome Annotation Versioning Engine. We used custom Python scripts to interact with CAVE via CAVEclient[120]. User authentication required to interface with CAVE related datasets.

We classified each md axon as either anterior or posterior based on whether the axon morphology branched anteriorly or posteriorly upon entering the VNC and which nerve bundle the axon traveled in. SPARC labeling confirmed the peripheral location of central md axons **(Figure S2.4).** We based the dorsal-ventral (DV) axes on SPARC labeling and python's scikit-learn cosine_similarity function.

To compare md axons based on their synaptic connectivity in the insets of **Figure 2.4D–E**, we constructed cosine similarity matrices from filtered synaptic data using the scikit-learn python package. This process involved several stages:

1. **Filtering Raw Synapse Data:** We began by filtering the raw synapse dataset to retain only meaningful connections (≥4 synapses). For each presynaptic neuron, we identified all postsynaptic partners and counted the number of synapses between each pair. We retained only connections with a synapse count equal to or exceeding our defined 4

synapse threshold. This ensured that weak or potentially spurious connections did not contribute to the similarity analysis.

2. **Generating a Directed Weighted Graph:** From the filtered synapse data, we generated a directed weighted graph using NetworkX[126]. Each node represented a neuron, and each edge represented a synaptic connection, with weights corresponding to the number of synapses.
3. **Extracting a Connectivity Matrix:** We extracted a connectivity matrix where rows represented source (presynaptic) neurons and columns represented target (postsynaptic) neurons. For asymmetric analyses, the matrix included only directed edges from each presynaptic neuron to each postsynaptic target.
4. **Clustering Cosine Similarity Scores:** We then hierarchically clustered cosine similarity scores using the agglomerative clustering methods from the scikit-learn Python package.
5. **Sorting the Similarity Matrix:** To sort the similarity matrix, we applied agglomerative hierarchical clustering. We used the resulting dendrogram to reorder rows and columns, which allowed visualization of structurally related neuron groups. When analyzing asymmetric matrices, we clustered rows and columns independently based on their respective similarity profiles (i.e., dorsal to ventral, anterior to posterior).

Analysis of central circuits downstream of md neurons.

For the analyses in **Figure S2.6**, we constructed the jumping and walking connectivity networks for corresponding postsynaptic partners using data from MANC and BANC datasets via flywire.ai. We focused our tertiary analysis on described neurons in literature and neurons annotated by subcluster class in BANC and MANC. Having two datasets—one from the VNC alone and one

from the entire nerve cord and brain—provides a more holistic view of circuits because some neurons only synapse in the brain, while others have connectivity in both the brain and nerve cord. We surveyed the broad connectivity of the ascending neurons, but for clarity chose to highlight specific connections to previously studied pathways that mediate behavioral phenotypes we observed in this study.

Reconstructed neurons table

Neurons	Dataset	Link
md neurons	FANC	link
md neurons	MANC	link
md neurons	BANC	link
SS01159	BANC	link
IS35283 lineage neurons	FANC	link
SS51024	FANC	link
IS35283 lineage neurons	MANC	link
SS51024	MANC	link
IS35283 lineage neurons	BANC	link
SS51024	BANC	link
IS35283 brain axons	FAFB	link
SS51024 brain axons	FAFB	link
all putative aversive sensory neurons	MANC	link
all putative aversive sensory neurons	BANC	link
putative labellum *ppk*+ neurons brain axons	FAFB	link

To analyze the connectivity of ascending neurons in each driver line, we cross-referenced each line to NeuronBridge to identify corresponding neurons in connectomic datasets. We queried postsynaptic targets of these neurons using three datasets: MANC (ventral nerve cord), FAFB (brain only), and BANC (brain and nerve cord combined). For each driver line, we identified ascending neurons based on morphological matching and analyzed their synaptic outputs to understand potential behavioral circuits.

For SS51024, we matched excitatory ascending neurons across datasets and analyzed their connectivity to the giant fibers, premotor networks, and brain circuits. For IS35283, we identified excitatory ascending neuron pairs and examined their connections to walking control circuits and descending neurons. For SS01159, we identified 60 ascending neurons (57 cholinergic, 3 glutamatergic based on predicted neurotransmitter classification) and focused analysis on the 6 neurons with strongest md connectivity (>5 synapses per neuron).

We quantified synaptic weights as total synapses between pre- and postsynaptic partners. We quantified VNC synapses in MANC, while we quantified brain synapses in FAFB. Cross-dataset analysis allowed us to integrate nerve cord and brain connectivity. We used BANC reconstructions for visualization of ascending neurons.

in vivo two-photon calcium imaging

We used a two-photon Movable Objective Microscopes (MOM; Sutter Instruments) with a 40x water-immersion objective (0.8 NA, 2.0 mm wd; Nikon Instruments) for calcium imaging.

We used a mode-locked Ti:sapphire laser (Chameleon Vision S; Coherent) to excite fluorophores at 920 nm. We maintained power at the back aperture of the objective below ~25 mW with a Pockels cell. Emitted fluorescence was directed to two high-sensitivity GaAsP photomultiplier tubes (Hamamatsu Photonics) through a 705 nm edge dichroic beamsplitter followed by a 580 nm edge image splitting dichroic beamsplitter (Semrock). Fluorescence was band-passed filtered by either a 525/50 (green) or 641/75 (red) emission filter (Semrock). Image acquisition was controlled with ScanImage 5.2[127] (Vidrio Technologies) in MATLAB (MathWorks). The microscope was equipped with a galvo-resonant scanner, and the objective was mounted onto a piezo actuator

(Physik Instrumente; digital piezo controller E-709). We focused our recordings on the abdominal ganglion, where the md axons project, using a fly holder and dissection similar to past work[128]. All experiments were performed in the dark at room temperature with 24C10AD;ppkDBD-GAL4>UAS-GCaMP7s-tdTomato flies. We used a 25W, 120V consumer soldering iron probe (Model SP25NKUS; Weller) attached to a 2000VA Auto Variable Voltage Transformer for temperature control (VEVOR). We calibrated the voltage necessary to achieve 40°C using a thermocouple attached to the iron tip and to a PID controller (Jaybva; PID temperature controller meter indicator).

In the experiments in **Figure 2.3,** we applied a 40°C heat or room temperature 25°C probe to dorsal abdominal segments 2-5. In **Figure S2.3C–E,** we applied 50 μM AITC in DMSO to the dorsal surface of the abdomen using a paintbrush. We pseudo-colored images to enhance the signal-to-noise ratio, where yellow represented the highest intensity and dark blue the lowest. We processed calcium imaging data to extract fluorescence signals and generate normalized activity traces for each experiment. We imported raw fluorescence data from tdTomato and GCaMP channels from individual CSV files and concatenated them into a single dataset. We parsed metadata such as recording date, fly identity, genotype, and trial number from filenames. For each recording, we calculated a fluorescence baseline (F_0) from the initial portion of the imaging period and computed $\Delta F/F$ values separately for the tdTomato and GCaMP channels. To account for motion or expression variability, we calculated the GCaMP-to-tdTomato fluorescence ratio for each frame and used its baseline to derive a normalized $\Delta R/R_0$ signal. We annotated stimulation periods by aligning fluorescence traces to a metadata table specifying the onset and offset frames of each heat stimulus. We labeled each frame as either “stimulus on” or “stimulus off,” and marked recordings identified as mechanical controls accordingly.

Extended Data

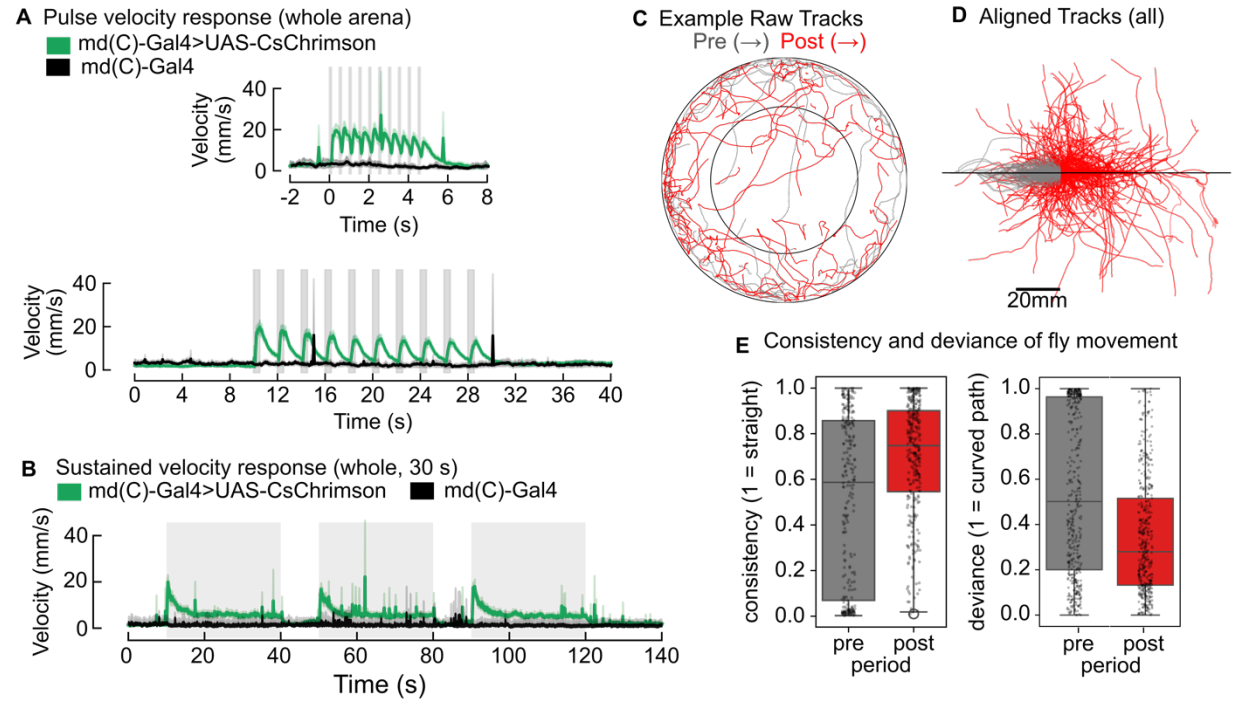

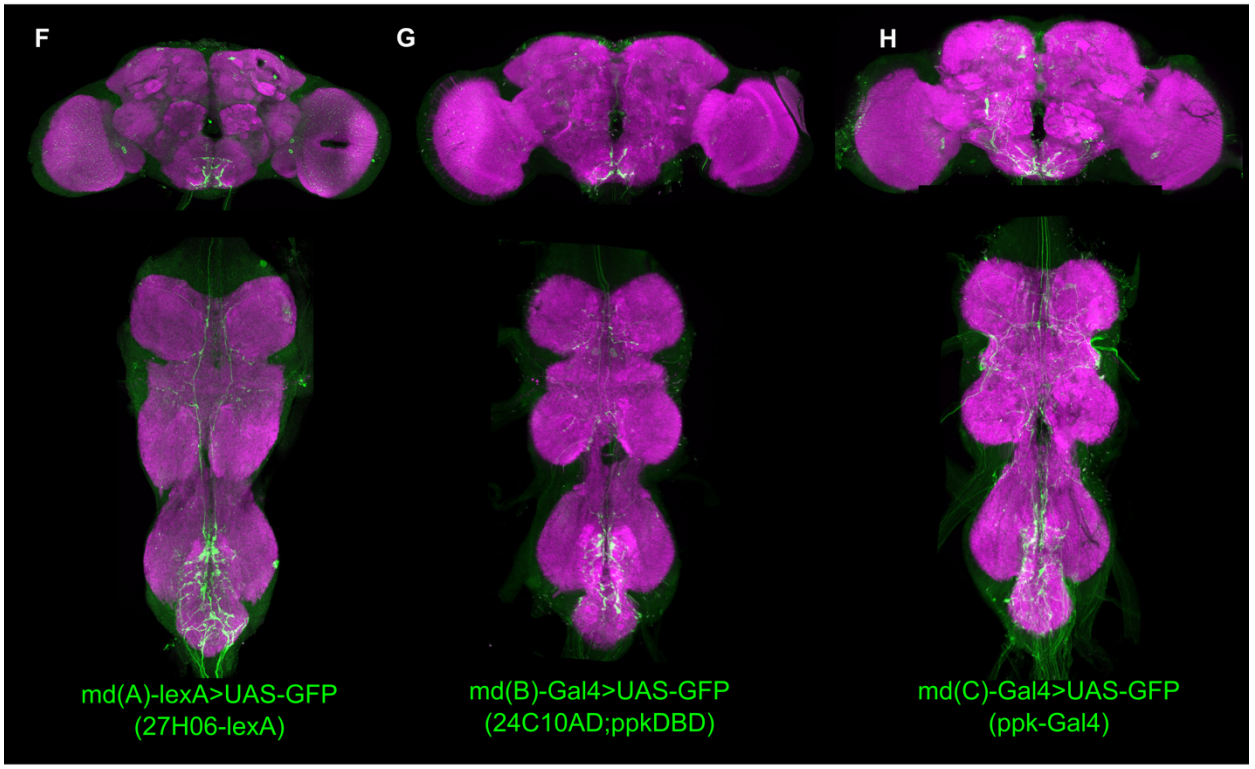

Extended Data Figure S2.1: Pulse activation experiments of md neurons and driver lines used. (A-B) Repeated activation of md(C)-GAL4 expressing UAS-CsChrimson (A), 500ms (A), and 30 seconds (B). C-E) Directional quantification of flies in quadrant arena assay. (C) Example raw tracks of flies pre (grey) and post(red). (D) Aligned tracks of all flies. (E). Quantification of consistency and deviance of fly movement. See Methods for details. (F-H) Genetic driver lines used to label abdominal multidendritic neurons (Figure 1C). Each driver line expressed in abdominal md neurons and other (non-overlapping) cell-types.

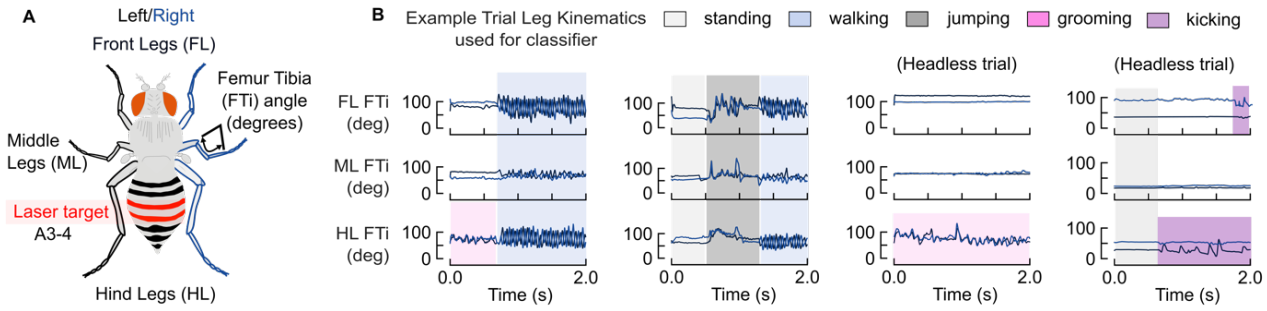

Extended Data Figure S2.2. Kinematics used to perform behavioral classification of flies on the ball. (A) Schematic of fly with front legs (FL), middle legs (ML), and hind legs (HL), with example femur-tibia angle (FTiº) used to plot joint kinematics. (B) Plotting of leg FTiº over time with highlighted stretches to signify standing (white) walking (blue) jumping (dark grey) abdomen grooming (pink) and single leg kicks (purple).

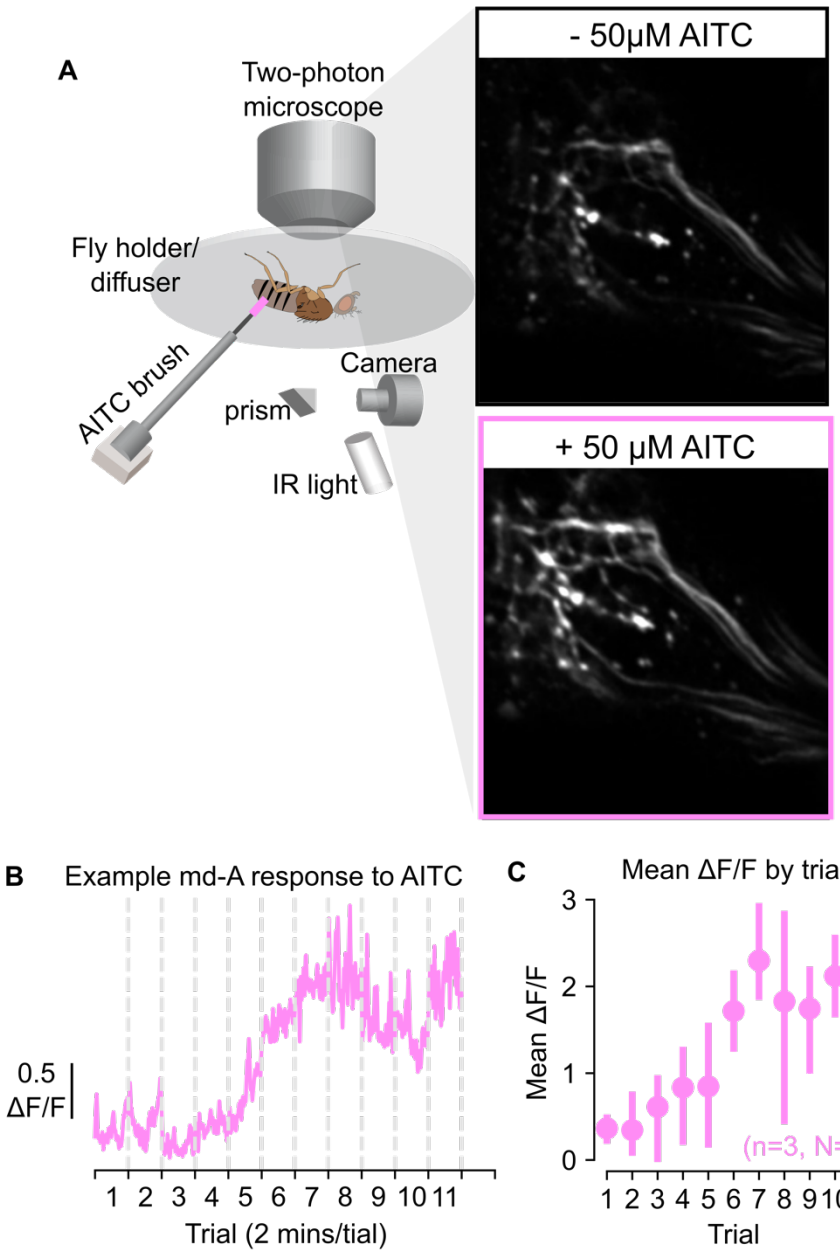

Extended Data Figure S2.3. Application of AITC increases calcium activity in md axon terminals. (A) We administered 50 μM AITC to the abdominal wall using a paintbrush and quantified the change in fluorescence over multiple imaging trials. (B) All trials were normalized to Trial 1. (C) Mean fluorescence of each trial. N=30 trials total across n=3 flies

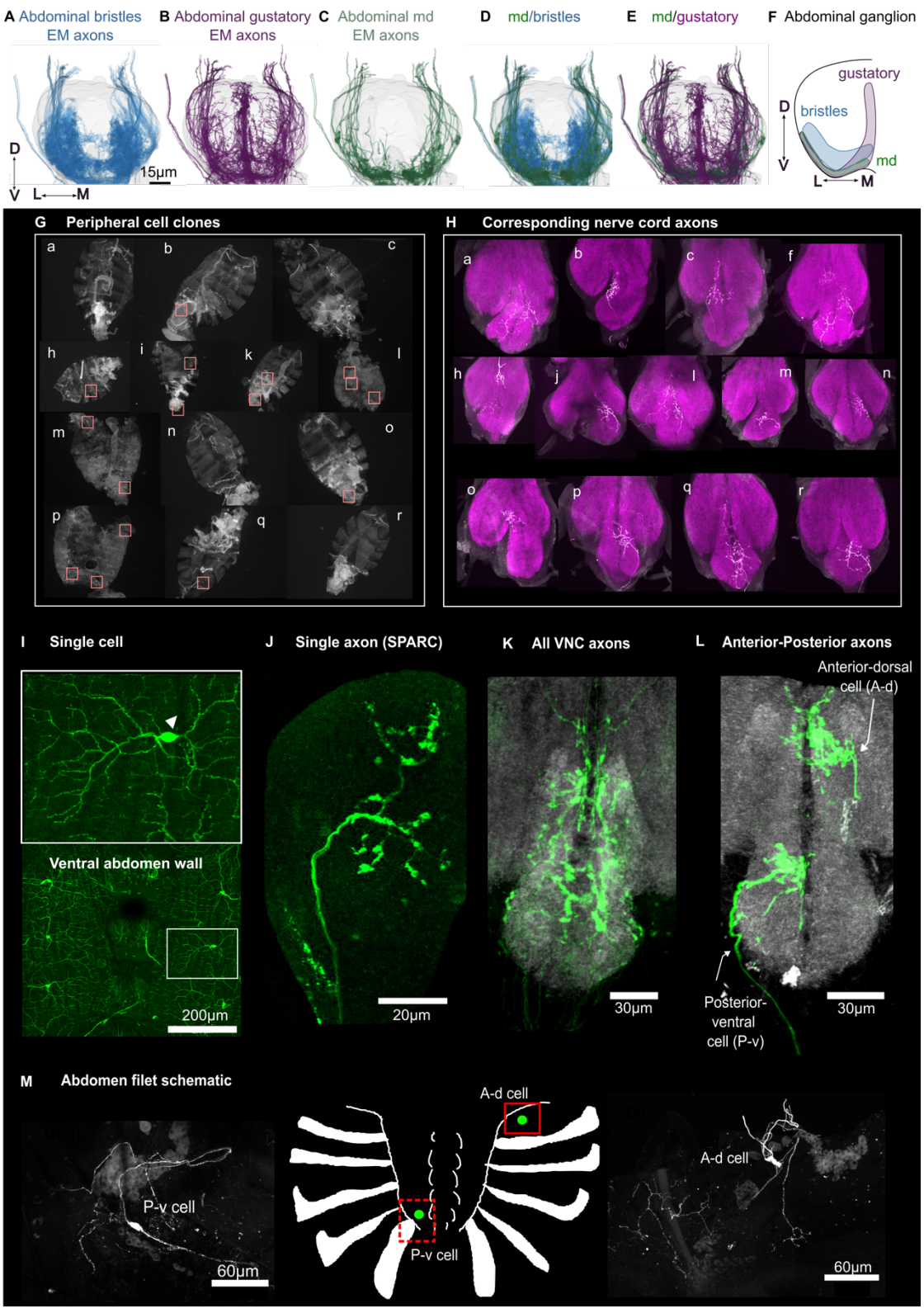
A Abdominal bristles EM axons
B Abdominal gustatory EM axons
C Abdominal md EM axons
D md/bristles
E md/gustatory
F Abdominal ganglion
gustatory
bristles
md
D
V
L
M
15µm
G Peripheral cell clones
H Corresponding nerve cord axons
I Single cell
Ventral abdomen wall
200µm
J Single axon (SPARC)
20µm
K All VNC axons
30µm
L Anterior-Posterior axons
Anterior-dorsal cell (A-d)
Posterior-ventral cell (P-v)
30µm
M Abdomen filet schematic
P-v cell
60µm
A-d cell
P-v cell
A-d cell
60µm

Extended Data Figure S2.4. Neuropil domains and SPARC labeling of 24C10AD;ppkDBD-GAL4. (A-E) MANC Dorsal-ventral EM reconstruction views of abdominal bristle axons (blue, A), abdominal putative gustatory neurons (purple, B), abdominal md axons (green, C), md-bristle axons (green-blue, D), and md-gustatory axons (green-purple, E). Scale bar is 15 microns. View is of abdominal ganglion. (F) Neuropil domains of each of the three sensory axon subtypes in the abdominal ganglion. Gustatory and md axons are more ventral than bristle axons, and bristle axons span more of the ventral domain of the abdominal ganglion. (G-H) Peripheral cell clones and their corresponding VNC axons. Lowercase letters are matched between abdominal and vnc labeled axons. Pink boxes denote locations of cell bodies. (I) Morphology of a peripheral md cell labeled by GFP. Bounding box encompasses one cell and its receptive field. Triangle denotes location of cell body. J) Single axon of a SPARC clone in the VNC labeled by GFP. (K) All VNC axons labeled by 24C10AD;ppkDBD-GAL4>UAS-GFP. (L) Anterior-dorsal and posterior-ventral single cell clones from SPARC protocol. (M). Abdomen filet schematic, origin location, and confocal images of anterior-dorsal (A-d) and posterior-ventral (P-v) cells. Genotype used throughout SPARC labeling was md(B)-GAL4 (24C10AD ; ppkDBD). SPARC procedure outlined in Methods

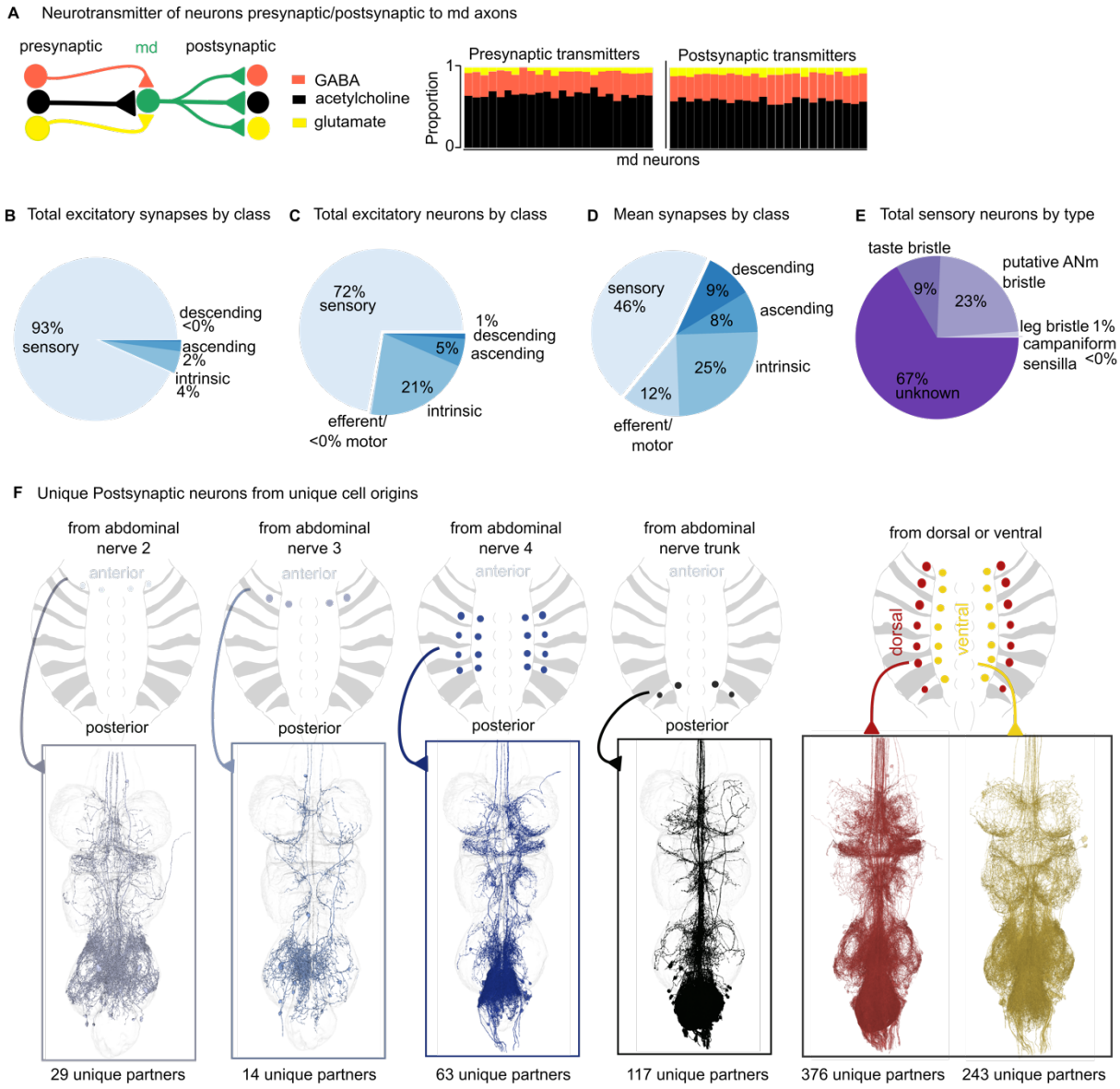

Extended Data Figure S2.5. Connectivity and neurotransmitter analysis of abdominal md neurons.
(A) Neurotransmitter identity of neurons presynaptic and postsynaptic to md axons. Md neurons predominantly receive excitatory cholinergic input and synapse onto cholinergic postsynaptic neurons. (B-D) Connectivity analysis of md neuron outputs by postsynaptic partner class. (B) Total excitatory synapses, (C) total excitatory neurons, and (D) mean synapses to md neurons. (E) Pie charts show sensory neurons by proportion presynaptic to md neurons (campaniform sensilla, leg bristles, putative ANm bristles, and taste bristles). (F) Spatial organization of md neuron connectivity by nerve of origin. Cross-sections of abdominal ganglion show postsynaptic partner distributions for md neurons entering via different nerves (nerve 2, 3, 4, and nerve trunk), with corresponding reconstructed axon morphologies below. Numbers indicate unique postsynaptic partners per nerve group. Md neurons originating from dorsal abdomen (red) and ventral abdomen (yellow) show distinct spatial distributions of their postsynaptic targets within the abdominal ganglion, preserving somatotopic organization. Cross-section shows target neuron locations with corresponding reconstructed md axon morphologies. Data from MANC connectome.

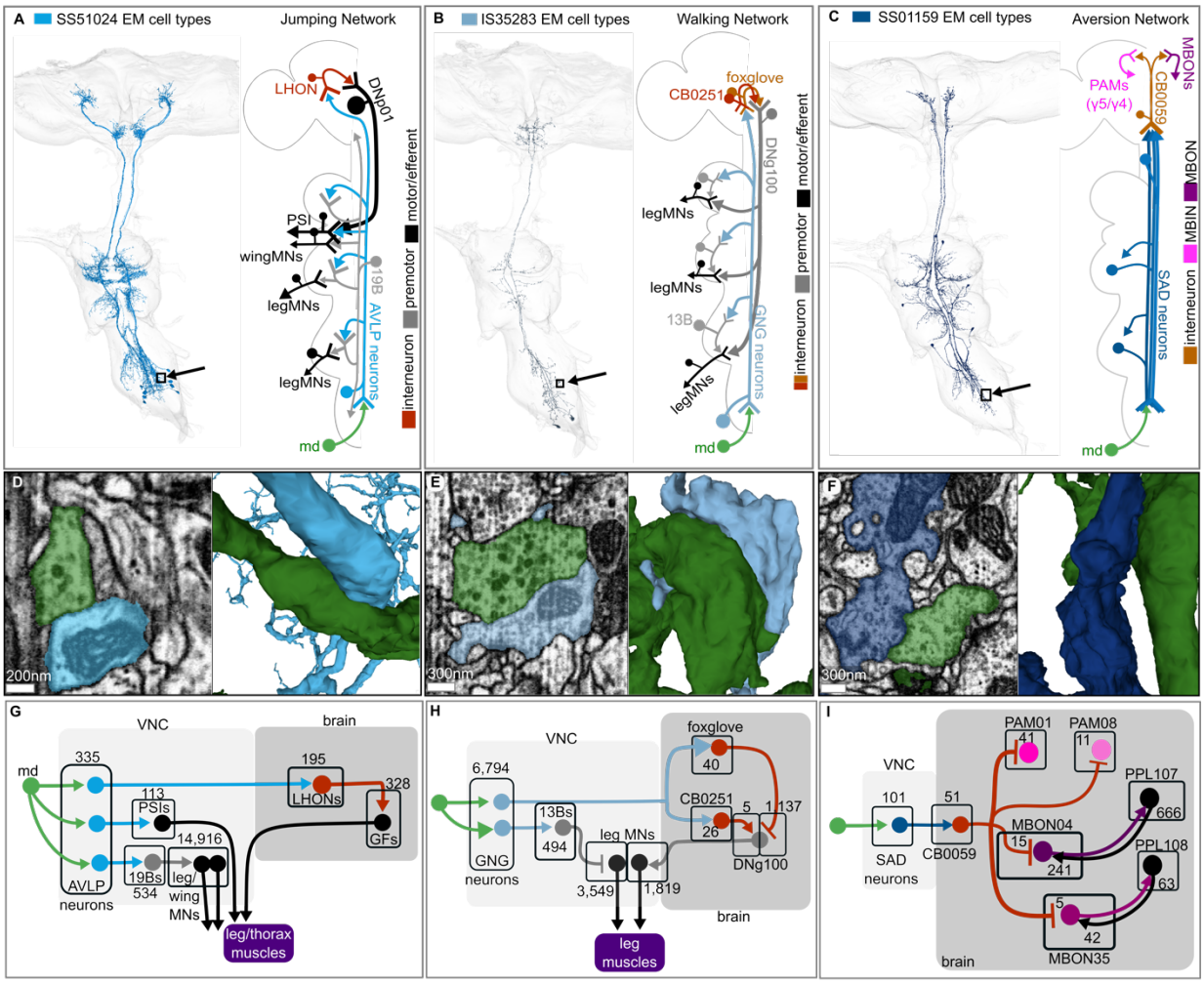

Extended Data Figure S2.6. Connectivity of ascending neurons to known circuits in the brain. (A-C) Circuit diagrams showing connectivity between md-related ascending neurons and established central brain neurons and networks. (A) SS51024 jumping network. md neurons connect to ascending neurons that integrate with giant fiber (GF) escape circuits through peripherally synapsing interneurons (PSIs) and lateral horn output neurons (LHONs). Pathway includes connections to 19B premotor neurons targeting leg and wing motor neurons (MNs), and descending neuron DNp01 controlling takeoff behavior. (B) IS35283 walking network. md neurons connect to ascending neurons projecting to gnathal ganglion (GNG) that integrate with walking control circuits. Key connections include CB0251 and foxglove interneurons that synapse onto descending neuron DNg100, and 13B premotor neurons targeting leg motor neurons. (C) SS01159 aversion network. md neurons connect to ascending neurons projecting to multiple brain regions including saddle (SAD). Circuit includes connections through CB0059 interneurons to PAM dopaminergic clusters (γ4, γ5) that drive mushroom body input neurons (MBINs) and output neurons (MBONs) involved in aversive learning. We hypothesize that these are the neurons involved in the avoidance we see, but further work is needed to validate these neurons. (D-F) Electron microscopy images showing synaptic connections between circuit components at coordinates indicated by the box and arrows on EM reconstructions in A-C. Scale bars: 200-300 nm as indicated. (G-I) Subcircuits downstream of ascending neurons. Numbers in black boxes indicate synapse counts between connected neuron types. Connectomic analysis performed across MANC and FAFB datasets. Gray boxes indicate VNC vs. brain. See Methods for circuit reconstruction details.

References

1. Dubin, A.E., and Patapoutian, A. (2010). Nociceptors: the sensors of the pain pathway. J. Clin. Invest. *120*, 3760–3772. https://doi.org/10.1172/JCI42843.
2. Loeser, J.D., and Melzack, R. (1999). Pain: an overview. Lancet Lond. Engl. *353*, 1607–1609. https://doi.org/10.1016/S0140-6736(99)01311-2.
3. Elwood, R.W. (2025). A History of Pain Studies and Changing Attitudes to the Welfare of Crustaceans. Animals *15*, 445. https://doi.org/10.3390/ani15030445.
4. Eisemann, C.H., Jorgensen, W.L., Merritt, D.J., Rice, M.J., Cribb, B.W., Webb, P.D., and Zalucki, M.P. (1984). Do insects feel pain? — A biological view. *40*, 164–167. https://doi.org/10.1007/bf01963580.
5. Sougoufara, S., Yorkston-Dives, H., Aklee, N.M., Rus, A.C., Zairi, J., and Tripet, F. (2022). Standardised bioassays reveal that mosquitoes learn to avoid compounds used in chemical vector control after a single sub-lethal exposure. Sci. Rep. *12*, 2206. https://doi.org/10.1038/s41598-022-05754-2.
6. Felsenberg, J., Jacob, P.F., Walker, T., Barnstedt, O., Edmondson-Stait, A.J., Pleijzier, M.W., Otto, N., Schlegel, P., Sharifi, N., Perisse, E., et al. (2018). Integration of Parallel Opposing Memories Underlies Memory Extinction. Cell *175*, 709-722.e15. https://doi.org/10.1016/j.cell.2018.08.021.
7. M. Gibbons, Elisa Pasquini, Amelia Kowalewska, Eva Read, Sam Gibson, A. Crump, Cwyn Solvi, Elisabetta Versace, and Lars Chittka (2024). Noxious stimulation induces self-protective behavior in bumblebees. bioRxiv. https://doi.org/10.1101/2024.01.15.575734.
8. Romero-González, J.E., Zhuo, Z., Chen, L., Peng, C., Solvi, C., and Peng, F. (2025). Positive affective contagion in bumble bees. Science *390*, 377–380. https://doi.org/10.1126/science.adr0216.
9. Jouandet, G.C., Alpert, M.H., Simões, J.M., Suhendra, R., Frank, D.D., Levy, J.I., Para, A., Kath, W.L., and Gallio, M. (2023). Rapid threat assessment in the Drosophila thermosensory system. Nat. Commun. *14*, 7067. https://doi.org/10.1038/s41467-023-42864-5.
10. Gibbons, M., Crump, A., Barrett, M., Sarlak, S., Birch, J., and Chittka, L. (2022). Can insects feel pain? A review of the neural and behavioural evidence. In Advances in Insect Physiology (Elsevier), pp. 155–229. https://doi.org/10.1016/bs.aiip.2022.10.001.
11. Jones, J.M., Foster, W., Twomey, C.R., Burdge, J., Ahmed, O.M., Pereira, T.D., Wojick, J.A., Corder, G., Plotkin, J.B., and Abdus-Saboor, I. (2020). A machine-vision approach for automated pain measurement at millisecond timescales. eLife *9*, e57258. https://doi.org/10.7554/eLife.57258.
12. Jeon, D., Kim, S., Chetana, M., Jo, D., Ruley, H.E., Young, C.-C., Rabah, D., Kinet, J.-P., and Shin, H.-S. (2010). Observational fear learning involves affective pain system and Cav1.2 Ca2+ channels in ACC. *13*, 482–488. https://doi.org/10.1038/nn.2504.

13. Johansen, J.P., Fields, H.L., and Manning, B.H. (2001). The affective component of pain in rodents: Direct evidence for a contribution of the anterior cingulate cortex. Proc. Natl. Acad. Sci. *98*, 8077–8082. https://doi.org/10.1073/pnas.141218998.

14. Berridge, K.C. (2019). Affective valence in the brain: modules or modes? *20*, 225–234. https://doi.org/10.1038/s41583-019-0122-8.

15. Azevedo, A., Lesser, E., Phelps, J.S., Mark, B., Elabbady, L., Kuroda, S., Sustar, A., Moussa, A., Khandelwal, A., Dallmann, C.J., et al. (2024). Connectomic reconstruction of a female Drosophila ventral nerve cord. Nature *631*, 360–368. https://doi.org/10.1038/s41586-024-07389-x.

16. Bates, A.S., Phelps, J.S., Kim, M., Yang, H.H., Matsliah, A., Ajabi, Z., Perlman, E., Delgado, K.M., Osman, M.A.M., Salmon, C.K., et al. (2025). Distributed control circuits across a brain-and-cord connectome. Preprint at Neuroscience, https://doi.org/10.1101/2025.07.31.667571 https://doi.org/10.1101/2025.07.31.667571.

17. Macrina, T., Lee, K.-S., Lu, R., Turner, N.J., Wu, J., Popovych, S., Silversmith, W., Kemnitz, N., Bae, J., Castro, M., et al. (2021). Petascale neural circuit reconstruction: automated methods. https://doi.org/10.1101/2021.08.04.455162.

18. Phelps, J.S., Hildebrand, D.F., Graham, B.H., Kuan, A.T., Thomas, L.A., Nguyen, T.Q., Buhmann, J., Azevedo, A.W., Sustar, A., Agrawal, S., et al. (2021). Reconstruction of motor control circuits in adult Drosophila using automated transmission electron microscopy. *184*, 759-774.e18. https://doi.org/10.1016/j.cell.2020.12.013.

19. Takemura, S., Hayworth, K.J., Huang, G.B., Januszewski, M., Lu, Z., Marin, E.C., Preibisch, S., Xu, C.S., Bogovic, J., Champion, A.S., et al. (2024). A Connectome of the Male Drosophila Ventral Nerve Cord. eLife *13*. https://doi.org/10.7554/eLife.97769.1.

20. Zheng, Z., Lauritzen, J.S., Perlman, E.S., Robinson, C.G., Nichols, M.A., Milkie, D.E., Torrens, O.N., William, J., Fisher, C.B., Sharifi, N., et al. (2018). A Complete Electron Microscopy Volume of the Brain of Adult Drosophila melanogaster. *174*, 730-743.e22. https://doi.org/10.1016/j.cell.2018.06.019.

21. Xiang, Y., Yuan, Q., Vogt, N., Looger, L.L., Jan, L.Y., and Jan, Y.N. (2010). Light-avoidance-mediating photoreceptors tile the Drosophila larval body wall. Nature *468*, 921–926. https://doi.org/10.1038/nature09576.

22. Neely, G.G., Keene, A.C., Duchek, P., Chang, E.C., Wang, Q.-P., Aksoy, Y.A., Rosenzweig, M., Costigan, M., Woolf, C.J., Garrity, P.A., et al. (2011). TrpA1 Regulates Thermal Nociception in Drosophila. PLOS ONE *6*, e24343. https://doi.org/10.1371/journal.pone.0024343.

23. Gong, J., Nirala, N.K., Chen, J., Wang, F., Gu, P., Wen, Q., Ip, Y.T., and Xiang, Y. (2023). TrpA1 is a shear stress mechanosensing channel regulating intestinal stem cell proliferation in *Drosophila*. Sci. Adv. *9*, eadc9660. https://doi.org/10.1126/sciadv.adc9660.

24. Tracey, W.D., Wilson, R., Laurent, G., and Benzer, S. (2003). painless, a Drosophila Gene Essential for Nociception. *113*, 261–273. https://doi.org/10.1016/s0092-8674(03)00272-1.

25. Gorczyca, D.A., Younger, S., Meltzer, S., Kim, S.E., Cheng, L., Song, W., Lee, H.Y., Jan, L.Y., and Jan, Y.N. (2014). Identification of Ppk26, a DEG/ENaC Channel Functioning

with Ppk1 in a Mutually Dependent Manner to Guide Locomotion Behavior in *Drosophila*. Cell Rep. *9*, 1446–1458. https://doi.org/10.1016/j.celrep.2014.10.034.

26. Kim, S.E., Coste, B., Chadha, A., Cook, B., and Patapoutian, A. (2012). The role of Drosophila Piezo in mechanical nociception. Nature *483*, 209–212. https://doi.org/10.1038/nature10801.

27. Clark, M.Q., Zarin, A.A., Carreira-Rosario, A., and Doe, C.Q. (2018). Neural circuits driving larval locomotion in Drosophila. Neural Develop. *13*, 6. https://doi.org/10.1186/s13064-018-0103-z.

28. Gowda, S.B.M., Salim, S., and Mohammad, F. (2021). Anatomy and Neural Pathways Modulating Distinct Locomotor Behaviors in Drosophila Larva. Biology *10*, 90. https://doi.org/10.3390/biology10020090.

29. Zhu, J., Boivin, J.-C., Garner, A., Ning, J., Zhao, Y.Q., and Ohyama, T. (2024). Feedback inhibition by a descending GABAergic neuron regulates timing of escape behavior in Drosophila larvae. eLife *13*, RP93978. https://doi.org/10.7554/eLife.93978.

30. Burgos, A., Honjo, K., Ohyama, T., Qian, C.S., Shin, G.J., Gohl, D.M., Silies, M., Tracey, W.D., Zlatic, M., Cardona, A., et al. (2018). Nociceptive interneurons control modular motor pathways to promote escape behavior in Drosophila. eLife *7*, e26016. https://doi.org/10.7554/eLife.26016.

31. Yoshino, J., Morikawa, R.K., Hasegawa, E., and Emoto, K. (2017). Neural Circuitry that Evokes Escape Behavior upon Activation of Nociceptive Sensory Neurons in Drosophila Larvae. *27*, 2499-2504.e3. https://doi.org/10.1016/j.cub.2017.06.068.

32. Agrawal, S., and Tuthill, J.C. (2022). The two-body problem: Proprioception and motor control across the metamorphic divide. Curr. Opin. Neurobiol. *74*, 102546. https://doi.org/10.1016/j.conb.2022.102546.

33. Tuthill, J.C., and Wilson, R. (2016). Mechanosensation and Adaptive Motor Control in Insects. *26*, R1022–R1038. https://doi.org/10.1016/j.cub.2016.06.070.

34. Cheng, L.E., Song, W., Looger, L.L., Jan, L.Y., and Jan, Y.N. (2010). The Role of the TRP Channel NompC in Drosophila Larval and Adult Locomotion. Neuron *67*, 373–380. https://doi.org/10.1016/j.neuron.2010.07.004.

35. Grueber, W.B., Ye, B., Yang, C.-H., Younger, S., Borden, K., and Jan, L.Y. (2007). Projections of Drosophila multidendritic neurons in the central nervous system: links with peripheral dendrite morphology. *134*, 55–64. https://doi.org/10.1242/dev.02666.

36. Grueber, W.B., Jan, L.Y., and Jan, L.Y. (2002). Tiling of the Drosophila epidermis by multidendritic sensory neurons. *129*, 2867–2878. https://doi.org/10.1242/dev.129.12.2867.

37. Shimono, K., Fujimoto, A., Tsuyama, T., Yamamoto-Kochi, M., Sato, M., Hattori, Y., Sugimura, K., Usui, T., Kimura, K., and Uemura, T. (2009). Multidendritic sensory neurons in the adult Drosophila abdomen: origins, dendritic morphology, and segment- and age-dependent programmed cell death. *4*. https://doi.org/10.1186/1749-8104-4-37.

38. Yaniv, S.P., and Schuldiner, O. (2016). A fly's view of neuronal remodeling. WIREs Dev. Biol. *5*, 618–635. https://doi.org/10.1002/wdev.241.

39. Yasunaga, K., Kanamori, T., Morikawa, R., Suzuki, E., and Emoto, K. (2010). Dendrite Reshaping of Adult *Drosophila* Sensory Neurons Requires Matrix Metalloproteinase-

Mediated Modification of the Basement Membranes. Dev. Cell *18*, 621–632. https://doi.org/10.1016/j.devcel.2010.02.010.

40. Williams, D.W., and Truman, J.W. (2005). Cellular mechanisms of dendrite pruning in *Drosophila* : insights from in vivo time-lapse of remodeling dendritic arborizing sensory neurons. Development *132*, 3631–3642. https://doi.org/10.1242/dev.01928.

41. Brown, H.M., Desai, T., Murphy, A.J., Pancholi, H., Schmidt, Z.W., Swahn, H., and Liebl, E.C. (2017). The function of Drosophila larval class IV dendritic arborization sensory neurons in the larval-pupal transition is separable from their function in mechanical nociception responses. *12*, e0184950–e0184950. https://doi.org/10.1371/journal.pone.0184950.

42. Messlinger, K. (1996). Chapter 17. Functional morphology of nociceptive and other fine sensory endings (free nerve endings) in different tissues. In Progress in Brain Research (Elsevier), pp. 273–298. https://doi.org/10.1016/S0079-6123(08)61094-8.

43. Gallio, M., Ofstad, T.A., Macpherson, L.J., Wang, J., and Zuker, C.S. (2011). The Coding of Temperature in the Drosophila Brain. *144*, 614–624. https://doi.org/10.1016/j.cell.2011.01.028.

44. Ache, J.M., Polsky, J., Alghailani, S., Parekh, R., Breads, P., Peek, M.Y., Bock, D.D., Von Reyn, C.R., and Card, G.M. (2019). Neural Basis for Looming Size and Velocity Encoding in the Drosophila Giant Fiber Escape Pathway. Curr. Biol. *29*, 1073-1081.e4. https://doi.org/10.1016/j.cub.2019.01.079.

45. Shuai, Y., Sammons, M., Sterne, G.R., Hibbard, K.L., Yang, H., Yang, C.-P., Managan, C., Siwanowicz, I., Lee, T., Rubin, G.M., et al. (2025). Driver lines for studying associative learning in Drosophila. eLife *13*, RP94168. https://doi.org/10.7554/eLife.94168.4.

46. Li, J., Zhang, W., Guo, Z., Wu, S., Jan, L.Y., and Jan, L.Y. (2016). A Defensive Kicking Behavior in Response to Mechanical Stimuli Mediated byDrosophilaWing Margin Bristles. *36*, 11275–11282. https://doi.org/10.1523/jneurosci.1416-16.2016.

47. Harris, R.M., Pfeiffer, B.D., Rubin, G.M., Truman, J.W., and Griffith, L.C. (2015). Neuron hemilineages provide the functional ground plan for the Drosophila ventral nervous system. eLife *4*, e04493–e04493. https://doi.org/10.7554/eLife.04493.

48. Sapkal, N., Mancini, N., Kumar, D.S., Spiller, N., Murakami, K., Vitelli, G., Bargeron, B., Maier, K., Eichler, K., Jefferis, G.S.X.E., et al. (2024). Neural circuit mechanisms underlying context-specific halting in Drosophila. Nature *634*, 191–200. https://doi.org/10.1038/s41586-024-07854-7.

49. Barik, A., Thompson, J.H., Seltzer, M., Ghitani, N., and Chesler, A.T. (2018). A Brainstem-Spinal Circuit Controlling Nocifensive Behavior. Neuron *100*, 1491-1503.e3. https://doi.org/10.1016/j.neuron.2018.10.037.

50. Liu, Z., Wu, M.H., Wang, Q.X., Lin, S.Z., Feng, X.Q., Li, B., and Liang, X. (2022). Drosophila mechanical nociceptors preferentially sense localized poking. eLife *11*, e76574. https://doi.org/10.7554/eLife.76574.

51. Im, S.H., and Galko, M.J. (2011). Pokes, sunburn, and hot sauce:Drosophilaas an emerging model for the biology of nociception. *241*, 16–26. https://doi.org/10.1002/dvdy.22737.

52. Hoyer, N., Petersen, M., Tenedini, F., and Soba, P. (2018). Assaying Mechanonociceptive Behavior in Drosophila Larvae. *8*. https://doi.org/10.21769/bioprotoc.2736.

53. Chattopadhyay, A., Gilstrap, A.V., and Galko, M.J. (2012). Local and global methods of assessing thermal nociception in Drosophila larvae. J. Vis. Exp. JoVE, e3837. https://doi.org/10.3791/3837.

54. Mandel, S.J., Shoaf, M.L., Braco, J.T., Silver, W.L., and Johnson, E.C. (2018). Behavioral Aversion to AITC Requires Both Painless and dTRPA1 in Drosophila. Front. Neural Circuits *12*, 45. https://doi.org/10.3389/fncir.2018.00045.

55. Terada, S.-I., Matsubara, D., Onodera, K., Matsuzaki, M., Uemura, T., and Usui, T. (2016). Neuronal processing of noxious thermal stimuli mediated by dendritic Ca2+ influx in Drosophila somatosensory neurons. eLife *5*, e12959. https://doi.org/10.7554/eLife.12959.

56. Hamada, F.N., Rosenzweig, M., Kang, K., Pulver, S.R., Ghezzi, A., Jegla, T.J., and Garrity, P.A. (2008). An internal thermal sensor controlling temperature preference in Drosophila. Nature *454*, 217–220. https://doi.org/10.1038/nature07001.

57. Tsubouchi, A., Yano, T., Yokoyama, T.K., Murtin, C., Otsuna, H., and Ito, K. (2017). Topological and modalityspecific representation of somatosensory information in the fly brain. Science *358*, 615–623. https://doi.org/10.1126/science.aan4428.

58. Asahina, K. (2018). Sex differences in Drosophila behavior: Qualitative and Quantitative Dimorphism. Curr. Opin. Physiol. *6*, 35–45. https://doi.org/10.1016/j.cophys.2018.04.004.

59. Isaacman-Beck, J., Paik, K.C., Wienecke, C.F.R., Yang, H.H., Fisher, Y.E., Wang, I.E., Ishida, I.G., Maimon, G., Wilson, R.I., and Clandinin, T.R. (2020). SPARC enables genetic manipulation of precise proportions of cells. Nat. Neurosci. *23*, 1168–1175. https://doi.org/10.1038/s41593-020-0668-9.

60. Gerhard, S., Andrade, I., Fetter, R.D., Cardona, A., and Schneider-Mizell, C.M. (2017). Conserved neural circuit structure across Drosophila larval development revealed by comparative connectomics. eLife *6*, e29089. https://doi.org/10.7554/eLife.29089.

61. Eckstein, N., Bates, A.S., Champion, A., Du, M., Yin, Y., Schlegel, P., Lu, A.K., Rymer, T., FinleyMay, S., Paterson, T., et al. (2023). Neurotransmitter Classification from Electron Microscopy Images at Synaptic Sites in Drosophila Melanogaster. bioRxiv, 2020.06.12.148775-2020.06.12.148775. https://doi.org/10.1101/2020.06.12.148775.

62. Lee, S.-Y.J., Dallmann, C.J., Cook, A., Tuthill, J.C., and Agrawal, S. (2025). Divergent neural circuits for proprioceptive and exteroceptive sensing of the Drosophila leg. Nat. Commun. *16*, 4105. https://doi.org/10.1038/s41467-025-59302-3.

63. Bessou, P., and Perl, E.R. (1969). Response of cutaneous sensory units with unmyelinated fibers to noxious stimuli. J. Neurophysiol. *32*, 1025–1043. https://doi.org/10.1152/jn.1969.32.6.1025.

64. Mizumura, K., Sugiura, T., Katanosaka, K., Banik, R.K., and Kozaki, Y. (2009). Excitation and sensitization of nociceptors by bradykinin: what do we know? Exp. Brain Res. *196*, 53–65. https://doi.org/10.1007/s00221-009-1814-5.

65. Jang, W., Oh, M., Cho, E.-H., Baek, M., and Kim, C. (2023). Drosophila pain sensitization and modulation unveiled by a novel pain model and analgesic drugs. PLOS ONE *18*, e0281874. https://doi.org/10.1371/journal.pone.0281874.

66. Babcock, D.T., Landry, C., and Galko, M.J. (2009). Cytokine Signaling Mediates UV-Induced Nociceptive Sensitization in Drosophila Larvae. Curr. Biol. *19*, 799–806. https://doi.org/10.1016/j.cub.2009.03.062.

67. Schlegel, P., Yin, Y., Bates, A.S., Dorkenwald, S., Eichler, K., Brooks, P., Han, D.S., Gkantia, M., Dos Santos, M., Munnelly, E.J., et al. (2024). Whole-brain annotation and multi-connectome cell typing of Drosophila. Nature *634*, 139–152. https://doi.org/10.1038/s41586-024-07686-5.

68. Dorkenwald, S., Matsliah, A., Sterling, A.R., Schlegel, P., Yu, S.-C., McKellar, C.E., Lin, A., Costa, M., Eichler, K., Yin, Y., et al. (2024). Neuronal wiring diagram of an adult brain. Nature *634*, 124–138. https://doi.org/10.1038/s41586-024-07558-y.

69. Scheffer, L.K., Xu, C.S., Januszewski, M., Lu, Z., Takemura, S.-Y., Hayworth, K.J., Huang, G.B., Shinomiya, K., Maitlin-Shepard, J., Berg, S., et al. (2020). A connectome and analysis of the adult Drosophila central brain. eLife *9*, e57443. https://doi.org/10.7554/eLife.57443.

70. Clements, J., Goina, C., Hubbard, P.M., Kawase, T., Olbris, D.J., Otsuna, H., Svirskas, R., and Rokicki, K. (2024). NeuronBridge: an intuitive web application for neuronal morphology search across large data sets. BMC Bioinformatics *25*, 114. https://doi.org/10.1186/s12859-024-05732-7.

71. Peek, M. (2018). Control of Escape Behavior by Descending Neurons in Drosophila Melanogaster. https://doi.org/10.6082/UCHICAGO.1415.

72. Kim, H., Park, H., Lee, J., and Kim, A.J. (2023). A visuomotor circuit for evasive flight turns in Drosophila. Curr. Biol. CB *33*, 321-335.e6. https://doi.org/10.1016/j.cub.2022.12.014.

73. Braun, J., Hurtak, F., Wang-Chen, S., and Ramdya, P. (2024). Descending networks transform command signals into population motor control. Nature *630*, 686–694. https://doi.org/10.1038/s41586-024-07523-9.

74. Dallmann, C.J., Luo, Y., Agrawal, S., Mamiya, A., Chou, G.M., Cook, A., Sustar, A., Brunton, B.W., and Tuthill, J.C. (2025). Selective presynaptic inhibition of leg proprioception in behaving Drosophila. Nature. https://doi.org/10.1038/s41586-025-09554-2.

75. Sterne, G.R., Otsuna, H., Dickson, B.J., and Scott, K. (2021). Classification and genetic targeting of cell types in the primary taste and premotor center of the adult Drosophila brain. eLife *10*, e71679. https://doi.org/10.7554/eLife.71679.

76. Cognigni, P., Felsenberg, J., and Waddell, S. (2018). Do the right thing: neural network mechanisms of memory formation, expression and update in Drosophila. Curr. Opin. Neurobiol. *49*, 51–58. https://doi.org/10.1016/j.conb.2017.12.002.

77. Owald, D., Felsenberg, J., Talbot, C.B., Das, G., Perisse, E., Huetteroth, W., and Waddell, S. (2015). Activity of Defined Mushroom Body Output Neurons Underlies Learned Olfactory Behavior in Drosophila. Neuron *86*, 417–427. https://doi.org/10.1016/j.neuron.2015.03.025.

78. Hampel, S., McKellar, C.E., Simpson, J.H., and Seeds, A.M. (2017). Simultaneous activation of parallel sensory pathways promotes a grooming sequence in Drosophila. eLife *6*, e28804. https://doi.org/10.7554/eLife.28804.

79. Mishra, A., Salari, A., Berigan, B.R., Miguel, K.C., Amirshenava, M., Robinson, A., Zars, B.C., Lin, J.L., Milescu, L.S., Milescu, M., et al. (2018). The Drosophila Gr28bD product is a non-specific cation channel that can be used as a novel thermogenetic tool. Sci. Rep. *8*, 901. https://doi.org/10.1038/s41598-017-19065-4.

80. Alpert, M.H., Gil, H., Para, A., and Gallio, M. (2022). A thermometer circuit for hot temperature adjusts Drosophila behavior to persistent heat. Curr. Biol. *32*, 4079-4087.e4. https://doi.org/10.1016/j.cub.2022.07.060.

81. Simões, J.M., Levy, J.I., Zaharieva, E.E., Vinson, L.T., Zhao, P., Alpert, M.H., Kath, W.L., Para, A., and Gallio, M. (2021). Robustness and plasticity in Drosophila heat avoidance. Nat. Commun. *12*, 2044. https://doi.org/10.1038/s41467-021-22322-w.

82. Levine, R.B., and Weeks, J.C. (1996). Cell Culture Approaches to Understanding the Actions of Steroid Hormones on the Insect Nervous System. Dev. Neurosci. *18*, 73–86. https://doi.org/10.1159/000111397.

83. Tissot, M., and Stocker, R.F. (2000). Metamorphosis in Drosophila and other insects: the fate of neurons throughout the stages. Prog. Neurobiol. *62*, 89–111. https://doi.org/10.1016/S0301-0082(99)00069-6.

84. Furusawa, K., and Emoto, K. (2021). Scrap and Build for Functional Neural Circuits: Spatiotemporal Regulation of Dendrite Degeneration and Regeneration in Neural Development and Disease. Front. Cell. Neurosci. *14*, 613320. https://doi.org/10.3389/fncel.2020.613320.

85. Caron, D.P., Rimniceanu, M., Scibelli, A.E., and Trimmer, B.A. (2020). Nociceptive neurons respond to multimodal stimuli in *Manduca sexta*. J. Exp. Biol., jeb.218859. https://doi.org/10.1242/jeb.218859.

86. Grueber, W.B., and Truman, J.W. (1999). Development and organization of a nitric-oxide-sensitive peripheral neural plexus in larvae of the moth,Manduca sexta. J. Comp. Neurol. *404*, 127–141. https://doi.org/10.1002/(SICI)1096-9861(19990201)404:1%253C127::AID-CNE10%253E3.0.CO;2-M.

87. Jang, W., Lim, J.Y., Kang, S., Kim, M., Hwang, S.W., and Kim, C. (2022). Drosophila ppk19 encodes a proton-gated and mechanosensitive ion channel. Sci. Rep. *12*, 18346. https://doi.org/10.1038/s41598-022-23236-3.

88. Gong, J., Chen, J., Gu, P., Shang, Y., Ruppell, K.T., Yang, Y., Wang, F., Wen, Q., and Xiang, Y. (2022). Shear stress activates nociceptors to drive Drosophila mechanical nociception. Neuron *110*, 3727-3742.e8. https://doi.org/10.1016/j.neuron.2022.08.015.

89. Guo, Y., Li, T., Tuomivaara, S.T., Teo, C.F., Feng, S., Chalkley, R.J., Zhu, R., Cheng, T., Li, K.H., Chen, W., et al. (2025). Identification of the peptide Vulnusin, a wound signal

that mediates mechanical-injury-induced nociception in Drosophila. Neuron *113*, 3352-3362.e5. https://doi.org/10.1016/j.neuron.2025.09.007.

90. Hwang, R.Y., Zhong, L., Xu, Y., Johnson, T., Zhang, F., Deisseroth, K., and Tracey, W.D. (2007). Nociceptive Neurons Protect Drosophila Larvae from Parasitoid Wasps. Curr. Biol. *17*, 2105–2116. https://doi.org/10.1016/j.cub.2007.11.029.

91. Moore, L.D., Chris Amuwa, T., Shaw, S.R., and Ballinger, M.J. (2024). Drosophila are hosts to the first described parasitoid wasp of adult flies. Nature *633*, 840–847. https://doi.org/10.1038/s41586-024-07919-7.

92. Ohyama, T., Jovanic, T., Denisov, G., Dang, T.C., Hoffmann, D., Kerr, R.A., and Zlatic, M. (2013). High-Throughput Analysis of Stimulus-Evoked Behaviors in Drosophila Larva Reveals Multiple Modality-Specific Escape Strategies. PLoS ONE *8*, e71706. https://doi.org/10.1371/journal.pone.0071706.

93. Ohyama, T., Schneider-Mizell, C.M., Fetter, R.D., Aleman, J.V., Franconville, R., Rivera-Alba, M., Mensh, B.D., Branson, K.M., Simpson, J.H., Truman, J.W., et al. (2015). A multilevel multimodal circuit enhances action selection in Drosophila. Nature *520*, 633–639. https://doi.org/10.1038/nature14297.

94. Takagi, S., Cocanougher, B.T., Niki, S., Miyamoto, D., Kohsaka, H., Kazama, H., Fetter, R.D., Truman, J.W., Zlatic, M., Cardona, A., et al. (2017). Divergent Connectivity of Homologous Command-like Neurons Mediates Segment-Specific Touch Responses in Drosophila. Neuron *96*, 1373-1387.e6. https://doi.org/10.1016/j.neuron.2017.10.030.

95. Heckscher, E.S., Zarin, A.A., Faumont, S., Clark, M.Q., Manning, L., Fushiki, A., Schneider-Mizell, C.M., Fetter, R.D., Truman, J.W., Zwart, M.F., et al. (2015). Even-Skipped+ Interneurons Are Core Components of a Sensorimotor Circuit that Maintains Left-Right Symmetric Muscle Contraction Amplitude. Neuron *88*, 314–329. https://doi.org/10.1016/j.neuron.2015.09.009.

96. Kaneko, T., Macara, A.M., Li, R., Hu, Y., Iwasaki, K., Dunnings, Z., Firestone, E., Horvatic, S., Guntur, A.R., Shafer, O.T., et al. (2017). Serotonergic Modulation Enables Pathway-Specific Plasticity in a Developing Sensory Circuit in Drosophila. *95*, 623-638.e4. https://doi.org/10.1016/j.neuron.2017.06.034.

97. Oikawa, I., Kondo, S., Hashimoto, K., Yoshida, A., Hamajima, M., Tanimoto, H., Furukubo-Tokunaga, K., and Honjo, K. (2023). A descending inhibitory mechanism of nociception mediated by an evolutionarily conserved neuropeptide system in Drosophila. *12*. https://doi.org/10.7554/elife.85760.

98. Jovanic, T., Schneider-Mizell, C.M., Shao, M., Masson, J.-B., Denisov, G., Fetter, R.D., Mensh, B.D., Truman, J.W., Cardona, A., and Zlatic, M. (2016). Competitive Disinhibition Mediates Behavioral Choice and Sequences in Drosophila. Cell *167*, 858-870.e19. https://doi.org/10.1016/j.cell.2016.09.009.

99. Schultzhaus, J.N., Saleem, S., Iftikhar, H., and Carney, G.E. (2017). The role of the Drosophila lateral horn in olfactory information processing and behavioral response. J. Insect Physiol. *98*, 29–37. https://doi.org/10.1016/j.jinsphys.2016.11.007.

100. Varela, N., Gaspar, M., Dias, S., and Vasconcelos, M.L. (2019). Avoidance response to CO2 in the lateral horn. PLOS Biol. *17*, e2006749. https://doi.org/10.1371/journal.pbio.2006749.

101. Das Chakraborty, S., Chang, H., Hansson, B.S., and Sachse, S. (2022). Higher-order olfactory neurons in the lateral horn support odor valence and odor identity coding in Drosophila. eLife *11*, e74637. https://doi.org/10.7554/eLife.74637.

102. Nässel, D.R. (2021). Leucokinin and Associated Neuropeptides Regulate Multiple Aspects of Physiology and Behavior in Drosophila. Int. J. Mol. Sci. *22*, 1940. https://doi.org/10.3390/ijms22041940.

103. Ohashi, H., and Sakai, T. (2018). Leucokinin signaling regulates hunger–driven reduction of behavioral responses to noxious heat in Drosophila. Biochem. Biophys. Res. Commun. *499*, 221–226. https://doi.org/10.1016/j.bbrc.2018.03.132.

104. Aso, Y., and Rubin, G.M. (2016). Dopaminergic neurons write and update memories with cell-type-specific rules. https://doi.org/10.7554/eLife.16135.001.

105. Masek, P., Worden, K., Aso, Y., Rubin, G.M., and Keene, A.C. (2015). A dopamine-modulated neural circuit regulating aversive taste memory in drosophila. Curr. Biol. *25*, 1535–1541. https://doi.org/10.1016/j.cub.2015.04.027.

106. Howard, C.E., Chen, C.-L., Tabachnik, T., Hormigo, R., Ramdya, P., and Mann, R.S. (2019). Serotonergic Modulation of Walking in Drosophila. Curr. Biol. *29*, 4218-4230.e8. https://doi.org/10.1016/j.cub.2019.10.042.

107. Tabuena, D.R., Solis, A., Geraldi, K., Moffatt, C.A., and Fuse, M. (2017). Central neural alterations predominate in an insect model of nociceptive sensitization. J. Comp. Neurol. *525*, 1176–1191. https://doi.org/10.1002/cne.24124.

108. Latremoliere, A., and Woolf, C.J. (2009). Central Sensitization: A Generator of Pain Hypersensitivity by Central Neural Plasticity. J. Pain *10*, 895–926. https://doi.org/10.1016/j.jpain.2009.06.012.

109. Dabbara, H., Schultz, A., and Im, S.H. (2021). Drosophila insulin receptor regulates diabetes-induced mechanical nociceptive hypersensitivity. MicroPublication Biol. *2021*. https://doi.org/10.17912/micropub.biology.000456.

110. Raja, S.N., Carr, D.B., Cohen, M., Finnerup, N.B., Flor, H., Gibson, S., Keefe, F.J., Mogil, J.S., Ringkamp, M., Sluka, K.A., et al. (2020). The revised International Association for the Study of Pain definition of pain: concepts, challenges, and compromises. Pain *161*, 1976–1982. https://doi.org/10.1097/j.pain.0000000000001939.

111. Mamiya, A., Sustar, A., Siwanowicz, I., Qi, Y., Lu, T.-C., Gurung, P., Chen, C., Phelps, J.S., Kuan, A.T., Pacureanu, A., et al. (2023). Biomechanical origins of proprioceptor feature selectivity and topographic maps in the Drosophila leg. Neuron *111*, 3230-3243.e14. https://doi.org/10.1016/j.neuron.2023.07.009.

112. Gorko, B., Siwanowicz, I., Close, K., Christoforou, C., Hibbard, K.L., Kabra, M., Lee, A., Park, J.-Y., Li, S.Y., Chen, A.B., et al. (2024). Motor neurons generate pose-targeted movements via proprioceptive sculpting. Nature *628*, 596–603. https://doi.org/10.1038/s41586-024-07222-5.

113. Seidner, G., Robinson, J.E., Wu, M., Worden, K., Masek, P., Roberts, S.W., Keene, A.C., and Joiner, W.J. (2015). Identification of Neurons with a Privileged Role in Sleep Homeostasis in Drosophila melanogaster. Curr. Biol. *25*, 2928–2938. https://doi.org/10.1016/j.cub.2015.10.006.

114. Sterne, G.R., Otsuna, H., Dickson, B.J., and Scott, K. (2021). Classification and genetic targeting of cell types in the primary taste and premotor center of the adult Drosophila brain. eLife *10*, e71679. https://doi.org/10.7554/eLife.71679.

115. Eyjolfsdottir, E., Branson, S., Burgos-Artizzu, X.P., Hoopfer, E.D., Schor, J., Anderson, D.E., and Perona, P. (2014). Detecting Social Actions of Fruit Flies. 772–787. https://doi.org/10.1007/978-3-319-10605-2_50.

116. Mathis, A., Mamidanna, P., Cury, K.M., Abe, T., Murthy, V.L., Mathis, A., and Bethge, M. (2018). DeepLabCut: markerless pose estimation of user-defined body parts with deep learning. *21*, 1281–1289. https://doi.org/10.1038/s41593-018-0209-y.

117. Karashchuk, P., Rupp, K.L., Dickinson, P.S., Walling-Bell, S., Sanders, E., Azim, E., Brunton, B.W., and Tuthill, J.C. (2021). Anipose: A toolkit for robust markerless 3D pose estimation. *36*, 109730–109730. https://doi.org/10.1016/j.celrep.2021.109730.

118. Moore, R.D., Taylor, G., Paulk, A.C., Pearson, T.A., Swinderen, B. van, and Srinivasan, M.V. (2014). FicTrac: A visual method for tracking spherical motion and generating fictive animal paths. *225*, 106–119. https://doi.org/10.1016/j.jneumeth.2014.01.010.

119. Maitin-Shepard, J., Baden, A., Silversmith, W., Perlman, E., Collman, F., Blakely, T., Funke, J., Jordan, C., Falk, B., Kemnitz, N., et al. (2021). google/neuroglancer. Version v2.23 (Zenodo). https://doi.org/10.5281/ZENODO.5573294 https://doi.org/10.5281/ZENODO.5573294.

120. Dorkenwald, S., Schneider-Mizell, C.M., Brittain, D., Halageri, A., Jordan, C., Kemnitz, N., Castro, M.A., Silversmith, W., Maitin-Shephard, J., Troidl, J., et al. (2025). CAVE: Connectome Annotation Versioning Engine. Nat. Methods *22*, 1112–1120. https://doi.org/10.1038/s41592-024-02426-z.

121. Pedregosa, F., Varoquaux, G., Gramfort, A., Michel, V., Thirion, B., Grisel, O., Blondel, M., Müller, A., Nothman, J., Louppe, G., et al. (2012). Scikit-learn: Machine Learning in Python. https://doi.org/10.48550/ARXIV.1201.0490.

122. Simon, J.C., and Dickinson, M.H. (2010). A New Chamber for Studying the Behavior of Drosophila. *5*, e8793–e8793. https://doi.org/10.1371/journal.pone.0008793.

123. Agrawal, S., Dickinson, E.S., Sustar, A., Gurung, P., Shepherd, D., Truman, J.W., and Tuthill, J.C. (2020). Central processing of leg proprioception in Drosophila. eLife *9*, e60299. https://doi.org/10.7554/eLife.60299.

124. Pratt, B.G., Lee, S.-Y.J., Chou, G.M., and Tuthill, J.C. (2024). Miniature linear and split-belt treadmills reveal mechanisms of adaptive motor control in walking Drosophila. Curr. Biol. *34*, 4368-4381.e5. https://doi.org/10.1016/j.cub.2024.08.006.

125. Hampel, S., Franconville, R., Simpson, J.H., and Seeds, A.M. (2015). A neural command circuit for grooming movement control. eLife *4*, e08758. https://doi.org/10.7554/eLife.08758.

126. Hagberg, A.A., Schult, D.A., and Swart, P.J. (2008). Exploring Network Structure, Dynamics, and Function using NetworkX. In, pp. 11–15. https://doi.org/10.25080/TCWV9851.

127. Pologruto, T.A., Sabatini, B.L., and Svoboda, K. (2003). ScanImage: Flexible software for operating laser scanning microscopes. Biomed. Eng. OnLine *2*, 13. https://doi.org/10.1186/1475-925X-2-13.

128. Mamiya, A., Gurung, P., and Tuthill, J.C. (2018). Neural Coding of Leg Proprioception in Drosophila. Neuron *100*, 636-650.e6. https://doi.org/10.1016/j.neuron.2018.09.009.

Chapter 3

Temperature Sensitivity and Transcriptomic Characterization of Adult md Neurons

Jessica M. Jones, Akira Mamiya, John Tuthill

Introduction

Nociceptors are not generalists. Their molecular identity determines what kinds of threats they respond to, how quickly they fire, and what circuits they engage downstream. The complement of ion channels, receptors, and signaling molecules a nociceptor expresses fundamentally shapes its sensory tuning and behavioral output.

During metamorphosis, larval md-IV nociceptors transform into adult md neurons, pruning their dendritic arbors and re-extending new processes into the adult cuticle. As we've seen in the previous chapter, these remodeled neurons drive both rapid escape responses and longer-term avoidance behaviors in adults. But a key question remains: does their molecular identity shift to match their new behavioral roles?

Adult flies inhabit a fundamentally different sensory world than larvae. Their abdomen is exposed, aerodynamic, and a frequent target of predators rather than a contact surface. This raises the possibility that abdominal nociceptors might evolve specialized molecular tuning—perhaps prioritizing mechanosensitive channels over the broad polymodal sensitivity characteristic of larval nociceptors. Alternatively, they might retain their diverse receptor repertoire to preserve flexibility across contexts.

To address this question, I analyzed single-cell RNA sequencing data from the FlyCellAtlas[1], examining transcripts enriched in adult md neurons and comparing their molecular profiles to larval nociceptors. The transcriptomic data reveal a clear shift: adult md neurons appear to downregulate many receptors that aid in polymodality (TrpA1, painless, Gr28b) while maintaining or upregulating mechanosensitive channels (Piezo, ppk, ppk26). This suggests a transition from broad threat detection to mechanical specialization.

However, when I test this prediction physiologically using calcium imaging, the results are more complex. Despite their apparent mechanical tuning, md neurons respond robustly to thermal stimuli but show surprisingly weak responses to mechanical stimulation. This discordance between transcriptomic prediction and physiological reality highlights the limits of inferring function from molecular identity alone—and suggests that sensory specialization may be more nuanced than gene expression profiles suggest.

Results

md Neurons Function as Temperature Sensors

As described in Chapter 2, we found that md neurons function as direct temperature sensors. Using two-photon calcium imaging, researchers observed robust calcium responses in md neurons when exposed to 40°C heat, but not at room temperature. These responses were consistent across individual neurons and flies, with calcium signals increasing rapidly upon heat application and remaining elevated during stimulation. This research establishes md neurons as thermal sensors that encode temperature information.

Single-cell RNA sequencing reveals molecular heterogeneity within adult sensory neuron populations.

To understand the molecular underpinnings of sensory neuron function and identify the transcriptomic signature of md neurons, we performed comprehensive single-cell RNA sequencing (scRNA-seq) analysis of adult *Drosophila* sensory neurons from the FlyCellAtlas[1]. We analyzed approximately 78,000 adult neurons using uniform manifold approximation and projection (UMAP) dimensionality reduction to visualize the cellular landscape and identify distinct neuronal subtypes **(Figure 3.1A).** We focused our analysis on relevant annotated cell types within the dataset (bitter-sensitive labellar taste bristle, Johnston organ neuron, mechanosensory neuron, gustatory receptor neuron, nociceptive neuron, pheromone-sensing neuron, photoreceptor, sacculus/arista neuron, olfactory receptor neuron, scolopidial neuron, and auditory sensory neuron). Mechanosensory neurons and JO/auditory neurons formed the largest clusters with the

most overlap across selected cell types, while nociceptive neurons formed the most distant UMAP

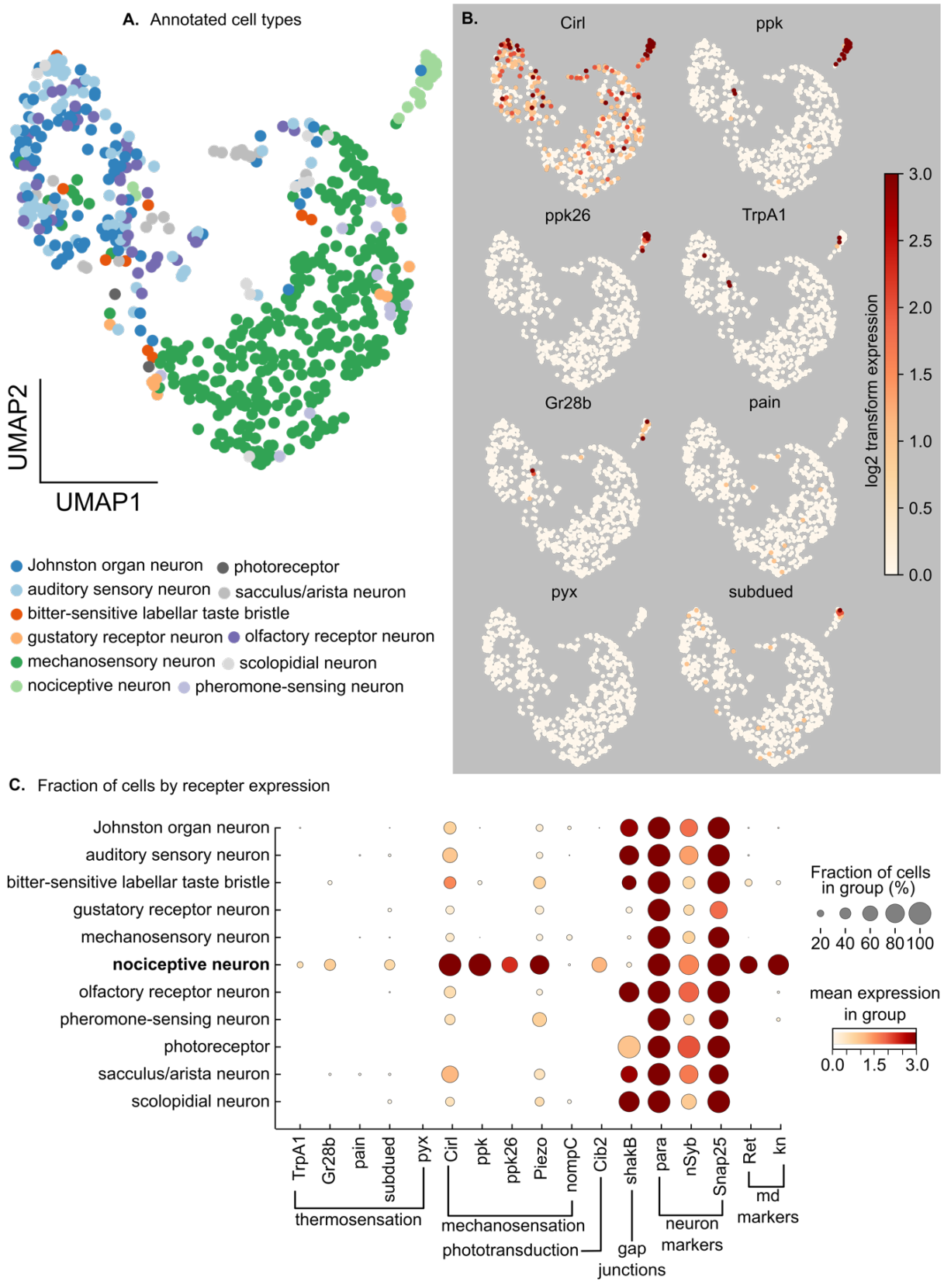

Figure 3.1. Single-cell transcriptomics of adult *Drosophila* sensory neurons reveals molecularly distinct populations. (A) UMAP embedding of adult peripheral sensory neurons clustered by transcriptomic identity and annotated by cell type, including mechanosensory neurons, nociceptors, and various chemosensory subclasses. (B) Gene expression of known nociceptor-enriched genes (Cirl, ppk, ppk26, TrpA1, pain, pyrexia, subdued, and gr28b) overlaid on the UMAP, showing spatial enrichment in a specific neuronal cluster. (C) Dot plot summarizing expression patterns of gene modules across annotated sensory neuron types. Each dot represents a gene's expression level (color) and proportion of expressing cells (size) within a cell type. Genes were clustered on the x-axis by known functional influences (thermosensation, mechanosensoation, phototransduction, gap junctions, neuron markers, and specific md markers)

distinct cluster. **(Figure 3.1A).** We focused on three critical mechanosensory markers: *Cirl* (a GPCR), *ppk* (pickpocket sodium channel), and *ppk26* (pickpocket 26), which showed distinct spatial expression patterns within the UMAP embedding. **(Figure 3.1B).** Cirl expression was broadly distributed across multiple sensory neuron types but showed enrichment in specific mechanosensory subclusters. *ppk* displayed more restricted expression, while *ppk26* showed the most selective expression pattern, being highly enriched in a distinct cluster of nociceptive neurons, suggesting a specialized functional role for this sodium channel subtype. We observed lower expression of thermosensory and chemosensory related genes, notably *TrpA1, Gr28b, painless, pyrexia,* and *subdued*.

We next quantified the fraction of cells with average expression of known genes for mechanosensation and thermosensation across cell-types **(Figure 3.1C).** Nociceptive neurons showed expression of thermosensory and mechanosensory related genes, confirming their role in noxious multimodal stimulus detection. We did not see strong expression of *nompC* (no mechanoreceptor potential C), pyrexia, or painless. Core molecular machinery genes (*para, nSyb, Snap25*) were broadly expressed across most neuronal types, while developmental and identity genes (Ret, kn) showed more restricted patterns localized to nociceptive neurons, likely defining lineage relationships and connectivity specificity. Interestingly, we saw that 60% of nociceptive cells expressed *Cib2*, which may signify that some nociceptive cells are involved in light

perception[13], and *shakB,* suggesting the presence of innexins and therefore gap junctions in nociceptors.

Comparative transcriptomic analysis reveals developmental stage-specific gene expression changes

To understand how sensory neuron molecular profiles change during development, we performed comparative analysis between larval and adult md neurons using published scRNA-seq datasets. We analyzed larval c4da neuron locations (n=400 cells) from Boiko et al., 2017[2], and adult c4da neuron locations (n=92 cells) from Li et al., 2022, focusing on genes that show significant expression changes between developmental stages **(Figure 3.2A).**

The comparative analysis revealed substantial transcriptomic remodeling during the larval-to-adult transition. We identified 4,000 genes showing significant differential expression ($p<0.001$), with most changes representing increased expression in adult neurons **(Figure 3.2B).** The distribution of expression changes showed a clear bias toward adult-specific upregulation, with many genes showing greater than 10-fold increases in adult expression levels. Detailed examination of specific gene families revealed stage-specific expression patterns that reflect functional maturation **(Figure 3.2D).**

Neurotransmitter-related genes showed mixed patterns. We observed an overall downregulation, but non-zero expression, in serotonergic, allatostatin, drosulfokinin, leuokinin, tachykinin, and dopamine-related neuropeptide receptors in adults. Conversely, we observed upregulation in

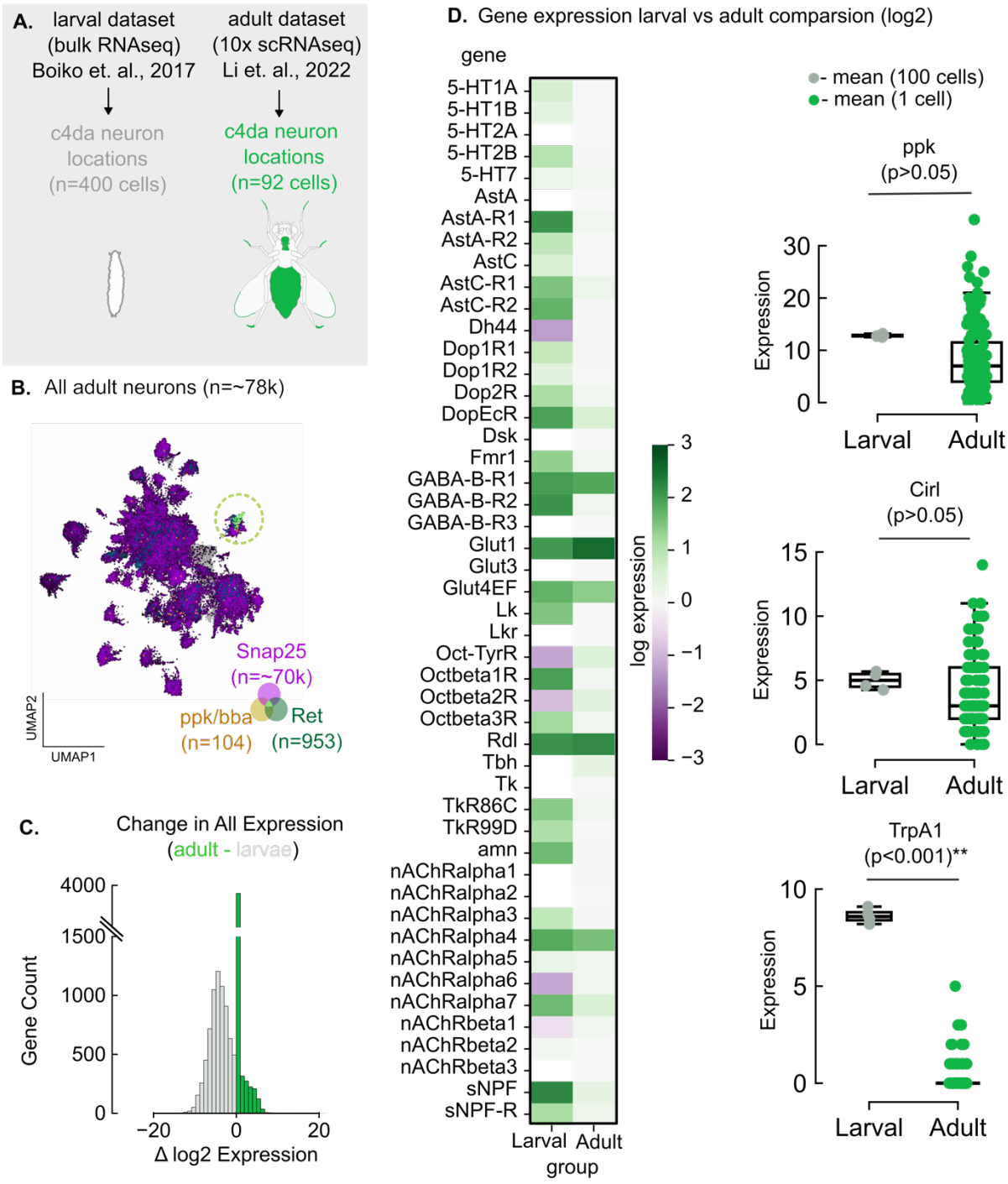

Figure 3.2. Adult-specific single-cell expression patterns differ from larval nociceptors and reveal developmental specialization. (A) Schematic comparing larval bulk RNA-seq data of c4da nociceptors (left) to adult c4da neuron single-cell RNA-seq data (right), identifying 92 c4da-like cells in the adult dataset. (B) UMAP of all adult neurons (~78,000) with expression of general (Snap25), nociceptor-specific (ppk, bba), and proprioceptor-specific (Ret) markers overlaid. (C) Histogram of genome-wide log2 fold change in gene expression between adult and larval c4da neurons. (D) Heatmaps comparing expression of select genes in larval vs. adult c4da neurons. A subset of nociceptive genes (e.g., TrpA1) is downregulated in adults, while other genes related to mechanosensation and neurotransmission show increased expression.

Glut1, Rdl, tyramine beta hydroxylase (*Tβh*), and octopamine beta 2 receptor (*Octβ2R*), suggesting an increase in the sensitivity or capacity of cells to respond to octopamine (*OA*) and, in the case of Oct-TyrR, tyramine (*TA*). The analysis also revealed developmental regulation of canonical neurotransmitters (glutamate, GABA, and acetylcholine), with many showing increased adult expression. This pattern suggests extensive synaptic remodeling during metamorphosis, potentially underlying the behavioral differences between larval and adult sensory responses or reflecting the maturation of cholinergic signaling pathways.

Notably, this comparative analysis revealed a consistent, non-zero, downregulation of genes associated with polymodal sensory detection in adults, including *TrpA1*, *painless*, pyrexia, and *Gr28b* ($p < 0.001$ for all comparisons, two-tailed t-tests with Bonferroni correction)[3–5].

Integration of physiological and transcriptomic data reveals possible molecular basis of temperature sensitivity.

The integration of our calcium imaging results with transcriptomic analysis provides compelling evidence for the molecular mechanisms underlying md neuron temperature sensitivity. The robust calcium responses to 40°C thermal stimulation **(Chapter 2, Figure 2.3)** is supported by subtle expression of *TrpA1, subdued,* and *Gr28b* in adults. Furthermore, the transcriptomic data reveals the molecular diversity within mechanosensory populations that could explain the heterogeneous

response magnitudes we observed in calcium imaging experiments. The variable expression levels of mechanotransduction machinery (*ppk, ppk26*) across individual neurons likely contribute towards conferring thermosensitive responses to innocuous and noxious touch.

These findings establish a comprehensive molecular and functional characterization of md neurons, demonstrating their evolution from primarily polymodal larvae sensors to multifunctional adult neurons capable of both thermal and potentially mechanical stimulus detection. The developmental transcriptomic remodeling we identified provides the molecular foundation for understanding how sensory systems adapt to meet the changing environmental demands across life stages. These results suggest that, despite transcriptional downregulation of *TrpA1* and other thermosensitive genes, adult md neurons retain functional responsiveness to noxious heat.

Discussion

The transcriptomic and physiological characterization of adult md neurons reveals a paradox that challenges our assumptions about the relationship between gene expression and sensory function. Single-cell RNA sequencing demonstrates that adult md neurons express high levels of mechanosensitive channels (*ppk, ppk26/Balboa, Piezo, Cirl*) while showing reduced expression of thermosensitive and polymodal receptors (*TrpA1, painless, Gr28b, pyrexia*) compared to their larval counterparts. This molecular signature would predict specialized mechanosensory function. However, calcium imaging reveals robust responses to thermal stimuli (40°C) and minimal responses to isolated mechanical perturbations, suggesting more complex sensory integration than transcriptomics alone would predict.

Methodological Limitations in Transcriptomic Inference

Important methodological caveats must be considered before interpreting this apparent contradiction. The adult RNAseq data come from sparsely sampled single nuclei that can underestimate genes with low or variable expression, while larval datasets were generated from bulk-isolated md-IV neurons. This difference in sampling depth likely contributes to the apparent downregulation of *TrpA1* and *painless* in adults. Additionally, single-cell RNAseq reveals mRNA presence, not protein translation, trafficking, or membrane functionality—a core limitation of transcriptomic inference. Low-level expression of thermosensitive channels may remain functionally sufficient but fall below single-cell detection thresholds.

Multimodal Integration as an Evolutionary Strategy

Rather than viewing this as a contradiction, these findings may reflect evolution of a sophisticated multimodal integration system requiring combinatorial stimuli for activation. Flying adults must rapidly discriminate between benign environmental contacts (wind, substrate vibrations) and genuine threats warranting costly escape responses. A system requiring both thermal and mechanical components[6] would provide enhanced specificity, reducing false alarms while maintaining sensitivity to dangerous stimuli that typically present both modalities simultaneously (contact with heated surfaces, predator attacks generating pressure and body heat). Even modest *TrpA1* expression—potentially below detection thresholds but functionally sufficient—could serve as a coincidence detector, gating mechanosensitive responses when thermal activation confirms threat relevance.

Developmental Functional Refinement

The developmental transition from larval polymodal responsiveness to adult multimodal integration represents an elegant solution to changing ecological demands. Larval md-IV neurons operate as broadly tuned danger detectors—any sufficiently intense stimulus triggers escape rolling because ground-dwelling larvae face relatively simple threat categories. Adult md neurons must support more nuanced behavioral decisions in three-dimensional environments where escape can involve jumping, flight initiation, or directional running.

In larvae, md-IVs are polymodal by necessity—everything from noxious heat to strong touch triggers rolling escape. In adults, behavioral demands are more complex and the cuticle is thicker and differently innervated. The transcriptomic shift toward mechanosensory specialization, combined with retained thermal sensitivity, may reflect functional refinement rather than simple modality switching.

Alternative Explanations for Mechanical Insensitivity

The physiological findings raise a fundamental question: why do these neurons respond to heat but not mechanical stimulation? One possibility is that mechanical responsiveness requires structural context that our preparation doesn't preserve. Mechanical force must transmit through cuticle and body wall to activate dendritic transduction channels, and physical coupling between cuticle and md dendrites may be compromised in restrained flies. In contrast, heat and AITC can passively diffuse and activate intracellular signaling without such coupling. Conversely, high mechanosensitive channel expression might not guarantee mechanosensitivity if critical co-factors, scaffolding proteins, or structural coupling are absent in adults. We did see a downregulation of *ppk26*, a critical co-factor used to form the heterodimer complex needed to confer mechanonociception in larvae, so the lack of mechanical response may be due to this.

Ecological Adaptive Value of TrpA1-Mediated Thermal Nociception

The evolution of TrpA1-mediated thermal nociception in abdominal *ppk*+ neurons likely represent critical adaptation to ecological challenges faced by adult *Drosophila*. For ectothermic insects, temperature profoundly affects physiology, ecology, and fitness, with extreme temperatures being damaging and potentially lethal. *TrpA1's* conserved role across developmental stages suggests thermal nociception is under strong evolutionary pressure as essential protection against tissue damage.

Unlike terrestrial larvae that thermoregulate through substrate selection and burrowing, adult *Drosophila* are exposed to direct solar radiation and temperature fluctuations during flight[7]. Adults must navigate three-dimensional thermal gradients while maintaining flight performance, requiring rapid integration of mechanical and thermal information. The abdominal location of

these thermosensors is particularly strategic, housing vital reproductive organs and metabolic machinery where thermal damage would be especially costly.

The integration of temperature sensitivity into preserved mechanosensory architecture provides an elegant solution that expands sensory capabilities without requiring complete neural reconstruction during metamorphosis. The preserved segmental organization and extensive peripheral innervation of *ppk*+ neurons create an ideal distributed sensor network for spatially precise thermal information. Recent evidence supporting *TrpA1* as mechanosensory[8,9] and chemosensory[10] in other systems points to potential channel co-opting during development to retain polymodality.

Future Directions and Knowledge Gaps

Significant gaps remain in understanding the ecological context and functional significance of abdominal thermal nociception. Most laboratory studies examine thermal responses under controlled conditions that may not reflect complex, spatially heterogeneous thermal environments wild *Drosophila* encounter. The discovery that nutritional status modulates thermosensation[11] highlights the importance of considering physiological state and ecological trade-offs. Precise thermal thresholds activating abdominal *ppk+/TrpA1+* neurons in naturalistic conditions remain unknown.

Our experimental paradigms may not recapitulate spatiotemporal dynamics of natural stimuli, particularly mechanical components likely accompanying thermal threats in ecological contexts. Future studies examining responses to naturalistic stimulus combinations—thermal gradients coupled with mechanical perturbations at physiologically relevant intensities—will be essential for resolving the apparent discrepancy between molecular expression and functional output.

While we have identified molecular machinery underlying temperature detection, specific behavioral outputs and downstream circuits integrating thermal and mechanical information remain poorly characterized. We have begun annotating peptidergic descending neurons providing presynaptic input to md neurons and downstream populations implicated in diuresis, stress tolerance, and pain, as well as integration with circulatory networks potentially regulating respiration[12] **(S3.1A—B).** We have also demonstrated potential roles in modulation with one notable GABAergic downstream partner pair that both receive substantial input from md and aversive sensory neurons and may play a pivotal role in nociceptive gain control **(Figure S3.2A, S3.2C)**. Disrupting 5B neuron function was hypothesized to eliminate the inhibitory gating mechanism on md neurons, leading to hypervigilant behavioral phenotypes **(S3.2D).** Additional analysis revealed that 5B neurons direct more than 60% of their output synapses back onto abdominal nociceptors and putative aversive sensory neurons, further emphasizing their role as feedback regulators **(Figure S3.2B)**. In silico modeling supports the interpretation that these inhibitory neurons downstream of nociceptors modulate both the magnitude and duration of the response **(S3.2E).** These results are consistent with known mechanisms of gain control and habituation in vertebrate pain pathways, where inhibitory circuits prevent hypersensitivity and maintain dynamic range **(S3.2F)**.

Summary

This chapter demonstrates both the power and limitations of transcriptomic approaches in defining sensory neuron identity. Adult md nociceptors adopt molecular profiles consistent with mechanosensory specialization yet respond robustly to thermal and chemical stimuli but not mechanical perturbation. These findings highlight developmental reprogramming of sensory gene expression that doesn't fully predict functional tuning, suggesting additional regulatory mechanisms at post-transcriptional or circuit levels. Future work combining high-resolution transcriptomic tools with in vivo physiology under naturalistic conditions will be essential to fully resolve how these neurons detect, interpret, and respond to threatening stimuli.

References

1. Li, H. *et al.* Fly Cell Atlas: A single-nucleus transcriptomic atlas of the adult fruit fly. *Science* **375**, eabk2432 (2022).

2. Boiko, N. *et al.* TrpA1 activation in peripheral sensory neurons underlies the ionic basis of pain hypersensitivity in response to vinca alkaloids. *PLOS ONE* **12**, e0186888 (2017).

3. Lee, Y. *et al.* Pyrexia is a new thermal transient receptor potential channel endowing tolerance to high temperatures in Drosophila melanogaster. *Nat. Genet.* **37**, 305–310 (2005).

4. Tracey, W. D., Wilson, R., Laurent, G. & Benzer, S. painless, a Drosophila Gene Essential for Nociception. **113**, 261–273 (2003).

5. Gallio, M., Ofstad, T. A., Macpherson, L. J., Wang, J. & Zuker, C. S. The Coding of Temperature in the Drosophila Brain. **144**, 614–624 (2011).

6. Haverkamp, A., Hansson, B. S. & Knaden, M. Combinatorial Codes and Labeled Lines: How Insects Use Olfactory Cues to Find and Judge Food, Mates, and Oviposition Sites in Complex Environments. *Front. Physiol.* **9**, 49 (2018).

7. Hamada, F. N. *et al.* An internal thermal sensor controlling temperature preference in Drosophila. *Nature* **454**, 217–220 (2008).

8. Gong, J. *et al.* Shear stress activates nociceptors to drive Drosophila mechanical nociception. *Neuron* **110**, 3727-3742.e8 (2022).

9. Gong, J. *et al.* TrpA1 is a shear stress mechanosensing channel regulating intestinal stem cell proliferation in *Drosophila*. *Sci. Adv.* **9**, eadc9660 (2023).

10. Arenas, O. M. *et al.* Activation of planarian TRPA1 by reactive oxygen species reveals a conserved mechanism for animal nociception. *Nat. Neurosci.* **20**, 1686–1693 (2017).

11. Ohashi, H. & Sakai, T. Leucokinin signaling regulates hunger–driven reduction of behavioral responses to noxious heat in Drosophila. *Biochem. Biophys. Res. Commun.* **499**, 221–226 (2018).

12. Bates, A. S. *et al.* Distributed control circuits across a brain-and-cord connectome. Preprint at https://doi.org/10.1101/2025.07.31.667571 (2025).

13. Sethna, S., Scott, P.A., Giese, A.P.J. *et al.* CIB2 regulates mTORC1 signaling and is essential for autophagy and visual function. *Nat Commun* 12, 3906 (2021). https://doi.org/10.1038/s41467-021-24056-1

Methods

Single cell RNA-seq

The methods for collection of the dataset and RNA-seq analysis are outlined as in Mamiya et al (2023)[1]. We accessed the dataset using SCope[2], an online platform for hosting and analyzing RNA-seq datasets, and analyzed data using python loompy and scanpy[3].

RNAseq comparison

To accurately compare RNA-seq gene expression data from *Drosophila* larval neurons (expressed in TPM and not yet log-transformed) with an adult dataset already log-transformed, the larval data must be appropriately transformed using a consistent log base, typically $\log_2$. In the provided code, after averaging the TPM values from four larval replicates, a conditional log transformation is applied to avoid mathematical errors due to zero values. Specifically, a mask (np.where) replaces zero or negative expression values with NaN, ensuring the np.log2 function only processes valid positive numbers. This results in a new column, avg_logFC_larvae, containing the $\log_2$-transformed average expression. This log transformation standardizes the larval dataset to a scale comparable with the adult neuron data, which is already $\log_2$-transformed. Subsequently, the adult neuron dataset is filtered to include only neuron-specific cells expressing marker genes (e.g., ppk, ppk26, Snap25, Ret) and transposed to align with gene labels as rows. The average expression across selected adult samples is then computed. Finally, both datasets are merged on gene identifiers, enabling a direct comparison between $\log_2$-scaled average gene expressions in larval and adult sensory neurons. This normalization and transformation process ensures analytical consistency when comparing datasets with different initial processing states, allowing for robust downstream statistical analyses such as differential expression or clustering.

Computational Modeling of Inhibitory Neurons

Model was adapted from Shiu et. al. 2024[4]. Detailed methods within manuscript. The network utilizes a leaky integrate-and-fire model as previously described. All parameters are taken from previous *Drosophila* modelling or electrophysiology efforts. To simulate experimental manipulations, input or output neurons could be "silenced" by removing their influence in the network. This was done by zeroing out the relevant columns in the weight matrix, effectively preventing those neurons from participating in the simulation.

Methods References

1. Mamiya, A. *et al.* Biomechanical origins of proprioceptor feature selectivity and topographic maps in the Drosophila leg. *Neuron* **111**, 3230-3243.e14 (2023).
2. Davie, K. *et al.* A Single-Cell Transcriptome Atlas of the Aging Drosophila Brain. *Cell* **174**, 982-998.e20 (2018).
3. Wolf, F. A., Angerer, P. & Theis, F. J. SCANPY: large-scale single-cell gene expression data analysis. *Genome Biol.* **19**, 15 (2018).
4. Shiu, P. K. *et al.* A Drosophila computational brain model reveals sensorimotor processing. *Nature* **634**, 210–219 (2024).

Extended Data

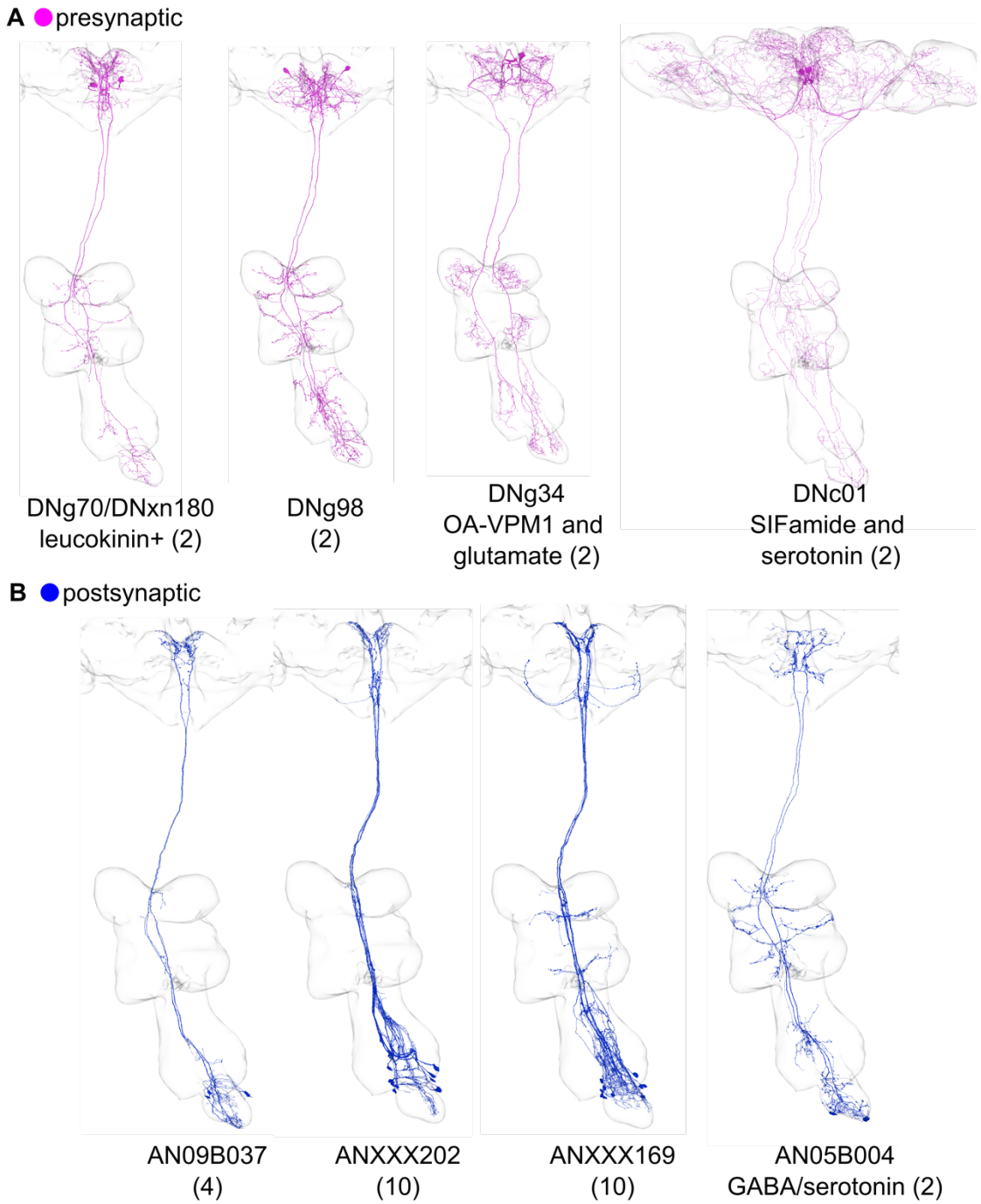

Extended Data Figure S3.1. Presynaptic to and postsynaptic from md neurons of future interest in pain modulation. A) Presynaptic (pink) and B) postsynaptic (blue) partners were chosen either based on independent connectivity to important peptidergic or circulatory neurons based on MANC/BANC synaptic query, verified and predicted peptidergic transmitter identity, or established literative implicating them as a part of a peptidergic or modulatory system of nociception in the adult or larvae.

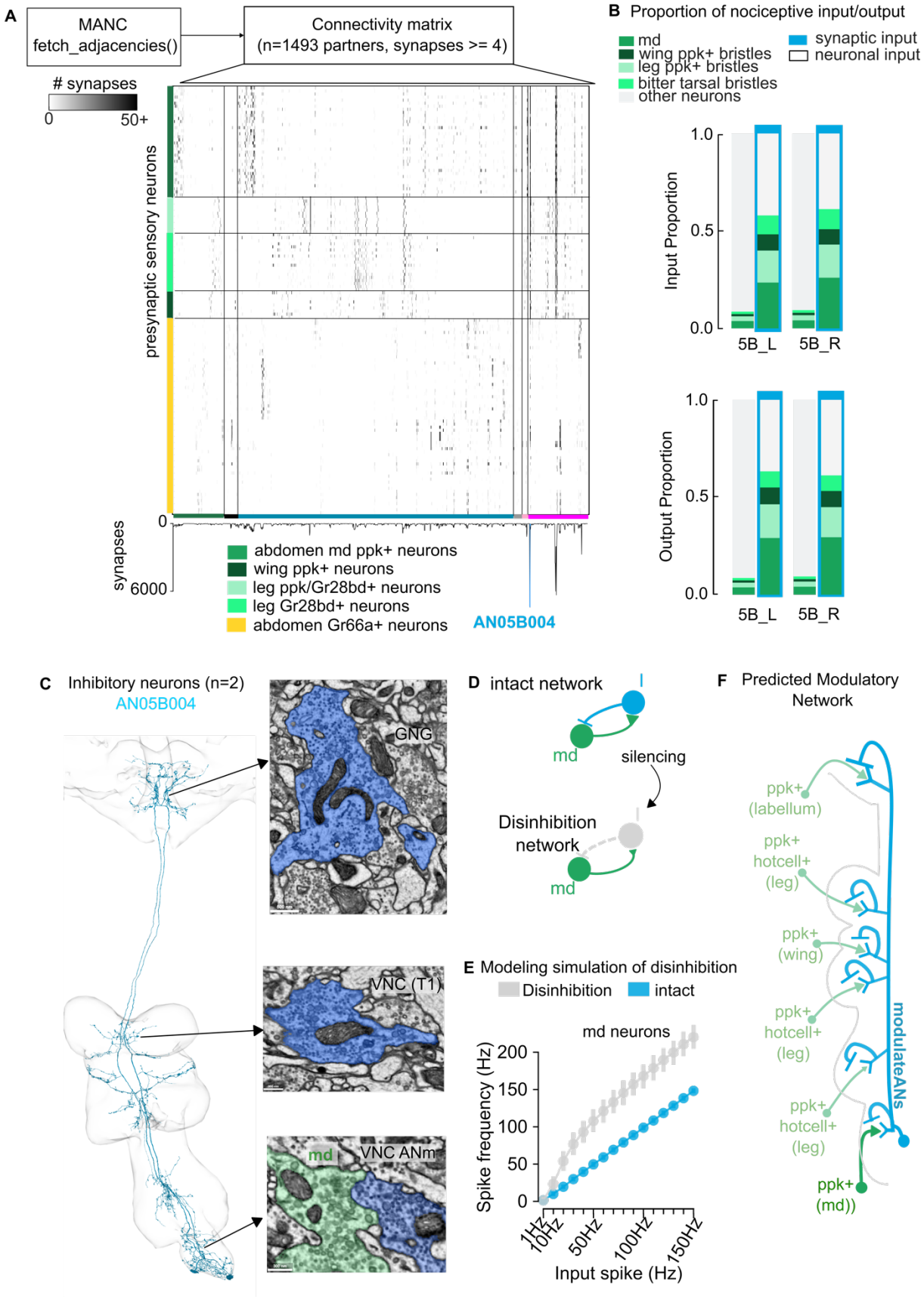
A
MANC
fetch_adjacencies()
Connectivity matrix
(n=1493 partners, synapses >= 4)
synapses
0
50+
presynaptic sensory neurons
synapses
0
6000
abdomen md ppk+ neurons
wing ppk+ neurons
leg ppk/Gr28bd+ neurons
leg Gr28bd+ neurons
abdomen Gr66a+ neurons
AN05B004
B Proportion of nociceptive input/output
md
wing ppk+ bristles
leg ppk+ bristles
bitter tarsal bristles
other neurons
synaptic input
neuronal input
Input Proportion
1.0
0.5
0.0
5B_L
5B_R
Output Proportion
1.0
0.5
0.0
5B_L
5B_R
C Inhibitory neurons (n=2)
AN05B004
GNG
VNC (T1)
md
VNC ANm
D intact network
I
md
silencing
Disinhibition
network
I
md
E Modeling simulation of disinhibition
Disinhibition
intact
md neurons
Spike frequency (Hz)
200
150
100
50
0
1Hz
10Hz
50Hz
100Hz
150Hz
Input spike (Hz)
F Predicted Modulatory
Network
ppk+
(labellum)
ppk+
hotcell+
(leg)
ppk+
(wing)
ppk+
hotcell+
(leg)
ppk+
hotcell+
(leg)
ppk+
(md))
modulateANs

Extended Data Figure S3.2. Modeling silencing AN05B004's influence on md neurons. **A)** Connectome matrix data from MANC showing the convergence onto AN05B004 neurons by categories of aversive sensory types. B) Proportion of nociceptive and aversive input and output to and from AN05B004 neurons. AN05B004 neurons give and receive 60% of their synapses from or to aversive sensory types. C) Reconstruction of AN05B004 neurons from the BANC dataset. EM images show the presences of dense core vesicles at synaptic terminals of both md (green) and AN05B004 neurons (blue) in various locations in the central nervous system. D) Schematic visualizing the loss of function hypothesis of AN05B004 neurons. E) Modeling AN05B004 disinhibition onto md neurons vs. an intact CNS. Modeling data based on connectivity matrix from MANC. F) Prediction modulatory network based on modeling data in E. AN05B004 neurons are used to modulate the gain of activity in md neurons, in addition to multiple other ppk+ aversive sensory types present in the VNC and brain.

Looking Forward

The work presented in this thesis has established a foundation for understanding how nociceptive circuits encode and modulate behavior across multiple timescales. By combining connectomics, transcriptomics, and behavioral analysis, we have revealed that *Drosophila* nociceptive processing encompasses sophisticated circuit integration, state-dependent modulation, and adaptive behavioral plasticity. However, this work also illuminates several compelling avenues for future inquiry that could deepen our understanding of pain-like processing across the animal kingdom.

Resolving the Transcriptomic-Physiological Paradox

One of the more intriguing finds of this thesis is the apparent contradiction between the transcriptome and physiological responses in adult md neurons. The precise molecular mechanisms underlying the functional-transcriptomic mismatch in Chapter 3 remain enigmatic. Future research should employ temporally controlled perturbations of key transcription factors, sensory channels, or post-translational regulatory elements to determine whether this represents genuine multimodal integration, experimental artifact, or developmental plasticity. Advanced techniques such as calcium imaging with behaving flies, targeted optogenetic manipulations of specific channel populations during in-vivo imaging, or CRISPR-based rescue experiments could directly test whether combinatorial thermal-mechanical stimuli activate these neurons more robustly than isolated modalities.

Additionally, the role of structural coupling between peripheral sensory dendrites and the adult cuticle remains unexplored. Future studies should examine whether mechanical responsiveness requires specific in vivo conditions—intact hemolymph pressure, cuticle tension, or mechanosensitive structures—that laboratory preparations may not preserve. Understanding

these requirements could resolve whether adult md neurons are truly specialized thermosensors or retain cryptic mechanosensitivity under appropriate conditions.

Circuit Plasticity and State-Dependent Processing

The discovery that ascending nociceptive pathways may regulate behavioral state rather than simply transmitting escape signals opens fruitful territory for investigating circuit plasticity. Our in vitro finding that the nociceptive VNC network that lacks these modulatory ascending neurons becomes hyperexcitable suggests these circuits broadly and actively calibrate threat sensitivity. Which is exciting because this is reminiscent of pain modulation in vertebrates. However, the mechanisms underlying this state regulation remain poorly characterized.

Future work should investigate how these circuits—particularly by recording from md neurons directly—adapt to injury, repeated stimulation, or changes in internal state using longitudinal behavioral assays combined with chronic manipulations or in vivo imaging. How do the inhibitory and excitatory ascending pathways interact to modulate behavioral state? What neuromodulatory systems influence the balance between these opposing circuits? How do factors like hunger, stress, or social context alter nociceptive processing? The connectomic identification of peptidergic descending neurons that provide presynaptic input to md neurons suggests a rich modulatory landscape worthy of systematic investigation. Understanding how these descending systems integrate with ascending nociceptive circuits could reveal fundamental principles of how nervous systems balance threat detection with behavioral flexibility.

Evolutionary Context and Comparative Analysis

The developmental transition from larval *polymodal* nociceptors to adult *multimodal* integrators represents an elegant evolutionary solution to changing ecological demands. However, this raises broader questions about how nociceptive systems adapt to different environmental niches and behavioral repertoires across species and life stages.

Comparative studies examining nociceptive circuit organization across *Drosophila* species with different ecological niches could reveal how environmental pressures shape circuit evolution. Do ground-dwelling species retain more larval-like polymodal responsiveness? How do nociceptive circuits differ between species with different flight capabilities or thermal tolerances? Such studies could illuminate general principles of how sensory systems evolve to match ecological demands.

Additionally, investigating other metamorphic insects could determine whether the larval-to-adult nociceptive transition observed in *Drosophila* represents a general feature of holometabolous development or a species-specific adaptation. Understanding these evolutionary patterns could provide insight into the origins and constraints of pain-like processing across invertebrates.

Toward a Unified Understanding of Affective Processing

One of the bigger implication of this work is its suggestion that *Drosophila* may possess distributed circuits for affective valence processing analogous to vertebrate pain networks. The capacity for learned aversion, state-dependent threat sensitivity, and persistent behavioral changes following nociceptor activation hints at an internal representation of "threat" that transcends simple stimulus-response relationships.

Future research should systematically investigate whether flies possess generalized affective processing systems that extend beyond nociception. Do other aversive modalities—bitter taste, noxious odors, extreme temperatures—engage similar ascending circuits and produce comparable state changes? Conversely, do appetitive stimuli activate opposing circuits that bias behavior toward approach rather than avoidance?

Advanced connectomic analysis could identify convergence points where different sensory modalities might integrate to produce unified affective states. Combined with sophisticated behavioral assays designed to measure sustained changes in exploration, risk-taking, or stimulus preference, such studies could reveal whether flies possess centralized systems for encoding stimulus valence that parallel mammalian emotional processing networks.

The integration of real-time neural monitoring during complex behavioral tasks could provide insight into how affective-like states emerge from circuit dynamics. Technologies like population calcium imaging or electrophysiology during naturalistic behaviors could reveal how nociceptive and other sensory signals converge to produce coherent behavioral states.

Ethical Considerations and Broader Implications

The findings presented in this thesis—that *Drosophila* possess dedicated nociceptors, ascending integration pathways, state-dependent modulation, and capacity for learned avoidance—raise questions that extend beyond neural mechanism into the domain of invertebrate welfare and research ethics. If a nervous system as compact as *Drosophila*'s can support pain-like processing, this raises fundamental questions about the evolutionary origins and neural requirements for subjective experience. While this work does not and cannot determine whether flies experience subjective pain in a manner analogous to humans, it does demonstrate that their nociceptive systems are far more sophisticated than simple stimulus-response reflexes would suggest. Understanding how simple nervous systems solve the fundamental challenge of converting sensory threat into adaptive behavior could inform approaches to treating chronic pain, developing more humane pest control strategies, and establishing ethical frameworks for invertebrate research and welfare.

The Limits and Utility of Mechanistic Understanding

A critical distinction must be maintained between demonstrating pain-like processing and inferring subjective experience. The circuits described here—parallel pathways for escape and state modulation, potential neuromodulatory and small molecule feedback, integration with learning and memory systems—satisfy multiple criteria proposed for identifying pain capacity across species. However, the relationship between circuit complexity and experience remains fundamentally uncertain, particularly in organisms whose neural architecture differs substantially from our own.

This uncertainty does not diminish the value of mechanistic understanding. Rather, it suggests a pragmatic approach: where we cannot definitively establish the presence or absence of suffering, we can optimize research practices to minimize potential harm while preserving scientific utility. This is already being utilized by the cultinary industry in establishing more humane ways to cook lobster and other kinds of shellfish species. Understanding how nociceptive circuits function enables more targeted experimental design, potentially reducing the number of animals required and refining stimulus parameters to answer specific questions without unnecessary activation of aversive pathways.

Current invertebrate research operates under minimal regulatory oversight compared to vertebrate studies, reflecting historical assumptions about insect nervous system simplicity. The demonstration that flies possess ascending nociceptive pathways, state-dependent threat sensitivity, and sustained behavioral changes following nociceptor activation—mechanisms that require brain substrates—suggests these assumptions warrant reconsideration.

Several practical refinements emerge from this work. First, the identification of specific driver lines and neural populations enables more precise circuit manipulations, potentially replacing *broad* pharmacological or thermal interventions (for example, with TrpA1) with targeted optogenetic approaches. Second, understanding that nociceptive activation produces long-lasting behavioral state changes—not just transient reflexes—suggests that recovery periods between experiments may be more important than previously recognized. Third, the discovery that context, internal state, and prior experience modulate nociceptive responses indicates that standardizing experimental conditions and minimizing stressors could reduce variability while improving animal welfare. Reducing uncontrolled variables and improving experimental reproducibility serves both scientific rigor and humane practice. The tens of thousands of flies used in laboratories worldwide

represent both a scientific resource and, potentially, a population whose experiences merit consideration.

Toward Informed Pest Management

Beyond the laboratory, this work has implications for how we approach pest control in agriculture and public health. Traditional broad-spectrum insecticides often work through nervous system disruption, potentially causing prolonged distress before death. Knowledge of specific nociceptive circuits and their downstream targets could enable development of compounds that rapidly incapacitate without activating aversive pathways, or that exploit these pathways to create more effective repellents. Similarly, understanding how flies integrate thermal and mechanical threat information could improve trap designs (for example, sticky traps) or environmental modifications that leverage natural avoidance behaviors.

This is not to argue that pest management should cease, but rather that mechanistic understanding enables optimization—approaches that are simultaneously more effective, more specific, and potentially less likely to cause unnecessary suffering. The economic and public health imperatives remain, but consideration of insect welfare where practical alternatives exist shouldn't be a burden or exist in conflict with these public health imperatives.

The Value of Uncertainty

Perhaps the most important ethical insight from this work is recognizing what we do not know. The transcriptomic-physiological paradox described in Chapter 3—molecular signatures suggesting mechanosensory specialization paired with robust thermal but minimal mechanical responses—illustrates how much remains uncertain about even well-characterized sensory

systems. If we cannot fully predict functional output from gene expression in a tractable model organism, our confidence in determining the presence or absence of subjective experience should be appropriately modest.

This uncertainty argues for continued investigation paired with proportional caution. As we map circuits, characterize molecular mechanisms, and observe behavior, we accumulate evidence that can inform—though perhaps never definitively answer—questions about experience and suffering. In light of this, we should continue to pursue better understanding while adopting precautionary practices where feasible.

Conclusion

To end, this thesis establishes *Drosophila* as a powerful model for understanding how parsimonious nervous systems integrate sensory information with internal states to regulate reflexive and adaptive threat responses. The identified circuits, spanning from peripheral nociceptors to brain-mediated state regulation, offer a foundation for understanding pain-like processing conserved across the animal kingdom.

By bridging invertebrate and vertebrate models, this research illuminates fundamental principles of how nervous systems translate sensory experience into adaptive action. The circuits identified in this study suggest that pain-like processing may not require human-like consciousness or vertebrate-specific brain structures, but rather emerges from ancient neural computation properties. This possibility should inform our approach to the broader diversity of animals whose nervous systems we are just beginning to understand. Future investigations building on this foundation promise to deepen our understanding of pain, affective processing, and the evolutionary origins of subjective experience.

The relationship between this work and ethical considerations is symbiotic. Rigorous mechanistic investigation provides the empirical basis for informed ethical reasoning, while ethical considerations motivate questions about function, experience, and welfare that drive scientific inquiry. Understanding nociceptive circuits illuminates both the engineering principles of nervous systems and the evolutionary origins of capacities associated with suffering.

Moving forward, the challenge is to maintain scientific rigor while acknowledging moral uncertainty. We must pursue mechanistic understanding that both advances knowledge and informs more thoughtful treatment of the organisms enabling that understanding.

The fly may be small, compact, but the questions it raises about pain, experience, and our responsibilities toward other sentient beings, including each other, are anything but.

Acknowledgments

It takes a village. And I am nothing without mine.

I first want to acknowledge the Tuthill lab. Every single one of you have cultivated me into the scientist I've always dreamed of being. To my advisor John—thank you for facilitating the cultivation. For instilling in me diligence, stamina, rigor, and humility in being a scientist. For teaching me how to write in, and for, science. Thank you for reaching out to me during the pandemic and extending warmth during a cold, trying time in the world. And thank you for encouraging me to go outside!

To the rest of the lab–thank you for your patience and comradery in these last five years and sharing a laugh a time or two to ease the stress of graduate school. You all were my home away from home. You all are the backbone of the lab, and it's been exciting watching every one of you grow, move on to careers, renovate houses, become parents for some, get married, win awards, publish papers, and sing karaoke, amongst other achievements.

Thank you to my committee for your willingness and excitement during times of showcasing my work at annual meetings. To Sama–for being authentically yourself, since meeting you in 2019. To Jay–for pointing me toward relevant larval literature, potential contacts for employment, and for being a realist when I really needed to hear it. To Ajay–for letting me rotate in your lab and being available for help, letters of recommendation, and reagents. For Amy and Bing, my dual GSRs–for being grounded, kind, and insightful, especially during this last sprint to the finish line. Thank you to all the PIs who've I've found community in during my time here.

Thank you to the HHMI for funding my research. To the Gilliam Fellows—thank you for being my science family for the last 3 years. It's becoming rarer to see collectives such as this one in science due to the changes in government, which is shameful. Despite these scary times, annual meetings with fellows past and present, and the Gilliam leadership, were the highlight of my years in the program and the most fun I've had in my science career. There's nothing like it, and I'm incredibly blessed to have participated in it when I did. Thank you to the NIH also for sponsoring summer REUs and part-time employment during my undergraduate career—a time when the government somewhat had it's act together…

I'd like to thank the Abdus-Saboor lab, past and present. To Ishmail—I would not be in grad school if it wasn't for you. And not just because you were my mentor, but because I realized I just wanted to be a version of you, and to step in that direction I needed to refine myself in graduate school and ground myself in science. I'm motivated to be the best person I can be because of seeing you *when* I saw you—during a transition period for both of us. Thank you for uplifting me. Thank you for teaching me that being black in this field is an act of protest. Thank you for being, and continuing to be, my mentor, my advisor, my sponsor, and my friend.

I'd like to thank the Graduate Program in Neuroscience staff and students. To the class of 2020–how did we do this for this long? We ride at dawn. To Kyle Shea—you are the reason I came to UW and stayed. You are irreplaceable.

To the many, many friends I've made in Seattle. Dancing, singing, crying, fighting misogynists and homophobes outside the club on a Saturday night, and licking the streets—you've been through it all with me. Highest highs, the lows, and everything in between. You are the actual life force behind this PhD because without you I would've absolutely mastered out; I was having

too much fun and simply forgot to. Nathalie, Olivia, Ayumi, Brittany, Addis, Stephen and Adrian—you are forever in my heart.

To my in-laws Joan and Paul—thank you for your acceptance. To Joan—for your steadfast love and support since the beginning. To Paul—I lost a father while pursuing this degree, and I gain a father while pursuing this degree. Nothing prepared me for the healing you've given me since the beginning. To my Lake brothers in Christ—thank you for continuing to be my knights and my best friends.

To my husband Eron—thank you for being, and continuing to be, my home for this last decade. You teach me by leading with tenacity and grace, and especially love. Thank you for reminding me to take care of, be patient with, and to love myself. Thank you for saving my life.

To UC Santa Cruz—for connecting me to lifelong friends and family. To my maids of honor and sisters in power Lina and Selamawit, to the skeetz squad—Aughviee, Jaelynn, Arianna—to the gworls Baylee and Kennedy—to everyone else. Thank you for your everlasting love and friendship.

To Central Virginia—with love. To the many families, and particularly mothers, who mothered me when I needed it. Thank you for adopting me. To Feda, Charlene, Toni, Demetria—thank you mom.

I'd like to thank Mr. Cannon, my kindergarten teacher at Olive Elementary in Novato, CA. My love for the natural world and science started with you and grew with my mother's help. Thank you for nurturing me and all your students. To all my STEM teachers and mentors who've carried me along the way, thank you.

To my family. *Nothing is too good for my family*. Thank you. I am an amalgamation of my entire family. Thank you for raising me to be the fierce, smart, and hilarious women I am today. To the men—my boy cousins, my uncles—thank you for teaching me how to be tough and stern. We're teaching each other now how to reflect and heal. To the women—Patricia, Rosie, Jeanie, Tish—thank you for teaching me how to be *resilient*.

To my mom—this document would reach thousands and thousands of pages if I had the space and time to write how much I am me because of you. Thank you for teaching and reminding me that it's okay to be soft, gentle, and thoughtful. Thank you for instilling in me the value of education and loving what you do, whatever that may be. I'm eternally grateful for your sacrifices. This thesis is for you especially.

And I love you to pieces…

free PALESTINE, free SUDAN, peace to the middle east

f*ck an oligarchy

protect trans and LGBTQIA+ rights

believe women, believe science

love and be kind to each other, have fun with your friends

and all BLACK lives matter